

RELEVANCE OF THE INTERACTION BETWEEN
SORLA AND THE ADAPTOR PROTEINS PACS1 AND
VPS35 FOR ALZHEIMER'S DISEASE PROCESSES

Dissertation zur Erlangung des akademischen Grades des
Doktors der Naturwissenschaften (Dr. rer. nat.)

eingereicht im Fachbereich Biologie, Chemie, Pharmazie
der Freien Universität Berlin

vorgelegt von

TILMAN ADRIAN BURGERT

aus Rastatt

2013

Diese Arbeit wurde von Oktober 2008 bis Mai 2013 unter der Leitung von Prof. Dr. Thomas Willnow am Max-Delbrück-Centrum für Molekulare Medizin (Berlin-Buch) durchgeführt.

1. Gutachter: Herr Prof. Dr. Fritz G. Rathjen

2. Gutachter: Herr Prof. Dr. Thomas E. Willnow

Disputation am 22.11.2013

DANKSAGUNG

Mein Dank gilt Prof. Dr. Thomas E. Willnow für die intensive Betreuung der Arbeit sowie für die hervorragenden Arbeitsbedingungen in seinem Labor.

Ebenfalls bin ich Prof. Dr. Fritz G. Rathjen sehr dankbar für die Bereitschaft meine Dissertation zu betreuen und zu begutachten.

Ein großer Dank gilt auch der Arbeitsgruppe Willnow sowie den vielen Kollegen und Freunden am Max-Delbrück-Centrum für ihre Unterstützung im Labor, die Bereitstellung von Reagenzien und Versuchsprotokollen, die Diskussion von wissenschaftlichen Ideen und nicht zuletzt für die lustige und schöne Zeit, die ich mit ihnen sowohl im als auch außerhalb des Labors verbringen durfte.

Meine Familie ist und war mir immer in jeglichen Belangen ein großer Rückhalt. Dafür danke ich ihr.

CONTENTS

LIST OF ABBREVIATIONS IX

LIST OF FIGURES XII

LIST OF TABLES XV

1. INTRODUCTION 1

1.1. ALZHEIMER’S DISEASE

1.1.1. Pathophysiology of Alzheimer’s disease.....1

Tau protein 1

The amyloid precursor protein 2

1.1.2. APP – the main etiologic agent
in Alzheimer’s disease.....3

The genetics of Alzheimer’s disease 3

*Physiological function of the APP protein
family in the nervous system* 3

1.1.3. APP processing products.....4

*APP cleavage products and their implications
in normal brain function and disease* 6

*Characteristics and physiological functions
of secretases* 7

Degradation of A β 8

1.1.4. Intracellular trafficking of APP.....	10
<i>Subcellular trafficking of APP and the secretases</i>	10
<i>Trafficking and processing of APP in neurons</i>	12
1.1.5. Interaction partners of APP.....	12
1.2. THE SORTING RECEPTOR SORLA	
1.2.1. Genetic evidences for the implication of SORLA in Alzheimer’s disease.....	14
1.2.2. Expression and physiological function of the VPS10p-domain receptor SORLA.....	14
<i>Structure and function of VPS10p receptor family members</i>	14
<i>Domain organization of SORLA</i>	15
<i>Tissue distribution of SORLA in mammals</i>	16
<i>Physiological functions of SORLA</i>	16
1.2.3. Intracellular trafficking of SORLA.....	17
Proteins regulating intracellular SORLA trafficking	
<i>The phosphofurin acidic cluster sorting protein (PACS) 1</i>	20
<i>The retromer complex</i>	21
<i>The GGA proteins</i>	23
<i>Implication of trafficking adaptor proteins in Alzheimer’s disease</i>	24
1.2.4. The role of SORLA in Alzheimer’s disease.....	25
<i>SORLA interacts with APP and influences its subcellular localization</i>	25
2. AIM OF THE STUDY	27

3.1. IMPACT OF TRAFFICKING ADAPTOR BINDING-DEFECTIVE SORLA MUTANTS ON APP SORTING AND PROCESSING *IN VIVO*

3.1.1. Generation of novel mouse models expressing SORLA mutants defective in binding trafficking adaptors.....	29
<i>Targeting of the Sorl1 locus</i>	30
<i>Targeting of the Rosa26 locus to knock-in cDNA expressing human SORLA trafficking adaptor binding-defective mutants</i>	32
3.1.2. <i>In vivo</i> characterization of the generated mouse models.....	36
<i>SORLA protein expression levels in various brain regions</i>	36
<i>Phenotypic characterization of the generated mouse models</i>	37
3.1.3. Intracellular trafficking of the SORLA variants in the brain.....	39
<i>Immunocytochemical analysis of the subcellular localization of SORLA variants in primary neurons</i>	40
<i>Expression of trafficking adaptor proteins in the brain</i>	47
<i>SORLA expression in purified synaptosomes</i>	48
3.1.4. Analysis of the mitogen-activated protein kinase pathway in the brain of mice expressing SORLA variants.....	50
3.1.5. Influence of SORLA variants on the localization and processing of APP in the brain.....	51
<i>Amyloidogenic processing in an Alzheimer's disease mouse model expressing human SORLA^{wt}, SORLA^{FSAF}, and SORLA^{acidic}</i>	51
<i>Synaptosomal localization of APP in 5xFAD mice expressing SORLA trafficking mutants</i>	53
<i>Phosphorylation of APP at Thr⁶⁶⁸ in 5xFAD mice expressing human SORLA variants</i>	55

3.2. ROLE OF PACS1 FOR SORLA TRAFFICKING AND APP PROCESSING IN THE NEURONAL CELL LINE SH-SY5Y	
3.2.1. Trafficking of SORLA in PACS1-deficient SY5Y-S/A cells.....	57
3.2.2. SORLA-dependent function for PACS1 in APP trafficking and amyloidogenic processing.....	60
3.2.3. Knockdown of PACS1 affects APP processing in SY5Y-S/A cells.....	63
3.2.4. Effects of siRNA-mediated PACS1 knockdown on β -secretase (BACE1) activity.....	64
3.2.5. SORLA-independent function for PACS1 in amyloidogenic processes.....	66
<i>Influence of PACS1 deficiency on APP processing in SY5Y cells expressing a SORLA mutant lacking the cytoplasmic domain</i>	66
<i>SORLA-independent function for PACS1 in the catabolism of $A\beta_{42}$</i>	67

4. DISCUSSION **71**

4.1. IMPLICATION OF SORLA FOR ALZHEIMER'S DISEASE

4.2. ROLE OF SORLA IN ALZHEIMER'S DISEASE *IN VIVO*

4.2.1. Generation of novel mouse models to study SORLA function in Alzheimer's disease processes <i>in vivo</i>	72
4.2.2. Human SORLA ^{wt} cDNA expression protects APP from processing in a mouse model of Alzheimer's disease.....	73

4.2.3. SORLA ^{FSAF} and SORLA ^{acidic} variants exhibit an altered subcellular localization and cause increased processing of APP in 5xFAD mice.....	75
4.2.4. SORLA ^{FSAF} and SORLA ^{acidic} differ in synaptic localization and provoke alterations in axonal transport of APP.....	80
4.3. THE ROLE OF PACS1 IN ALZHEIMER'S DISEASE-RELATED PROCESSES	
4.3.1. SORLA-dependent function for PACS1 in APP processing in SY5Y cells.....	83
4.3.2. SORLA-independent function for PACS1 in amyloid processes.....	87
4.4. FUTURE PERSPECTIVES.....	89
5. MATERIAL AND METHODS	91
5.1. MATERIAL	
5.1.1. Oligonucleotides.....	91
<i>Mouse specific primer sequences</i>	91
<i>Primer used für genotyping</i>	91
<i>Human specific primer sequences</i>	92
<i>Human specific siRNA</i>	92
5.1.2. Antibodies.....	92
<i>Primary antibodies</i>	92
<i>Secondary antibodies</i>	94
5.1.3. Media, buffers and solutions.....	94

<i>Media</i>	94
<i>Buffers and solutions</i>	95
5.1.4. Bacteria strains and mammalian cells.....	96
5.1.5. Chemicals.....	96
5.2. MOUSE-BASED EXPERIMENTS	
<i>Animal experimentation</i>	97
5.2.1. Brain tissue sections.....	97
<i>Nissl staining</i>	98
<i>Immunohistochemistry on free-floating sections</i>	98
5.2.2. Preparation and immunocytochemistry of primary neurons.....	98
5.2.3. Isolation of proteins from mouse brains.....	99
<i>Purification of membrane proteins</i>	99
<i>Fractionation of nervous tissue</i>	99
5.3. CELL CULTURE BASED EXPERIMENTS	
5.3.1. Cultivation and storage of SH SY5Y cells.....	100
5.3.2. Experimental procedures.....	100
<i>siRNA treatment</i>	100
<i>Immunocytochemistry</i>	100
<i>Protein isolation from eukaryotic cells</i>	101
5.4. PROTEINBIOCHEMISTRY	
<i>Determination of protein concentration</i>	101
<i>Dephosphorylation of protein lysates</i>	101
<i>SDS-PAGE (polyacrylamide gel electrophoresis)</i>	101
<i>Western blotting / Immunoblotting</i>	102

<i>Biological assays</i>	102
5.5. MOLECULAR BIOLOGY	
5.5.1. Molecular cloning.....	103
<i>Enzymatic digest of DNA</i>	103
<i>Amplification of DNA fragments by polymerase chain reaction</i>	103
<i>Agarose gel electrophoresis of DNA</i>	103
<i>Isolation of DNA from agarose gels</i>	103
<i>Determination of DNA concentration</i>	104
<i>Ligation of DNA fragments</i>	104
<i>DNA transformation of bacteria</i>	104
<i>Cryopreservation of bacteria</i>	104
<i>Isolation of plasmid DNA from bacteria</i>	105
<i>Sequencing of DNA</i>	105
5.5.2. DNA isolation and genotyping.....	105
<i>Isolation of genomic DNA for southern blot</i>	105
<i>Isolation of genomic DNA for genotyping by PCR</i>	106
<i>Genotyping by PCR</i>	106
<i>Genotyping by southern blot</i>	107
5.6. MICROSCOPY	107
5.7. STATISTICAL ANALYSIS	
<i>Statistical testing</i>	108
<i>Densitometric scanning of western blots</i>	108
<i>Colocalization analysis</i>	108
5.8. GENERATION OF MOUSE MODELS	
5.8.1. Cloning of the targeting vector.....	109
<i>Targeting of the Sor11 locus</i>	109
<i>Targeting of the Rosa26 locus</i>	109

5.8.2. Embryonic stem cell culture.....	110
<i>Cultivation of embryonic stem cells</i>	110
<i>Electroporation of embryonic stem cells</i>	110
<i>Isolation of embryonic stem cell clones</i>	111
<i>Freezing of embryonic stem cell clones</i>	111
<i>Injection of embryonic stem cell clones into blastocysts</i>	111
6. ZUSAMMENFASSUNG	113
7. SUMMARY	115
8. BIBLIOGRAPHY	117
9. PUBLICATIONS	129
CURRICULUM VITAE	131

LIST OF ABBREVIATIONS

A β	amyloid β
AD	Alzheimer's disease
ADAM	a disintegrin and metalloprotease
AICD	APP intracellular domain
AKT	protein kinase B
AP	adaptor protein
APH	anterior-pharynx defective
AP2M1	adaptor protein 2 μ subunit
APOE	apolipoprotein E
APOER2	apolipoprotein E receptor 2
APP	amyloid precursor protein
BACE	β -site APP cleaving enzyme
BAR	Bin, amphiphysin and Rvs
BCA	bicinchoninic acid
BDNF	brain-derived neurotrophic factor
bp	basepairs
BSA	bovine serum albumin
CAG	cytomegalovirus early enhancer/chicken β -actin promoter
CD-MPR	cation-dependent mannose-6-phosphate receptor
CHO	chinese hamster ovary
CI-MPR	cation-independent mannose-6-phosphate receptor
CK2	casein kinase 2
CTF	C-terminal fragment
DMEM	Dulbecco's Modified Eagle's Medium
DMSO	dimethyl sulfoxide
DNA	desoxyribonucleic acid
DTA	diphtheria toxin A expression cassette
EDTA	ethylene-diamine-tetra acetic acid
EEA	early-endosome associated
EOAD	early-onset Alzheimer's disease
ERK	extracellular-signal regulated kinase
ES	embryonic stem cell
FAD	familial Alzheimer disease
FBR	furin-binding region
FBS	fetal bovine serum
flAPP	amyloid precursor protein (full length)
GAE	γ -adaptin ear
GAT	GGA and TOM
GDNF	glial cell line-derived neurotrophic factor
GGA	Golgi-localized, γ -adaptin ear containing ADP ribosylation-binding factor
g	gram

HEK	human embryonic kidney
HEPES	2-(4-(2-Hydroxyethyl)-1-piperazinyl)-ethansulfonacid
JIP	c-jun NH(2)-terminal kinase-interacting protein
kb	kilo base pairs
kDa	kilo dalton
KPI	Kunitz-type protease inhibitor domain
Lamp	lysosomal-associated membrane protein
LB	lysogeny broth
LDL	low density lipoprotein
LDLR	LDL receptor
l	liter
LOAD	late-onset Alzheimer's disease
LRP	LDLR-related protein
LTD	long-term depression
LTP	long-term potentiation
M	molar
min	minutes
MR	middle region
mRNA	messenger ribonucleic acid
NaK-ATPase	sodium-potassium ATPase
NCT	nicastatin
NeoR	neomycin-conferring resistance cassette
NeuN	neuron-specific nuclear protein
NFT	neurofibrillary tangles
P2	synaptosomes
P3	light membranes
PACS1	phosphofurin acidic cluster sorting protein 1
PAGE	polyacrylamide gel electrophoresis
pAPP	phosphorylated amyloid precursor protein (here: at Thr ⁶⁶⁸)
PBS	phosphate buffered saline
PCR	polymerase chain reaction
PFA	paraformaldehyde
polyA	polyadenylation signal
PEN	PS enhancer
PS/ <i>PSEN</i>	presenilin
PSD95	post synaptic density protein 95
r	Pearson's correlation coefficient
Rab	Ras-related in brain
rel.	Relative
RT	room temperature

s	second
S	supernatant
sAPP	soluble amyloid precursor protein
SDS	sodium dodecyl sulfate
SNP	single nucleotide polymorphism
SOC	super optimal broth with catabolite repression
SORCS	sortilin-related VPS10 domain-containing receptors
SORLA	sortilin-related receptor with LDLR class A repeats
<i>Sorll</i>	gene encoding SORLA
TBS	tris-buffered saline
tg	transgene
TGN	trans-Golgi network
Thr	threonine
tM	thresholded Manders' value
TM	transmembrane domain
U	unit
V	volt
VHS	Vps27, Hrs, Stam
VPS	vacuolar protein sorting
Vti	vesicle transport through interaction with t-SNAREs homolog
w/	with
w/o	without
w/phosph.	treated with phosphatase
wt	wild-type

LIST OF FIGURES

Figure 1: Domain organization of APP695	3
Figure 2: Proteolytic processing of APP	5
Figure 3: Intracellular trafficking of APP	10
Figure 4: Domain organization of SORLA	16
Figure 5: Intracellular trafficking of SORLA is dependent on trafficking adaptor binding motifs in the cytoplasmic tail	19
Figure 6: Domain organization and cargo binding motifs of PACS1	20
Figure 7: Regulation of endosome-to-TGN retrieval by the retromer complex.	22
Figure 8: Domain organization and cargo binding motifs of GGA1.	23
Figure 9: Model for the function of SORLA in trafficking and processing of APP.	25
Figure 10: Binding motifs in the cytoplasmic tail of SORLA.	29
Figure 11: Targeting of the <i>Sorll</i> locus.	31
Figure 12: Generation of transgenic mice expressing human SORLA mutants.	33
Figure 13: Generation of transgenic mice expressing human SORLA mutants controlled by the CAG promoter.	35
Figure 14: Expression levels of SORLA ^{wt} , SORLA ^{FSAF} , and SORLA ^{acidic} in the mouse brain.	36
Figure 15: Brain architecture in mice expressing SORLA ^{wt} , SORLA ^{FSAF} , and SORLA ^{acidic} .	38
Figure 16: Immunohistological detection of SORLA in cortex and hippocampus of mice expressing SORLA ^{wt} , SORLA ^{FSAF} or SORLA ^{acidic} .	40
Figure 17: Trans-Golgi network localization (Vti1b) of SORLA ^{wt} , SORLA ^{FSAF} , and SORLA ^{acidic} in primary neurons.	41
Figure 18: Trans-Golgi network localization (γ -adaptin) of SORLA ^{wt} , SORLA ^{FSAF} , and SORLA ^{acidic} in primary neurons.	42
Figure 19: Endosomal localization of SORLA ^{wt} , SORLA ^{FSAF} , and SORLA ^{acidic} in primary neurons.	44
Figure 20: Lysosomal localization of SORLA ^{wt} , SORLA ^{FSAF} , and SORLA ^{acidic} in primary neurons.	46
Figure 21: Expression of trafficking adaptor proteins in the brain of SORLA ^{wt} , SORLA ^{FSAF} , and SORLA ^{acidic} mice.	48

Figure 22: Subcellular protein separation of cortical extracts of mice expressing SORLA ^{wt} , SORLA ^{FSAF} , and SORLA ^{acidic} .	49
Figure 23: Protein expression of components of the mitogen-activated protein kinase pathway in mice expressing SORLA ^{wt} , SORLA ^{FSAF} , and SORLA ^{acidic} .	50
Figure 24: APP metabolites in the brain of an Alzheimer's disease mouse model (5xFAD) expressing SORLA ^{wt} , SORLA ^{FSAF} , and SORLA ^{acidic} .	52
Figure 25: APP expression levels in cortical brain lysates of 5xFAD mice expressing SORLA ^{wt} , SORLA ^{FSAF} , and SORLA ^{acidic} .	53
Figure 26: APP and SORLA localization in subcellular fractions of 5xFAD mice expressing SORLA ^{wt} , SORLA ^{FSAF} , and SORLA ^{acidic} .	54
Figure 27: APP phosphorylation levels in cortical brain lysates of 5xFAD mice expressing SORLA ^{wt} , SORLA ^{FSAF} , and SORLA ^{acidic} .	55
Figure 28: Knockdown of PACS1 in SY5Y cells.	57
Figure 29: Effect of PACS1 knockdown on the trans-Golgi network localization of SORLA in SY5Y cells.	58
Figure 30: PACS1 knockdown alters the endosomal localization of SORLA in SY5Y-S/A cells.	59
Figure 31: Effect of PACS1 knockdown on the subcellular trafficking of APP in SY5Y-S/A cells.	61
Figure 32: Loss of PACS1 enhances APP processing in SY5Y-S/A cells.	63
Figure 33: Effect of PACS1 knockdown on GGA3 and BACE1 expression and activity in SY5Y-S/A cells.	65
Figure 34: Knockdown of PACS1 in SY5Y cells expressing a tailless SORLA mutant.	66
Figure 35: Effect of PACS1 knockdown on APP processing in SY5Y cells expressing a tailless SORLA mutant.	67
Figure 36: Model for PACS1-dependent sorting of the CI-MPR	68
Figure 37: Knockdown of PACS1 affects protein levels of the cation-independent mannose-6 phosphate receptor and of cathepsin B in SY5Y-S/A cells.	69
Figure 38: Loss of PACS1 does not impair CD-MPR expression levels in SY5Y-S/A cells.	70
Figure 39: Model for the role of the interaction between SORLA and PACS1 or the retromer complex in trafficking and processing of APP.	77

Figure 40: Role of PACS1 in SORLA transport and APP processing.

84

Figure 41: Model for PACS1-dependent sorting of the CI-MPR.

87

LIST OF TABLES

Table 1: Viability in transgenic mice expressing SORLA variants.	38
Table 2: Quantification of the trans-Golgi network localization of SORLA ^{wt} , SORLA ^{FSAF} , and SORLA ^{acidic} in primary neurons.	43
Table 3: Quantification of the endosomal localization of SORLA ^{wt} , SORLA ^{FSAF} , and SORLA ^{acidic} in primary neurons.	45
Table 4: Quantification of the lysosomal localization of SORLA ^{wt} , SORLA ^{FSAF} , and SORLA ^{acidic} in primary neurons.	47
Table 5: Quantification of the trans-Golgi network localization of SORLA in SY5Y-S/A cells.	59
Table 6: Quantification of the endosomal localization of SORLA in SY5Y-S/A cells.	60
Table 7: Quantification of the subcellular localization of APP in SY5Y-S/A cells.	62

1. INTRODUCTION

1.1. ALZHEIMER'S DISEASE

1.1.1. Pathophysiology of Alzheimer's disease

Alzheimer's disease (AD) is a senile dementia and the most common neurodegenerative disease in the elderly with more than 20 million cases worldwide. In 1906, Alois Alzheimer reported mental dysfunctions of a female patient. When analyzing the brain post mortem, Alzheimer found two types of structural anomalies: intraneuronal filamentous inclusions within pyramidal neurons, nowadays termed neurofibrillary tangles (NFT), and amyloid plaques (Goedert and Spillantini 2006).

NFTs are intracellular aggregates of misfolded and hyperphosphorylated Tau protein, that emerge in the entorhinal cortex and the hippocampus and spread, in later stages of the disease, to the isocortex (Braak and Braak 1991).

Amyloid plaques are extracellular deposits that accumulate mainly in the isocortex (Jellinger, Braak et al. 1991) and are composed of A β , a processing product of the amyloid precursor protein (APP) (Kang, Lemaire et al. 1987).

Interestingly, the amount and distribution of NFTs, but not of amyloid plaques, correlate with the severity of AD (Arriagada, Growdon et al. 1992).

Neuropathologic observations in AD patients are accompanied by synapse loss and, more drastically, cortical atrophy, mainly in the medial temporal lobes (Armstrong 2011). More specifically, areas around NFTs or amyloid deposits are surrounded by dystrophic neurites, reactive astrocytes and activated microglia suggesting a causal role for these deposits in loss of functional neurons (Takata and Kitamura 2012).

Tau protein

The genomic locus of human *TAU* is located on chromosome 17q21 (Neve, Harris et al. 1986). Tau is a microtubule-associated protein that mainly resides in the axon of neurons where it stabilizes microtubules and thereby enables transport along axons (Weingarten, Lockwood et al. 1975; Binder, Frankfurter et al. 1985). Upon phosphorylation, Tau loses its binding activity and detaches from microtubules (Biernat, Gustke et al. 1993). Post-

translational modifications like phosphorylation and oxidation as well as genomic mutations in *TAU* influence the aggregation potential of the protein (Schweers, Mandelkow et al. 1995; Schneider, Biernat et al. 1999; Lewis, McGowan et al. 2000).

The role of NFTs in AD is still controversial. In AD patients, the number of phosphate residues per Tau molecule is 4-fold higher than in healthy controls (Kopke, Tung et al. 1993). But, whether NFTs are a protective response of damaged neurons or inducers of neuronal death, is still a matter of debate.

The amyloid precursor protein

APP is an evolutionary conserved protein with homologues in *Caenorhabditis elegans* (Daigle and Li 1993), *Drosophila melanogaster* (Rosen, Martin-Morris et al. 1989) and zebrafish (Musa, Lehrach et al. 2001). In humans, *APP* is localized on chromosome 21. The genomic locus in mice is on chromosome 16.

APP is a member of a gene family that also includes the two APP homologues APLP1 and APLP2 (Wasco, Bupp et al. 1992; Slunt, Thinakaran et al. 1994). Being type-I transmembrane proteins, their amino terminal extracellular moiety is subdivided into two different subunits E1 and E2. E1 at the N-terminus consists of a heparin- and a copper-binding domain and is followed by E2, that contains another heparin-binding domain and a motif comprised of the five amino acids RERMS (Fig. 1). Finally, a cytoplasmic region that contains phosphorylation and binding motifs for interaction with cytosolic proteins completes the receptors of the APP family.

Although the family members are structurally related, only APP and APLP2 contain a Kunitz-type protease inhibitor domain (KPI). Furthermore, APP is alternatively spliced yielding three isoforms. Of those, APP695 (isoform specific number of amino acids) lacks the KPI domain and is the predominant isoform expressed in neurons (Neve, Finch et al. 1988). Notably, the most interesting difference between receptors of the APP family is the uniqueness of the A β sequence in APP.

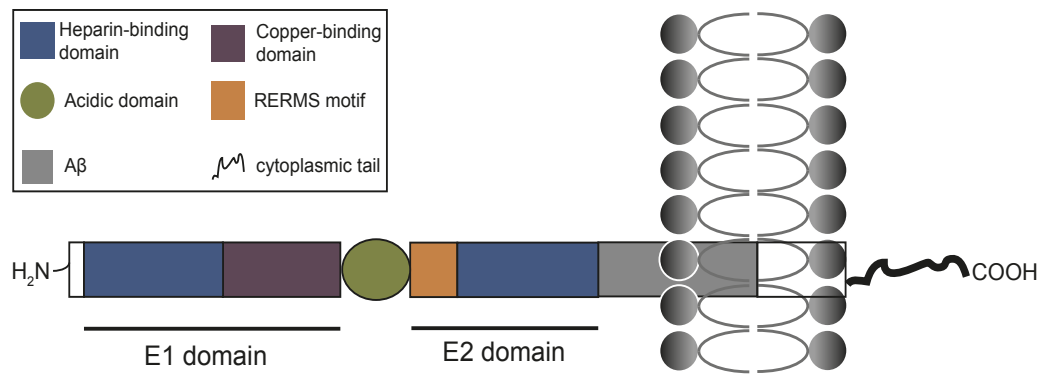


Figure 1: Domain organization of APP695.

The APP695 isoform is mainly expressed in neurons. Structurally, the N-terminus is governed by the E1 domain, consisting of a heparin-binding domain that is followed by a copper-binding domain. Thereafter, an acidic domain and the E2 domain follows, which comprises a RERMS motif and another heparin-binding domain. The 42 amino acid spanning A β sequence is located at the very C-terminal end of the extracellular region and reaches in part into the transmembrane domain. Finally, the intracellular, cytoplasmic tail at the C-terminus of APP is supposed to be important for various regulatory and cellular processes (see below).

1.1.2. APP – the main etiologic agent in Alzheimer’s disease

The genetics of Alzheimer’s disease

AD can be divided into two forms. More than 98% of cases are diagnosed from an age of 65 years onward (late-onset of Alzheimer’s disease (LOAD)). In contrast, the early-onset familial Alzheimer’s disease (EOAD) starts around 30 years of age and is mainly caused by autosomal-dominant inherited mutations in *APP*. Patients suffering from down syndrome/trisomy 21 also show clinical and neuropathological hallmarks of AD, due to increased levels of APP (and its processing products) pinpointing the central importance of APP in Alzheimer’s disease. Interestingly, no mutations in *TAU* have been identified so far to cause EOAD.

Physiological function of the APP protein family in the nervous system

APP family members are highly expressed during embryonic development and in the adult brain. Due to their structural similarity, suggesting overlapping and redundant functions, much effort has been put into elucidating the physiological role of APP, APLP1 and APLP2 in the brain.

APP-deficient mice are viable and fertile, but exhibit a reduction in body and brain weight as well as diminished forelimb grip strength and deficits in learning and spatial memory (Zheng, Jiang et al. 1995; Dawson, Seabrook et al. 1999). Whereas the synaptic bouton counts and number of neurons are unchanged (Phinney, Calhoun et al. 1999), *APP* null mice exhibit reduced synaptic activity and neurite outgrowth explaining in part their neurophysiological phenotype (Qiu, Ferreira et al. 1995; Perez, Zheng et al. 1997).

In contrast, *APLP1* deficient mice show only minor phenotypes, including a postnatal growth deficit (Heber, Herms et al. 2000). *APLP2* null animals reveal no obvious abnormalities (von Koch, Zheng et al. 1997).

Surprisingly, simultaneous genetic disruption of all APP family genes results in early postnatal death (Herms, Anliker et al. 2004). Affected embryos display focal dysplasia, loss of cortical Cajal-Retzius cells, and migration defects pointing towards an important function of APP, *APLP1* and *APLP2* in brain development.

Interestingly, combined genetic disruption of *APLP1/APLP2* or *APP/APLP2* leads to death shortly after birth as well (Heber, Herms et al. 2000). A detailed analysis of the *APP/APLP2* null mice revealed a malfunction of the neuromuscular synapse and suggested transsynaptic APP interactions to be crucial for synaptic transmission and cholinergic synaptic function (Wang, Yang et al. 2005; Wang, Wang et al. 2009). In contrast, *APP/APLP1* double-deficient mice show no abnormalities (Heber, Herms et al. 2000) suggesting a redundancy between *APLP2* and *APP/APLP1*.

In summary, *in vivo* loss-of-function studies ascribe the APP gene family a pivotal role in normal brain development and synaptic function and point towards a partial redundancy between the various APP family members.

1.1.3. APP processing products

A β , the major component of amyloid plaques, arises as a consequence of a physiological proteolytic process (Haass, Schlossmacher et al. 1992). In detail, A β is generated upon APP cleavage mediated by protease activities called secretases (Shoji, Golde et al. 1992). Two different pathways are implicated in APP processing. Whereas A β arises only in the amyloidogenic pathway, the non-amyloidogenic pathway prevents its generation (Fig. 2).

In the amyloidogenic pathway, APP is cleaved by a secretase called beta-site APP cleaving enzyme (BACE) 1 liberating a large part of APP's extracellular domain, termed sAPP β

(Vassar, Bennett et al. 1999). The remaining membranous part (β -CTF) is further processed by the γ -secretase complex generating two fragments: the APP-intracellular domain (AICD) that is released into the cytosol and the $A\beta$ peptide that is secreted into extracellular fluids (Seubert, Vigo-Pelfrey et al. 1992; De Strooper 2003).

In contrast, the non-amyloidogenic pathway is initiated by an α -secretase-dependent cleavage of APP in the $A\beta$ region liberating an APP ectodomain fragment termed $sAPP\alpha$ (Sisodia, Koo et al. 1990). The subsequent processing of the membranous stub (α -CTF) by the γ -secretase generates the AICD and a truncated peptide called p3 (Haass, Hung et al. 1993).

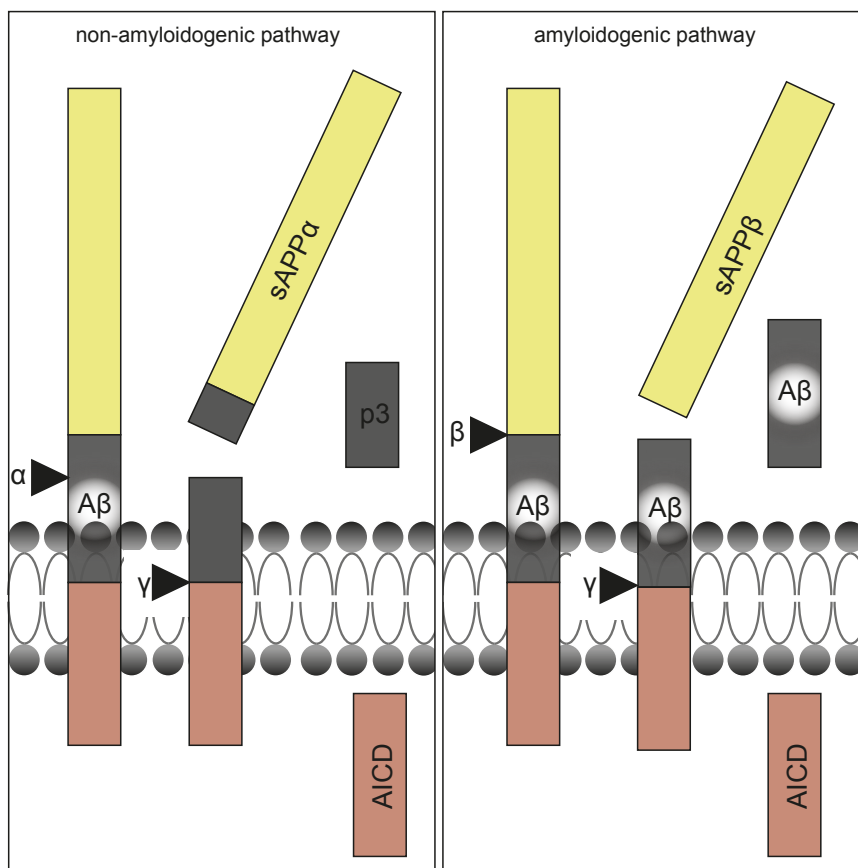


Figure 2: Proteolytic processing of APP.

APP undergoes cleavage by entering two different proteolytic pathways:

In the non-amyloidogenic pathway, APP is processed by an α -secretase yielding soluble (s)APP α and a membranous stub that is further cleaved by γ -secretase resulting in APP-intracellular domain (AICD) and p3. On the other hand, a β -secretase-induced cleavage of APP is the initial step in the amyloidogenic pathway resulting in $sAPP\beta$ production. The remaining membrane-embedded stub is subjected to γ -secretase cleavage producing $A\beta$ and AICD.

The physiological relevance of APP processing and $A\beta$ generation is still a matter of debate. However, studies suggest that APP cleavage is regulated by neuronal activity. More precisely, blocking neuronal activity diminishes $A\beta$ production whereas, in turn, a higher activity

increases A β generation. On the other hand, A β release at synaptic terminals decreases excitability and synaptic activity suggesting a negative feedback loop balancing neuronal activity and APP processing (Kamenetz, Tomita et al. 2003).

In addition, processing of APP is differently regulated by receptor stimulation. For example, activation of muscarinic M1 acetylcholine receptors results in an increased sAPP α release (Nitsch, Slack et al. 1993) and decreased A β levels (Hock, Maddalena et al. 2003). Conversely, stimulation of NMDA receptors upregulates A β production, paralleled by a decreased α -secretase activity (Lesne, Ali et al. 2005).

APP cleavage products and their implications in normal brain function and disease

In AD brains, the most devastating pathological hallmark is synaptic dysfunction and widespread neuronal cell loss. Microscopically, dystrophic neurites are surrounded by amyloid plaques containing high amounts of A β .

At pathologically high levels, plaque-derived, diffusible A β oligomers provoke synaptotoxicity by modulating pre- and postsynaptic functions leading to the inhibition of long term potentiation (LTP) and increase of long term depression (LTD) ultimately resulting in neuronal degeneration (Shankar, Li et al. 2008). In contrast, A β levels within a physiological range facilitate an increase in neuronal activity (Puzzo, Privitera et al. 2008; Abramov, Dolev et al. 2009) explaining the synaptic defects in mice displaying low levels of A β (Seabrook, Smith et al. 1999).

High levels of A β are supposed to be caused by an increased amyloid processing at the expense of non-amyloid processing. Hence, neuronal dysfunction in AD may also be caused by decreased levels of sAPP α . Indeed, sAPP α is supposed to mediate synaptotrophic and neuroprotective functions by increasing LTP and spatial memory (Taylor, Ireland et al. 2008). Additionally, sAPP α stimulates neurogenesis and neurite outgrowth via the Erk signaling cascade (Rohe, Carlo et al. 2008).

In contrast to sAPP α , the 17 amino acids shorter peptide sAPP β seems to adopt minor, yet important physiological functions in brain metabolism. It binds to the DR6 receptor and triggers axon degeneration (Nikolaev, McLaughlin et al. 2009).

The AICD of APP forms a transcriptionally active complex with Fe65 and Tip60 in the nucleus (Cao and Sudhof 2001). A number of transcriptional targets have been identified (including GSK3 β , neprilysin, EGFR, LRP1, APP, p53), yet the relevance of AICD-dependent gene regulation remains disputed (Hebert, Serneels et al. 2006; Waldron, Isbert et al. 2008).

Characteristics and physiological functions of secretases

BACE1 is a membrane-bound aspartyl protease with high expression levels in the brain. BACE1-deficient mice display decreased levels of A β indicating BACE1 to be the sole β -secretase (Roberds, Anderson et al. 2001). Additional to APP, BACE1 cleaves neuregulin-1 (Hu, He et al. 2008), a protein implicated in Schwann-cell mediated myelination, explaining the hypomyelination phenotype seen in *BACE1* null mice (Willem, Garratt et al. 2006).

The γ -secretase is a multi-protein complex consisting of the four subunits aspartyl protease activity-conveying enzymes Presenilin (PS) 1 or PS2, nicastrin (NCT), anterior-pharynx defective (APH)-1a or APH-1b, and the PS enhancer (PEN)-2. The concerted action of these four factors facilitates a regulated intramembranous protein cleavage of target proteins (Steiner 2008). Known substrates of γ -secretase are Notch, a receptor involved in cell signaling during embryogenesis (De Strooper, Annaert et al. 1999), as well as the membrane-bound stub (CTF) produced by α - or β -secretase cleavage of APP (see Fig. 2).

Interestingly, intramembrane proteolysis is not limited to a single site in APP. Rather, β -CTFs are subjected to a stepwise endoproteolysis resulting in A β species of different size designated A β ₃₈ to A β ₄₂ (Qi-Takahara, Morishima-Kawashima et al. 2005; Takami, Nagashima et al. 2009). This mechanism is of particular importance for amyloid plaque deposition, since A β ₄₂ (number indicates the amount of amino acids) is more prone to aggregation and, therefore, suspected to represent a seed for A β oligomers. In contrast, A β ₄₀ and shorter forms have a reduced propensity to aggregate (Haass and Selkoe 2007). Interestingly, inhibiting the dimerization of the transmembrane domains of APP by small molecules or disrupting the dimerization motif lowers A β ₄₂ generation in favour of shorter A β species, indicating a modulatory effect of APP dimerization on γ -secretase cleavage specificity (Munter, Voigt et al. 2007; Munter, Botev et al. 2010; Richter, Munter et al. 2010).

Mutations in *PSEN1* and *PSEN2* (genes encoding PS1 or PS2, respectively) identified in EOAD patients (<http://www.molgen.ua.ac.be/ADMutations>) cause an increase in the ratio of A β ₄₂ to A β ₄₀ and thereby enhance the potential for plaque formation (Scheuner, Eckman et al. 1996).

The α -secretase cleavage is the first event in non-amyloidogenic processing of APP preventing the production of toxic A β species. Besides APP, various other proteins like Notch, cadherins, and tumor necrosis factor α are subjected to α -secretase-mediated processing (Hooper, Karran et al. 1997). Several members of the a disintegrin and metalloprotease (ADAM) family comprising ADAM9, ADAM10, ADAM17 and ADAM19 potentially function as α -secretase (Allinson, Parkin et al. 2003). Although α -secretase activity is shared by many ADAMs, siRNA-mediated knockdown of ADAM10 suggested ADAM10 to be the main active form in neurons (Kuhn, Wang et al. 2010). Consequently, ADAM10 overexpression in neurons shifts the APP processing fate towards the non-amyloidogenic pathway (Postina, Schroeder et al. 2004).

Degradation of A β

Brain levels of A β are not only determined by the kinetics of APP breakdown but also by proteolytic degradation of the peptide by various proteases.

For example, the insulin-degrading enzyme degrades monomeric A β (Farris, Mansourian et al. 2003).

The zinc metalloprotease neprilysin, the by far most extensively studied A β degrading enzyme, is expressed in neurons where it localizes to presynaptic terminals (Fukami, Watanabe et al. 2002). Being a type-II membrane associated protein, neprilysin is active in the extracellular space and in lumenal compartments of the endoplasmic reticulum and Golgi apparatus (Roques, Noble et al. 1993). Although the A β -degrading nature of the protease was confirmed in loss- and gain-of-function studies in transgenic animals (Iwata, Tsubuki et al. 2001; Iwata, Mizukami et al. 2004), neprilysin fails in degrading A β oligomers – a diffusible form originating from plaques and responsible for the synaptotoxic property of A β (Shankar, Li et al. 2008). Consequently, overexpression of neprilysin in a mouse model does not affect AD-induced memory defects (Meilandt, Cisse et al. 2009).

Cathepsins B and D are also A β degrading proteases acting predominantly in acidic cellular compartments (and in the extracellular space) (Hamazaki 1996; Mort and Buttle 1997). Being synthesized as inactive proenzymes, cathepsin B and D are targeted to the lysosome for activation – an active transport process mediated by the cation-independent mannose-6-phosphate receptor (CI-MPR). Cathepsin B is also secreted from cells and found in amyloid plaques *in vivo* (Mueller-Steiner, Zhou et al. 2006).

Neuron-specific overexpression of cathepsin B or enhancement of this enzyme activity *in vivo* reduces the relative abundance of A β ₄₂, suggesting a substrate preference of the protease for this highly aggregation-prone form of the peptide (Wang, Sun et al. 2012). In line with this finding, viral overexpression or genetic inactivation of cathepsin B in a mouse model of AD decreased or increased plaque deposition, respectively (Mueller-Steiner, Zhou et al. 2006).

1.1.4. Intracellular trafficking of APP

Subcellular trafficking of APP and the secretases

The prerequisite for proteolytic processing is the spatial vicinity of APP and the secretases as well as the subcellular milieu (e.g. pH) that facilitates protease activity.

Accordingly, the subcellular trafficking of APP (and of the secretases) is a tightly regulated process as it determines amyloidogenic versus non-amyloidogenic processing fates (Fig. 3).

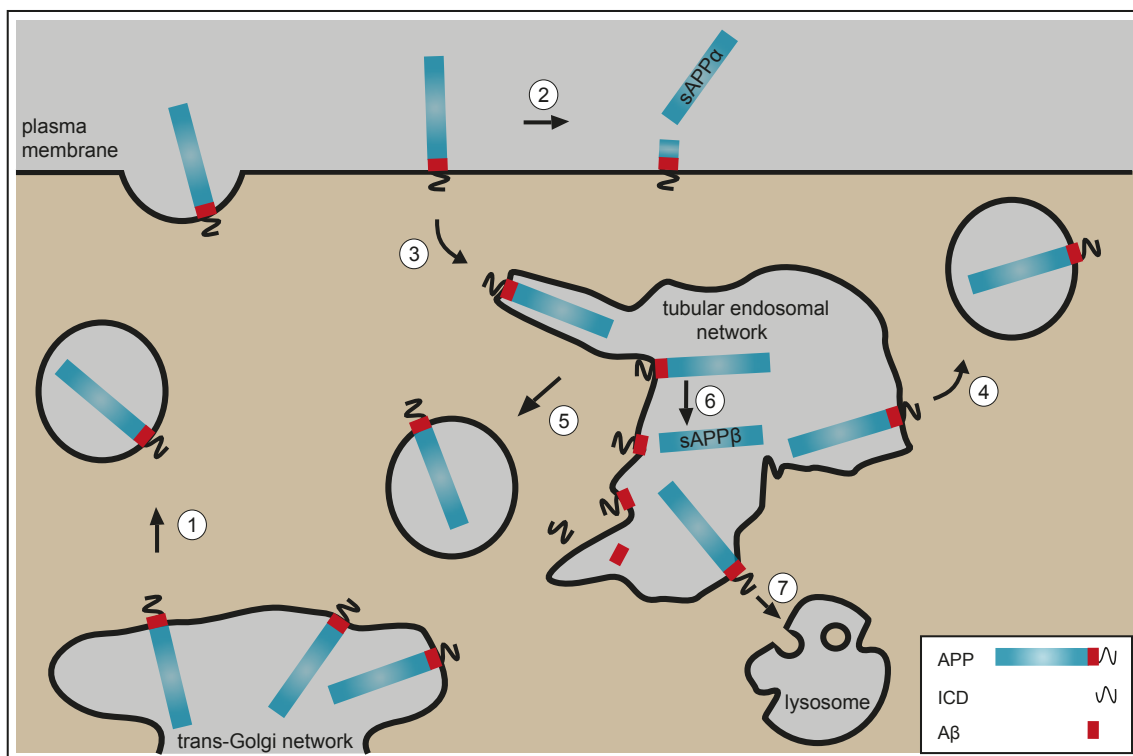


Figure 3: Intracellular trafficking of APP.

Newly synthesized APP matures during transit of the Golgi and exits the trans-Golgi network (TGN) by default to the cell surface (1). There, APP is either subjected to α -secretase cleavage (2) or internalized via clathrin-coated pits (3) (Koo and Squazzo 1994). In the tubular endosomal network, APP is rerouted back to the cell surface (4) or sorted to the TGN (5). APP molecules that escape regulated transport to TGN or cell surface move to endosomes, where they encounter BACE1 and γ -secretase, resulting in processing into sAPP β and A β (6). APP molecules that are not rerouted to the TGN or processed in the endosome may be degraded in lysosomes (7). ICD, intracellular tail of APP.

Following co-translational transport into the endoplasmic reticulum, APP follows the constitutive secretory pathway to the cell surface. En route, APP matures in the Golgi and moves via secretory vesicles to the cell surface, where the main α -secretase activity resides (Sisodia 1992). Although it is well accepted that the non-amyloidogenic pathway is initiated at the cell surface, studies in polarized Madin-Darby canine kidney (MDCK) cells also

suggest α -secretase activity in the trans-Golgi network (TGN) (Haass, Koo et al. 1995), the compartment, where the major fraction of APP is localized (Weidemann, König et al. 1989). APP that escapes α -secretase-mediated cleavage at the plasma membrane is internalized in a process dependent on the Y⁶⁸²ENTPY motif (numbering according to the APP695 isoform) in the cytoplasmic tail of APP (Lai, Sisodia et al. 1995). Following endocytosis, APP localizes to the endosomal network and is either recycled to the plasma membrane (Yamazaki, Koo et al. 1996), retrogradely transported to the TGN (Schmidt, Spörbert et al. 2007) or degraded in lysosomes (Haass, Koo et al. 1992). Of note, mutation of the Y⁶⁸²ENTPY motif decreases the internalization rate of APP and, in turn, blocks generation of A β suggesting the acidic endosomal compartment as the prominent site for A β generation (Perez, Soriano et al. 1999). As well as its substrate APP, secretases also follow a complex trafficking path in neurons. Following post-translational modification in the secretory pathway (Benjannet, Elagoz et al. 2001), BACE1 reaches the cell surface where it is enriched in lipid rafts (Riddell, Christie et al. 2001), a microdomain that favours amyloidogenic cleavage of APP (Ehehalt, Keller et al. 2003). A dileucine-motif and an adjacent phosphorylatable serine residue in the cytoplasmic tail of BACE1 regulates its internalization (Huse, Pijak et al. 2000; Pastorino, Ikin et al. 2002). This motif also represents the binding site for the Golgi-localized, γ -ear containing ADP ribosylation-binding factors (GGA) 1, 2 and 3 (He, Zhu et al. 2003), trafficking adaptors that regulate BACE1 recycling to the cell surface (He, Li et al. 2005) as well as its degradation (Tesco, Koh et al. 2007). As aspartyl protease, BACE1 is most active in an acidic environment (pH 4.5) (Vassar, Bennett et al. 1999) suggesting endosomes as the favoured organelle for amyloidogenic processing to proceed. Consequently, inhibition of lysosomal acidification results in enrichment of β -CTFs in endosomes (Haass, Koo et al. 1992). Interestingly, BACE1 activity is not restricted to endosomes and may to a minor extent also take place at the cell surface, probably due to aberrant trafficking of BACE1 (Prabhu, Burgos et al. 2012).

Much effort has been put into deciphering the localization of the active γ -secretase complex but the relative contribution of the subcellular compartments to A β generation remain elusive. Since γ -secretase has an acidic pH optimum (Pasternak, Bagshaw et al. 2003), and since APP processing by BACE1 precedes γ -secretase cleavage, A β generation is proposed to occur in the endosomal network or in lysosomes. However, the cell surface also represents a compartment that enables γ -secretase-mediated processing (Kaether, Haass et al. 2006).

Additionally, recent studies also suggest the TGN as a compartment for A β production (Burgos, Mardones et al. 2010; Choy, Cheng et al. 2012).

Taken together, most evidences point towards an amyloidogenic cleavage in endosomal compartments and a non-amyloidogenic processing at the cell surface.

Trafficking and processing of APP in neurons

Much emphasis has been put on elucidating APP trafficking and processing in neurons where APP cleavage and A β production has an important (patho)physiological impact. Transport vesicles deliver APP to neuronal axons and dendrites along microtubules (Koo, Sisodia et al. 1990), a process mediated by kinesin-1 and c-jun NH(2)-terminal kinase-interacting protein (JIP)-1 (Matsuda, Matsuda et al. 2003). Interestingly, JIP-1 predominantly interacts with APP phosphorylated at Thr⁶⁶⁸ (numbering according to the APP695 isoform) (Muresan and Muresan 2005). Furthermore, CTFs carrying this specific phosphorylation are increased in human AD brains (Lee, Kao et al. 2003) suggesting a link between APP phosphorylation, APP trafficking and AD progression.

Indeed, phosphorylated APP undergoes a conformational change that interferes with its interaction with Fe65, a cytosolic adaptor, involved in APP trafficking and processing (Ando, Iijima et al. 2001). Furthermore, the noxious role of the Thr⁶⁶⁸ phosphorylation is strengthened by the fact that ablation of phosphorylation by either application of a kinase inhibitor or by mutating Thr⁶⁶⁸ to alanine, reduces the production of A β (Lee, Kao et al. 2003) and prevents memory and synaptic plasticity deficits in a mouse model of AD (Lombino, Biundo et al. 2013).

1.1.5. Interaction partners of APP

Since neuronal transport of APP does not strictly depend on JIP-1 (Kins, Lauther et al. 2006), the activity of interacting factors for APP sorting in neurons has been proposed. In support of this hypothesis, a number of proteins have been shown to affect APP processing by altering localization of the amyloid precursor protein.

Foremost, various proteins interacting with the cytoplasmic tail of APP have been identified. Overexpression of such interacting proteins, including Fe65, X11 α or X11 β inhibits A β production and decreases plaque burden in mouse models (Lee, Lau et al. 2003; Lee, Lau et al. 2004; Santiard-Baron, Langui et al. 2005).

Another APP interacting factor is the Reticulon family protein-binding Nogo-66 receptor that interacts with the ectodomain of APP. Genetic disruption of Nogo-66 in mice results in elevated A β levels and an increased plaque burden in the brain (Park, Gimbel et al. 2006).

Finally, a number of endocytic receptors of the low-density lipoprotein (LDL) receptor gene family (LRPs) have been implicated in APP transport and processing. For example, LRP1 interacts with APP at the cell surface, an interaction that involves Fe65 linking the intracellular domains of both proteins (Pietrzik, Yoon et al. 2004). Because of the high endocytic activity of LRP1, interaction with this receptor promotes internalization of APP, resulting in increased generation of A β in the endocytic compartment of cells in culture (Cam, Zerbinatti et al. 2005) and in a mouse model *in vivo* (Zerbinatti, Wozniak et al. 2004). Fe65 also bridges APP with LRP1B, a protein sharing high sequence similarity with LRP1. However, the interaction with LRP1B reduces amyloidogenic processing due to the lower internalization rate of LRP1B compared to LRP1 (Cam, Zerbinatti et al. 2004).

Overexpression of the apolipoprotein E receptor 2 (APOER2), another member of the LDL receptor gene family, counteracts LRP1-mediated endocytosis and shifts APP into lipid rafts, thereby promoting amyloidogenic processing resulting in increased A β levels (Fuentelba, Barria et al. 2007). Adding F-spondin, an extracellular APOER2 ligand that links the extracellular domains of APOER2 and APP, decreases A β generation presumably due to the slower internalization rate of APOER2 as compared to APP (Hoe, Wessner et al. 2005).

1.2. THE SORTING RECEPTOR SORLA

1.2.1. Genetic evidences for the implication of SORLA in Alzheimer's disease

Much is known about receptors that regulate the endocytosis of APP and thereby influence amyloidogenic processing. However, proteins regulating the intracellular sorting of APP to and from compartments, where APP breakdown occurs, remained dubious. Hints towards novel interaction partners possibly involved in intracellular sorting of APP came in 2004 when gene expression profiling studies identified the sortilin-related receptor with LDLR class A repeats (SORLA) as being downregulated in the brain of AD patients (Scherzer, Offe et al. 2004). Subsequently, analysis of post-mortem brain tissue of AD patients by western blot confirmed a reduction of SORLA protein levels (Andersen, Reiche et al. 2005).

In parallel, the identification of several LOAD-associated single nucleotide polymorphisms (SNPs) in *Sorll* (the gene encoding SORLA) confirmed SORLA as a risk factor for AD at the genetic level (Rogaeva, Meng et al. 2007). One particular two-SNP haplotype in *Sorll* was shown to result in a decreased SORLA expression suggesting genetically determined low SORLA levels as a risk factor for LOAD (Caglayan, Bauerfeind et al. 2012). Recently, mutations in *SORLI* have even been shown to cause familial EOAD (Pottier, Hannequin et al. 2012).

1.2.2. Expression and physiological function of the VPS10p-domain receptor SORLA

Structure and function of VPS10p receptor family members

SORLA is a member of the VPS10p domain receptor family. A characteristic feature of all family members is a VPS10p domain in the extracellular moiety, first described in the vacuolar sorting 10 protein, a sorting receptor in yeast that directs lysosomal hydrolases from the TGN to the vacuole (Marcusson, Horazdovsky et al. 1994).

Apart from SORLA, the VPS10p domain receptor family comprises four additional family members in mammals termed sortilin, and the sortilin-related VPS10 domain-containing

receptors (SORCS) 1, SORCS2, and SORCS3. The best studied VPS10p-domain receptor is sortilin, which is implicated in neurotrophic signaling during acute and chronic insults to the brain, in frontotemporal dementia, and in AD (Jansen, Giehl et al. 2007; Hu, Padukkavidana et al. 2010; Carlo, Gustafsen et al. 2013). Additionally, sortilin was identified as a genetic risk factor for myocardial infarction (Kjølby, Andersen et al. 2010). SORCS1, SORCS2, and SORCS3 are mainly expressed in the brain and play a role in the progression of AD (Lane, Raines et al. 2010), in type 2 diabetes (Clee, Yandell et al. 2006), and in axonal growth control, respectively (Deinhardt, Kim et al. 2011).

Domain organization of SORLA

SORLA is a 250 kDa type-I transmembrane receptor that combines several structural elements found in either the LDL receptor (LDLR) family or the VPS10p-domain receptor family.

In detail, SORLA has seven distinct domains (Fig. 4). The N-terminal VPS10p domain is implicated in ligand binding (Jacobsen, Madsen et al. 2001). It is followed by five epidermal growth factor (EGF) precursor-type repeats and 11 tandemly arranged cysteine-rich repeats that resemble those in the LDLR ligand binding domain (Yamazaki, Bujo et al. 1996). These structural elements are followed by six fibronectin-type III repeats that are also found in cell-adhesion molecules (Patthy 1990). The intracellular part of SORLA is preceded by a transmembrane domain that contains 25 residues. The cytoplasmic tail carries various amino acid motifs implicated in intracellular trafficking of SORLA (discussed below).

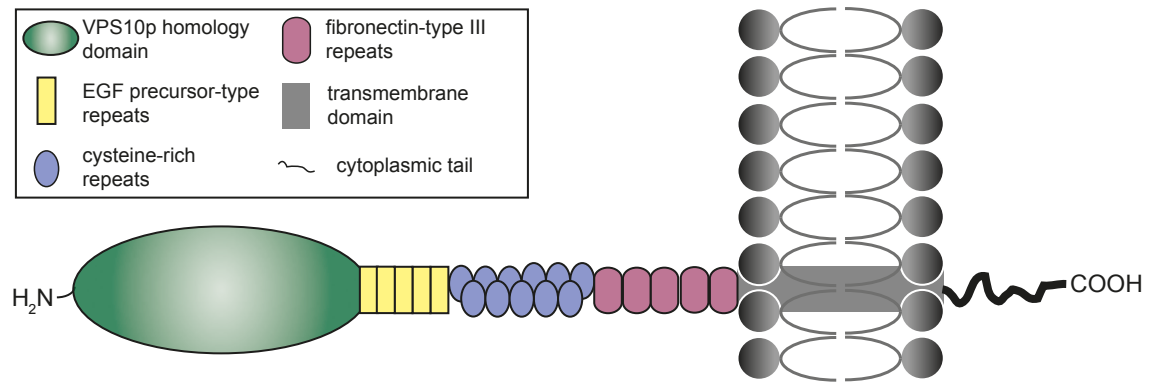


Figure 4: Domain organization of SORLA.

SORLA is a multidomain receptor that contains structural elements found in proteins of the LDL- and VPS10p-receptor families. A VPS10p homology domain locates at the N-terminus and is crucial for the binding of neurotensin (Jacobsen, Madsen et al. 2001). Five EGF precursor-type repeats situate between the VPS10p homology domain and a cluster of eleven cysteine-rich repeats that mediate binding of ligands like the lipoprotein lipase and APOE (Jacobsen, Madsen et al. 2001). Adjacent to the cysteine repeats locate six fibronectin-type III domains that complete the extracellular part of the receptor. A hydrophobic membrane-spanning domain anchors SORLA in the plasma membrane. The cytoplasmic tail contains various binding motifs for cytosolic proteins that regulate the intracellular trafficking of the receptor.

Tissue distribution of SORLA in mammals

SORLA is expressed in various mammalian tissues including brain, testis, lung, kidney, heart, smooth muscle cells and skeletal muscle (Jacobsen, Madsen et al. 1996; Morwald, Yamazaki et al. 1997). SORLA in the brain is especially abundant in neurons of the hippocampus, the cerebral cortex, the cerebellum, and, to a lower extent, in the thalamus, hypothalamus, and in the retina (Kanaki, Bujo et al. 1998; Motoi, Aizawa et al. 1999). In neurons, SORLA mainly localizes to the neuronal cell body (Posse De Chaves, Vance et al. 2000). The *Sorl1*-mRNA has not been detected in glia cells suggesting SORLA expression to be restricted to neurons (Hermans-Borgmeyer, Hampe et al. 1998).

Physiological functions of SORLA

High SORLA expression levels during embryogenesis suggested a role for this receptor in developmental processes (Hermans-Borgmeyer, Hampe et al. 1998). However, *Sorl1* deficient animals proved viable and fertile and showed no obvious developmental defects (Andersen, Reiche et al. 2005).

In cultured cells, SORLA binds APOE and neurotensin, proteins that are important for the cellular uptake of lipoprotein particles or implicated in modulating of the dopaminergic system, respectively (Jacobsen, Madsen et al. 2001). However, the physiological relevance of their interaction with SORLA is unknown to date.

In the brain, SORLA influences neurotrophic activity by regulating glia cell-line derived neurotrophic factor (GDNF) secretion and clearance (Geng, Xu et al. 2011; Glerup, Lume et al. 2013) and may, due to the receptor's role in lipoprotein lipase trafficking, indirectly affect synaptic remodeling (Blain, Paradis et al. 2004; Klinger, Glerup et al. 2011).

Furthermore, SORLA increases the migration of smooth muscle cells by immobilizing the urokinase-type plasminogen receptor at the cell surface, thereby facilitating an increased degradation of extracellular matrix components (Zhu, Bujo et al. 2004). Since enhanced cell migration represents an important determinant of arterial remodeling, SORLA levels are correlated with an expansion of carotid-intima media thickness, an established marker of atherosclerosis (Jiang, Bujo et al. 2008).

Although functions for SORLA in various physiological processes have been ascribed based on circumstantial evidence, by far the most studies support a role for SORLA in APP processing in AD (Willnow, Petersen et al. 2008). This function is based on the ability of SORLA to sort APP between various intracellular compartments thereby controlling its processing fate. In the following, the intricate trafficking path of SORLA is discussed - how it is controlled by the interaction with distinct cytosolic adaptors and how it ultimately controls APP processing fates and determines risk of AD.

1.2.3. Intracellular trafficking of SORLA

Central to the role of SORLA in APP processing is its unique trafficking behavior in cells. Upon synthesis, the 2215 amino acid polypeptide chain of SORLA is core-glycosylated in the endoplasmic reticulum followed by complex oligosaccharide modifications in the Golgi (Fiete, Mi et al. 2007). During transit of the biosynthetic pathway, the receptor's propeptide supports proper folding of the VPS10p domain and prevents premature ligand binding. In the late Golgi compartment, the protease furin removes the propeptide, activating the receptor's ligand binding ability (Jacobsen, Madsen et al. 2001).

The majority of SORLA molecules at any given time are found in Golgi compartments (Jacobsen, Madsen et al. 2001) (Fig. 5), while only a minor portion of SORLA (10 %)

trafficks to the cell surface. Shedding by ADAM17 at the plasma membrane liberates the ectodomain of SORLA (Hermeijer, Sjøgaard et al. 2006). The remaining membranous stub is further subjected to γ -secretase cleavage followed by translocation of the intracellular domain to the nucleus with yet unknown consequences (Bohm, Seibel et al. 2006).

SORLA that is not processed at the plasma membrane undergoes endocytosis and is re-routed to the TGN (Nielsen, Gustafsen et al. 2007). Alternatively, SORLA escapes the tubular endosomal network via recycling endosomes and moves back to the cell surface (Schmidt, Sporbert et al. 2007).

The predominant localization and rerouting of SORLA to the TGN supports a role for this receptor in sorting of target proteins to and from this organelle, a central hub to distribute proteins between endocytic and secretory compartments. To fulfill such a proposed role as trafficking receptor, the intracellular transport of SORLA must be tightly regulated. Several studies revealed amino acid motifs in the receptor's cytoplasmic tail that are necessary for the specific interaction with adaptors controlling the subcellular trafficking fate of SORLA (Fig. 5B).

Whereas the internalization of SORLA is mediated by the adaptor protein (AP) 2, the intracellular transport is regulated by several proteins (Nielsen, Gustafsen et al. 2007). Retrograde transport from the endosomal network to the TGN involves interaction of SORLA with sorting adaptors phosphofurin acidic cluster sorting protein (PACS) 1 and the retromer complex, whereas GGA1 is supposed to anterogradely transport SORLA from the TGN to the endosomal compartment (Schmidt, Sporbert et al. 2007; Fjorback, Seaman et al. 2012; Herskowitz, Offe et al. 2012).

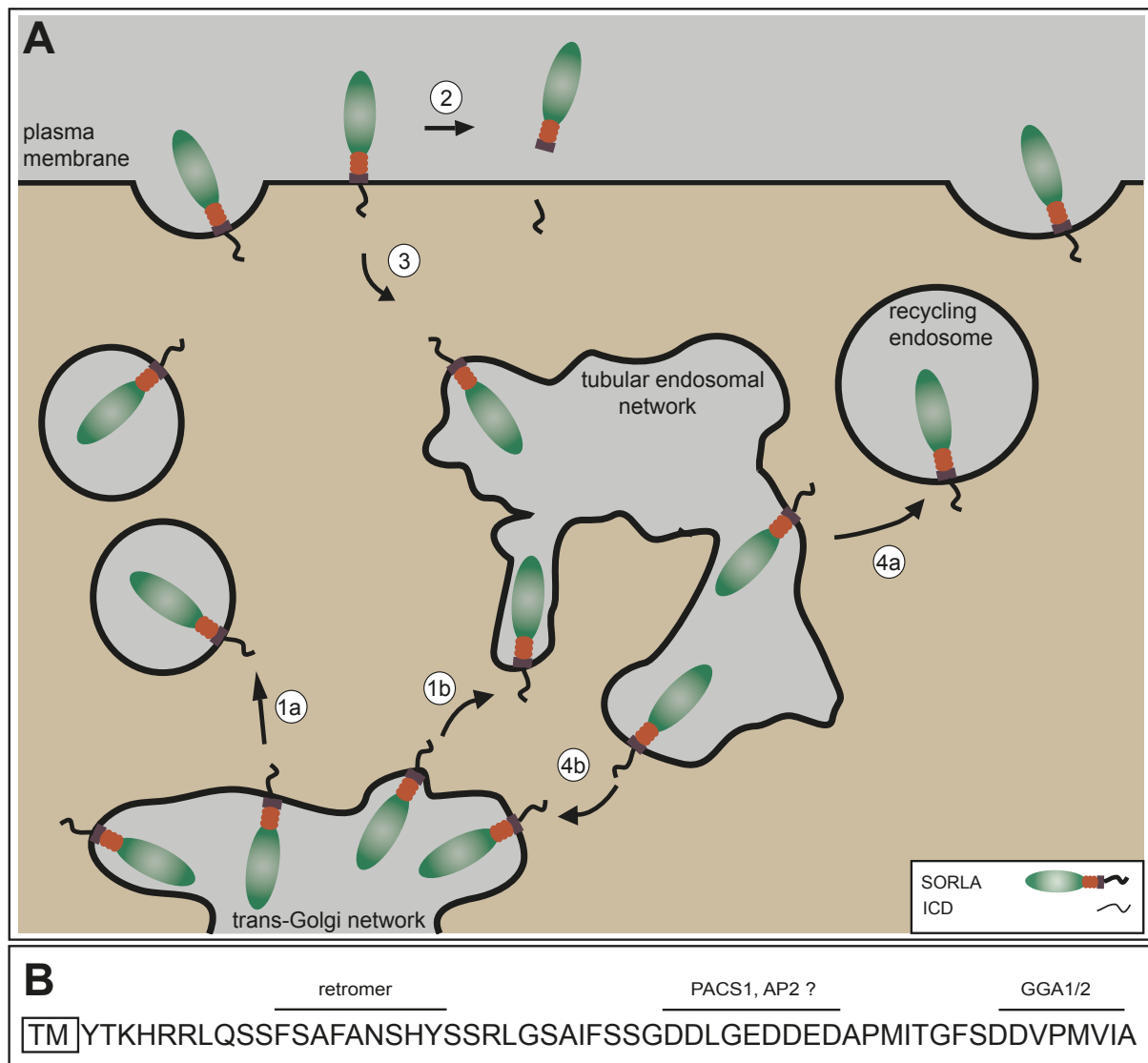


Figure 5: Intracellular trafficking of SORLA is dependent on trafficking adaptor binding motifs in the cytoplasmic tail.

(A) SORLA is posttranslationally modified in the Golgi and exits the trans-Golgi network (TGN) either to the plasma membrane (via secretory vesicles) (1a) or to the early endosomal compartments (1b). At the cell membrane, SORLA may be subjected to shedding of its ectodomain (2). Alternatively, SORLA may be internalized (3) and sorted to endosomal compartments from where it either recycles back to the plasma membrane (4a) or reroutes to the TGN (4b).

(B) The human SORLA cytoplasmic tail harbours various trafficking adaptor binding sites. A stretch enriched in aromatic amino acids binds VPS35 and VPS26, components of the retromer complex (Fjorback, Seaman et al. 2012). A cluster composed of acidic amino acids serves as binding site for PACS1 (and potentially the μ -subunit of AP2). Finally, a DXXLL-like motif at the C-terminus mediates interaction with GGA1 and 2. ICD, intracellular tail of SORLA.

Proteins regulating intracellular SORLA trafficking

The phosphofurin acidic cluster sorting protein (PACS) 1

In 1998, PACS1 was identified as a mediator of clathrin-dependent TGN retrieval of the membrane proteins furin and CI-MPR (Wan, Molloy et al. 1998). Follow up studies revealed SORLA, VAMP4, TRPP2, HIV-nef and several other viral proteins as additional binding partners that depend on PACS1-regulated intracellular sorting (Youker, Shinde et al. 2009).

PACS1 can be detected in various tissues including the brain, where it is highly expressed in neurons. Target proteins interact with PACS1 via a cluster of acidic amino acids in their cytoplasmic moieties (Fig. 6A). PACS1, in turn, binds its cargo via the furin(cargo)-binding region (FBR) (Fig. 6B) (Crump, Xiang et al. 2001). Binding depends on the phosphorylation state of a serine residue embedded in an acidic cluster located in the middle region of PACS1 as alanine substitution of this serine residue yields a dominant-negative PACS1 protein (Scott, Gu et al. 2003). Upon binding, the FBR domain of PACS1 links the cargo to the clathrin machinery components AP1 and AP3.

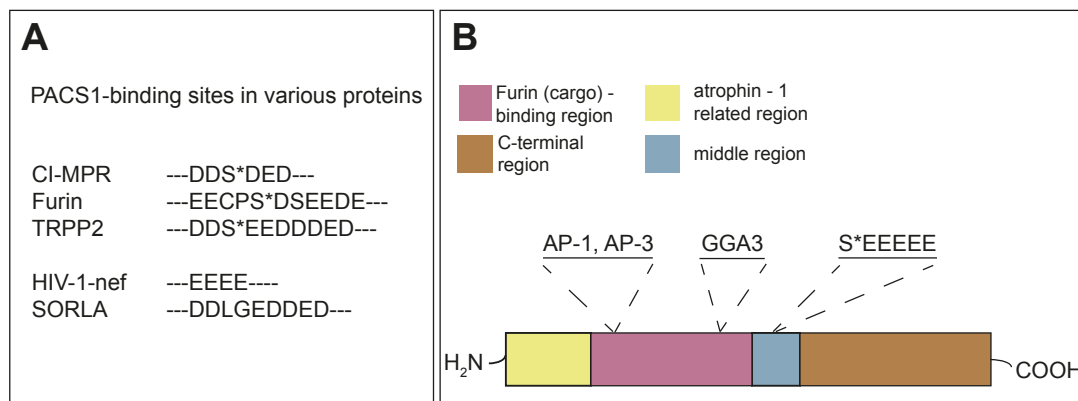


Figure 6: Domain organization and cargo binding motifs of PACS1.

(A) PACS1 is implicated in subcellular trafficking of various proteins. The recognition by PACS1 depends on a cluster of acidic amino acids in the cytoplasmic tail of cargo proteins. Additionally, the phosphostatus of a serine residue (S*) embedded in the binding motif may modulate the binding affinity and transport by PACS1. For example, a phosphorylatable serine in the PACS1 binding site can be found in CI-MPR, furin and TRPP2 but is absent in HIV-nef and SORLA.

(B) PACS1 comprises five domains but not much is known about the function of the very C- and very N-terminal domains. The furin-binding domain (FBR) is important for various functions of the protein. It is crucial for cargo recognition and facilitates the interaction with protein adaptor proteins AP1 and AP3 that link the cargo to the clathrin machinery which, in turn, initiates vesicle trafficking. Furthermore, the furin-binding domain harbours a binding site for GGA3 – a protein involved in a complex, PACS1-dependent trafficking of cargo proteins between the TGN and endosomes. (*Figure legend continues.*)

(*Figure legend continued.*) The middle region (MR) contains a stretch of acidic amino acids that bind to the cargo recognition motif in the FBR domain, thereby blocking cargo binding of PACS1 (S*EEEE) (Scott, Gu et al. 2003). This binding depends on the phosphorylation of a serine residue (S*) embedded in the MR. Phosphorylation loosens binding to the FBR and enables cargo binding.

The role of PACS1 in protein trafficking has mainly been elucidated through studies of furin and CI-MPR. CI-MPR sorting between the TGN and endosomes is regulated by a concerted action of PACS1 and GGA3 in combination with a casein kinase (CK) 2-controlled phosphorylation cascade. In this process, GGA3 mediates TGN export whereas PACS1 directs endosome-to-TGN rerouting of the CI-MPR (Scott, Fei et al. 2006). In contrast, PACS1 recycles endocytosed furin back to the plasma membrane following phosphorylation of a serine residue in furin's acidic cluster (Fig. 6A). However, retrieval to the TGN depends on a dephosphorylated acidic cluster (Wan, Molloy et al. 1998).

In contrast to furin, the acidic cluster in the cytoplasmic tail of SORLA is not interrupted by a phosphorylatable serine residue (Fig. 6A). PACS1 binds to SORLA and mutation of the acidic amino acids in the cytoplasmic tail (DDLGEDDED → AALGAAAA) abolishes the PACS1-SORLA interaction. This mutation, in turn, shifts the receptor away from the TGN, suggesting a role of PACS1 in the TGN retrieval of SORLA (Schmidt, Sporbart et al. 2007).

The retromer complex

Retromer was first described in yeast as a mediator for endosome-to-Golgi retrieval of VPS10p, a receptor for the carboxypeptidase Y (Seaman, Marcusson et al. 1997). Consisting of highly conserved subunits, the retromer complex regulates protein trafficking in various organisms including mammals, *Caenorhabditis elegans*, *Drosophila melanogaster*, and *Arabidopsis thaliana* (Bonifacino and Hurley 2008).

In mammalian cells, retromer is a heteropentameric protein complex composed of a cargo-recognition trimer (VPS26, VPS29 and VPS35) and a SNX dimer (SNX1 or SNX2 with SNX5 or SNX6).

Upon interaction with the accessory proteins Rab7a and SNX3, the cargo recognition trimer localizes to endosomes and binds aromatic motifs in the cytoplasmic tail of target proteins (Rojas, van Vlijmen et al. 2008; Vardarajan, Bruesegem et al. 2012).

SNX proteins contain a phosphatidylinositol-3-phosphate-binding phox-homology domain and thereby facilitate the recruitment of the retromer SNX dimer at endosomes,

organelles highly enriched in phosphatidylinositol-3-phosphate (Cozier, Carlton et al. 2002). Following binding to the endosomal membrane, the Bin, amphiphysin and Rvs (BAR) domain in SNX proteins enables - upon dimerization - sensing and induction of membrane curvature, provoking a vesicle-to-tubule transition, a characteristic hallmark of endosomal substructures (Peter, Kent et al. 2004) (Carlton, Bujny et al. 2004). So far, it is not known how the tubule inducing SNX dimer and the cargo recognition trimer interact. But, SNX5 or SNX6 facilitate cargo linkage to the dynein complex enabling trafficking along microtubules to the Golgi (Fig. 7) (Hong, Yang et al. 2009; Wassmer, Attar et al. 2009).

An aromatic motif in the cytoplasmic tail of SORLA (Fig. 5B) was shown to be crucial for the interaction with VPS26 and VPS35 (Fjorback, Seaman et al. 2012). Knockdown of the retromer components VPS35 or SNX1 in HepG2 cells decreased SORLA levels, presumably due to a defect in TGN-retrieval and a subsequent degradation of the receptor in lysosomes (Nielsen, Gustafsen et al. 2007). Abolishing the interaction between retromer and SORLA by knockdown of VPS26 or by mutating the recognition motif in the tail of the receptor shifted SORLA away from the TGN pinpointing the importance of the retromer complex for the trafficking of the receptor (Fjorback, Seaman et al. 2012).

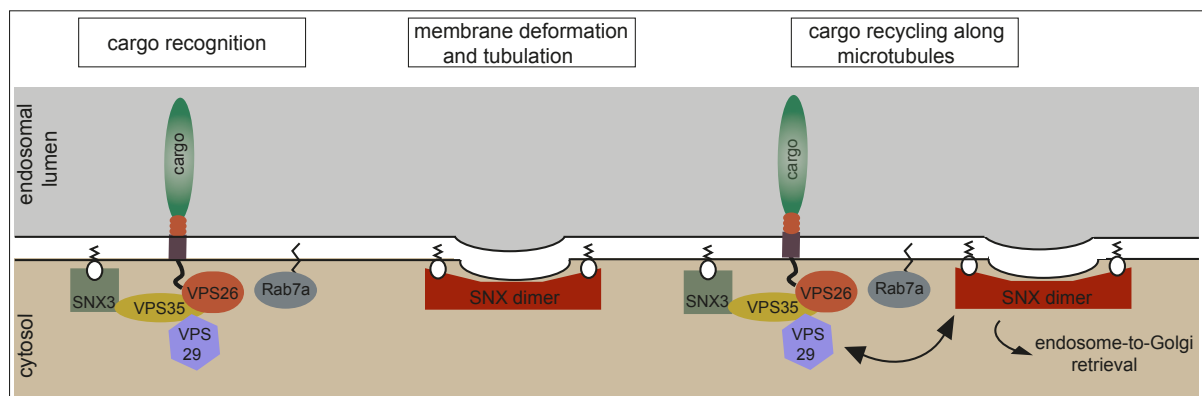


Figure 7: Regulation of endosome-to-TGN retrieval by the retromer complex.

The retromer complex contains five proteins (VPS26, VPS29, VPS35, SNX1/SNX2 and SNX5/SNX6) that are crucial for cargo recognition and membrane tubulation. A trimer (VPS26, VPS29, VPS35) is important for the binding of the respective cargo. Since these proteins lack the ability to interact with the endosomal membrane, two proteins that contain a lipid moiety (Rab7a) or bind to phosphatidylinositol-3-phosphate (SNX3) are thought to facilitate the recruitment of the cargo recognition complex. In detail, SNX3 associates with VPS35 whereas the interaction partner for Rab7a in the retromer complex is still elusive (Vardarajan, Bruesegem et al. 2012). A dimer composed of SNX1 or SNX2 and SNX5 or SNX6 completes the retromer complex. The SNX proteins interact with the endosomal membrane by binding to phosphatidylinositol-3-phosphate. Additionally, they contain a Bin, amphiphysin and Rvs domain that induces curvature of the membrane ultimately resulting in a tubulation process.

Finally, it is suggested that the cargo recognition complex is captured in the tubules and subjected to retrograde transport along microtubules. However, the molecular details, especially the regulation of cargo capture, are still unknown.

The GGA proteins

Discovered in 2000, GGA1, GGA2 and GGA3 represent a family of monomeric adaptors, implicated in intracellular protein trafficking (Boman, Zhang et al. 2000). Whereas GGA1 and 2 are responsible for the sorting of cargo from the TGN to endosomes, GGA3 plays a role in lysosome targeting of ubiquitinated membrane proteins (Puertollano, Aguilar et al. 2001; Zhu, Doray et al. 2001; Puertollano and Bonifacino 2004).

GGA1 binds to an acidic cluster dileucine (DXXLL) motif in the cytoplasmic tail of various proteins (Fig. 8A). This binding is facilitated by the Vps27, Hrs, Stam (VHS) domain, one of three domains that comprise the protein (Takatsu, Katoh et al. 2001) (Fig. 8B). Localization of GGA1 to the TGN is accomplished by the GGA and TOM (GAT) domain facilitating binding to Arf-GTP, a protein enriched in membranes of the TGN (Takatsu, Yoshino et al. 2002). A hinge region connecting the GAT domain and the γ -adaptin ear (GAE) domain, serves as a linker to the clathrin machinery enabling proper vesicle transport (Puertollano, Randazzo et al. 2001). Finally, the GAE domain contains binding sites for various accessory proteins that are implicated in formation, budding, trafficking and targeting of the vesicle (Bonifacino 2004).

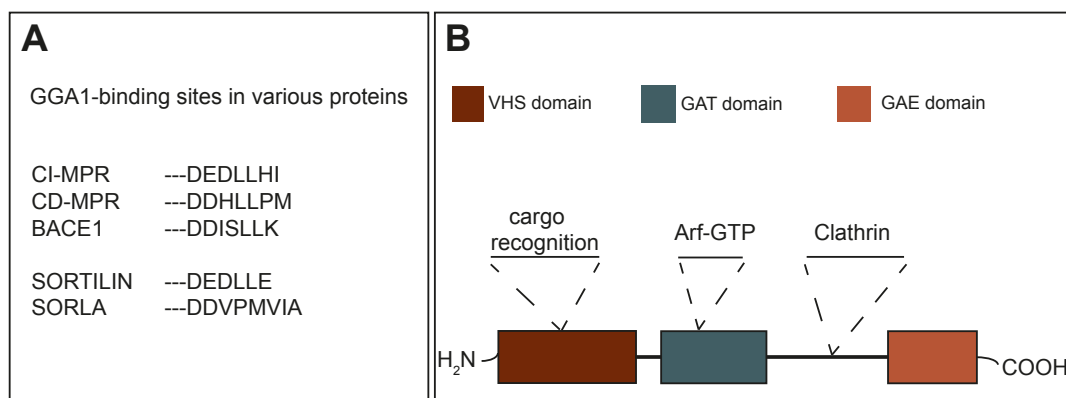


Figure 8: Domain organization and cargo binding motifs of GGA1.

(A) GGA1 facilitates the anterograde sorting of receptors from the TGN to the endosomal compartment. The prerequisite for GGA1-dependent sorting is a „DXXLL“-like motif in the cytoplasmic tail of the cargo. This motif can be found in various receptors like CI- and CD-MPR, BACE1, sortilin and SORLA.

(B) GGA1 and GGA2 regulate anterograde transport from the TGN to endosomes. Structurally, they can be subdivided in three domains. Interaction with the TGN depends on an amino acid stretch in the GAT domain that is crucial for the binding of Arf-GTP, a protein enriched in membranes of the TGN. The VHS domain comprises an amino acid motif that facilitates recognition and binding of the cargo. Finally, the hinge region that is situated between GAE and GAT domain links the GGA-cargo complex to the clathrin machinery.

The cytoplasmic tail of SORLA harbours a DXXLL-like motif that was shown to be important for the interaction with GGA1 and GGA2 (Jacobsen, Madsen et al. 2002) (Fig. 8A). Mutation of this motif abolished binding of GGA and lead to a decreased anterograde TGN-endosome shuttling of the receptor (Schmidt, Sporbert et al. 2007). Additionally, knock-down of GGA1 in HEK293 cells negatively affected SORLA stability, highlighting GGA1 as an important regulator of SORLA trafficking (Herskowitz, Offe et al. 2012).

Implication of trafficking adaptor proteins in Alzheimer's disease

Since intracellular localization of APP affects amyloidogenic and non-amyloidogenic processing, various trafficking-related proteins were implicated in AD.

In 2009, a genome-wide association study identified the phosphatidylinositol-binding clathrin-assembly protein, a protein involved in clathrin-mediated endocytosis, as a risk factor for AD (Harold, Abraham et al. 2009).

Also, disrupting the interaction of APP and the sorting adaptor protein 4 reduces the pool of APP molecules in endosomes and decreases A β generation (Burgos, Mardones et al. 2010).

The implication of GGAs in AD is based on their impact on BACE1 trafficking. siRNA mediated silencing or overexpression of GGA1 resulted in increased or decreased A β and CTF levels, respectively (Wahle, Thal et al. 2006), presumably due to a shift in the cellular localization of BACE1. Furthermore, GGA3 haploinsufficiency lead to elevated A β production as a consequence of increased BACE1 levels (Walker, Kang et al. 2012).

Two accessory proteins of the retromer complex, SNX3 and Rab7a, are also genetically linked to LOAD suggesting a role of the retromer complex in APP trafficking (Vardarajan, Bruesegem et al. 2012). In support of this hypothesis, knockdown of the retromer component VPS35 in primary hippocampal neurons shifts APP into early endosomes where amyloidogenic processing occurs, thereby explaining the increase in A β levels in the supernatant as well as in the brain of heterozygous *VPS26* null mice suffering from decreased VPS26 and VPS35 protein expression (Muhammad, Flores et al. 2008; Bhalla, Vetanovetz et al. 2012). However, direct interaction between APP and the retromer complex could not be shown, suggesting another protein (such as SORLA) that may link retromer and APP.

1.2.4. The role of SORLA in Alzheimer's disease

SORLA interacts with APP and influences its subcellular localization

Both genetic and pathophysiological studies discussed above have linked low SORLA expression with an increased risk for LOAD. The underlying molecular mechanism was suggested by studies in cultured cells, documenting a direct interaction of SORLA with APP in a 1:1 stoichiometric complex (Andersen, Schmidt et al. 2006). Since SORLA mainly localizes to the TGN, co-expression of APP and SORLA in non-neuronal cell lines traps APP in the TGN and thereby prevents APP from reaching the cell surface and endosomal compartments where processing occurs (Fig. 9)(Andersen, Reiche et al. 2005).

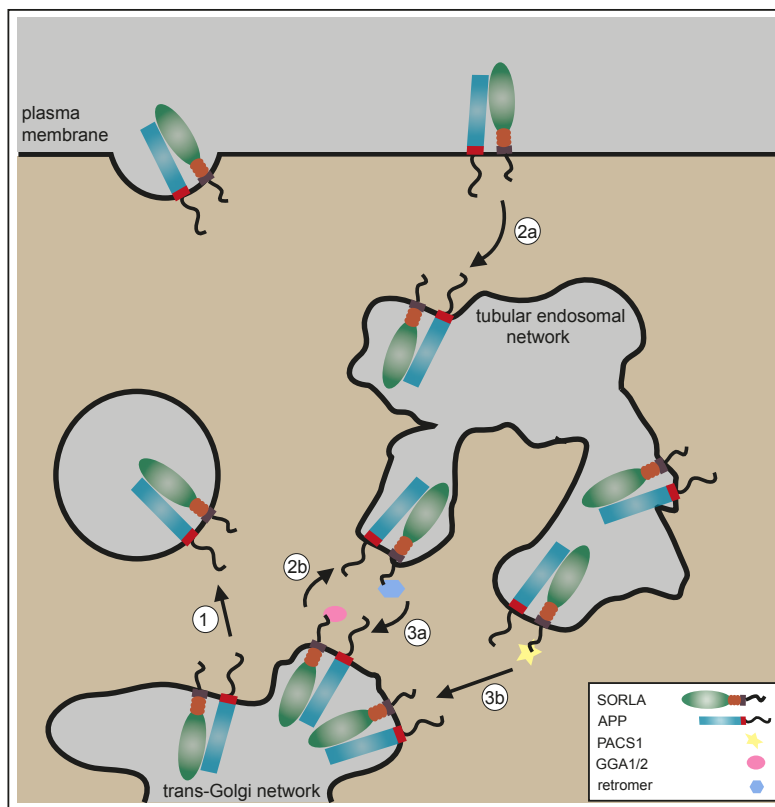


Figure 9: Model for the function of SORLA in trafficking and processing of APP.

SORLA interacts with APP in the trans-Golgi network (TGN) and blocks the release of APP to the cell surface (1) where non-amyloidogenic processing happens. Since only 10% of the total SORLA pool is present at the cell surface, only a small fraction of SORLA/APP reaches the plasma membrane, thereby protecting APP from non-amyloidogenic cleavage (Willnow, Petersen et al. 2008). SORLA/APP complexes enter the endosomal network either via endocytosis from the cell surface potentially via AP2-mediated clathrin-coated pits (2a) or via anterograde transport from the TGN, presumably involving an interaction of SORLA with GGA1/2 (2b). Since amyloidogenic processing is supposed to happen in endosomes, SORLA protects APP from cleavage by β - and γ -secretase via rerouting of the receptor to the trans-Golgi network (TGN). TGN retrieval of SORLA/APP complexes involves interaction of SORLA with the retromer complex (3a) and PACS1 (3b).

In further support of this model, increasing SORLA expression levels decrease APP processing and A β load in the brain (Rohe, Synowitz et al. 2009) and in chinese hamster ovary cells (Schmidt, Sporbert et al. 2007).

In the opposite scenario, SORLA deficiency in mice or knockdown of SORLA in cells lead to an increased processing of APP, ultimately resulting in increased A β levels and plaque deposition (Andersen, Reiche et al. 2005; Rogaeva, Meng et al. 2007; Rohe, Carlo et al. 2008).

Since SORLA harbours binding motifs for various cellular trafficking adaptors in the cytoplasmic tail, the hypothetical concept of SORLA being a trafficking receptor for APP was challenged by generating cell lines expressing various SORLA mutants, carrying disrupted adaptor binding sites.

In line with a role of the retromer complex in TGN-retrieval, mutation of the retromer binding site in SORLA shifted the receptor away from the TGN and resulted in an increased amyloidogenic and non-amyloidogenic processing of APP (Fjorback, Seaman et al. 2012).

A SORLA mutant lacking the cytoplasmic domain or carrying a mutation in the PACS1-binding site, shifted SORLA and APP to the plasma membrane and into endosomes, provoking an increased amyloidogenic and non-amyloidogenic processing of APP (Schmidt, Sporbert et al. 2007).

2. AIM OF THE STUDY

The intracellular trafficking of APP is of central importance to the processing fate of this precursor protein. Yet, the molecular mechanisms governing APP routing in neurons *in vivo* remain poorly understood. A key factor in APP sorting may be SORLA that binds APP in the TGN and controls the release of the precursor protein to the cell surface and to endocytic compartments where proteolytic processing occurs. This hypothesis is supported by studies in non-neuronal cell lines (such as CHO and HEK293) showing that mutations in the cytoplasmic tail of SORLA to disrupt sorting adaptor interaction, impacts SORLA localization and, consequently, A β peptide production.

Although studies in established non-neuronal cell lines support a role for adaptor-mediated sorting of SORLA in APP transport and processing, no *in vivo* evidence to support this model has been put forward so far. Thus, the aim of my thesis project was to further substantiate the relevance of sorting adaptor interaction for SORLA trafficking and APP processing in cultured neurons and in the brain *in vivo*. More specifically, I focused on the interaction of SORLA with the adaptor proteins PACS1 and with the retromer complex in neuroblastoma cell lines, in primary neurons, and in novel transgenic mouse models generated by myself.

3. RESULTS

3.1. IMPACT OF TRAFFICKING ADAPTOR BINDING-DEFECTIVE SORLA MUTANTS ON APP SORTING AND PROCESSING *IN VIVO*

3.1.1. Generation of novel mouse models expressing SORLA mutants defective in binding trafficking adaptors

The concerted action of various trafficking adaptor proteins regulate the subcellular localization of SORLA. Mutating adaptor binding sites in the cytoplasmic tail drastically influence the trafficking of the receptor (Nielsen, Gustafsen et al. 2007; Schmidt, Sporbert et al. 2007; Fjorback, Seaman et al. 2012; Herskowitz, Offe et al. 2012). However, functional *in vivo* studies regarding the intracellular routing of SORLA in the brain have been missing so far.

Therefore, I aimed to generate new mouse models expressing SORLA variants lacking binding sites for proteins that regulate SORLA routing. In detail, I focused on the interaction of SORLA with PACS1 and the retromer complex. As demonstrated in studies before, an alanine scan of trafficking adaptor-binding motifs disrupting the interaction of SORLA with PACS1 ($^{2191}\text{GDDLGEDDEDAP}^{2222} \rightarrow ^{2191}\text{GAALGAAAAAAP}^{2222}$) (Schmidt, Sporbert et al. 2007) or with the retromer complex ($^{2169}\text{SSFSAFAN}^{2176} \rightarrow ^{2169}\text{SSAAAAAN}^{2176}$) (Fjorback, Seaman et al. 2012) (Fig. 10) was performed to shed light on their contribution to the functionality of the receptor *in vivo*.



Figure 10: Binding motifs in the cytoplasmic tail of SORLA.

Amino acid sequence in the cytoplasmic domain of SORLA. Binding motifs for trafficking adaptor proteins retromer, PACS1 and GGA are shown above. The mutated amino acids in SORLA^{acidic} or SORLA^{FSAF} are depicted in bold. TM, transmembrane domain.

Targeting of the Sor11 locus

In a first approach, I intended to insert mutations of the binding site for PACS1 or the retromer complex into the endogenous *Sor11* locus using homologous recombination in embryonic stem cells (Fig. 11A). To that aim, a vector was generated carrying the respective mutations flanked by 8 kb of genomic DNA, essential to mediate targeting of the *Sor11* locus. Additionally, the vector contained a diphtheria toxin A expression (DTA) cassette adjacent to the homologous DNA stretch killing embryonic stem cells undergoing non-homologous integration of the vector sequence. Following electroporation of the targeting vector, the DNA of 600 selected embryonic stem cell clones was isolated and screened for a targeting event. Southern blotting of the isolated NsiI-digested DNA confirmed the presence of the wild-type allele but failed to detect a targeted allele (Fig. 11B).

To increase the propability of a homologous recombination event, stretches of homologous DNA in the vector were elongated, resulting in vectors carrying 9.2 kb or 13 kb of genomic DNA, respectively (Fig. 11C). Transfection of the targeting vectors followed by analysis of the DNA of 600 embryonic stem cell clones for each construct by southern blot failed in identifying any targeted clones (data not shown).

Taken together, in total 1800 embryonic stem cell clones from targetings with three different vectors were screened for homologous recombination. The radioactively labeled DNA probe used for the southern blot analysis hybridized with genomic DNA at the expected size for the wild-type allele (Fig. 11B). Therefore, problems with the detection method as the cause for failure in identifying a targeted allele seems unlikely. Rather, an inaccessibility due to a locked chromatin configuration of the endogenous *Sor11* locus at the targeted position may account for the lack of any homologous recombination event.

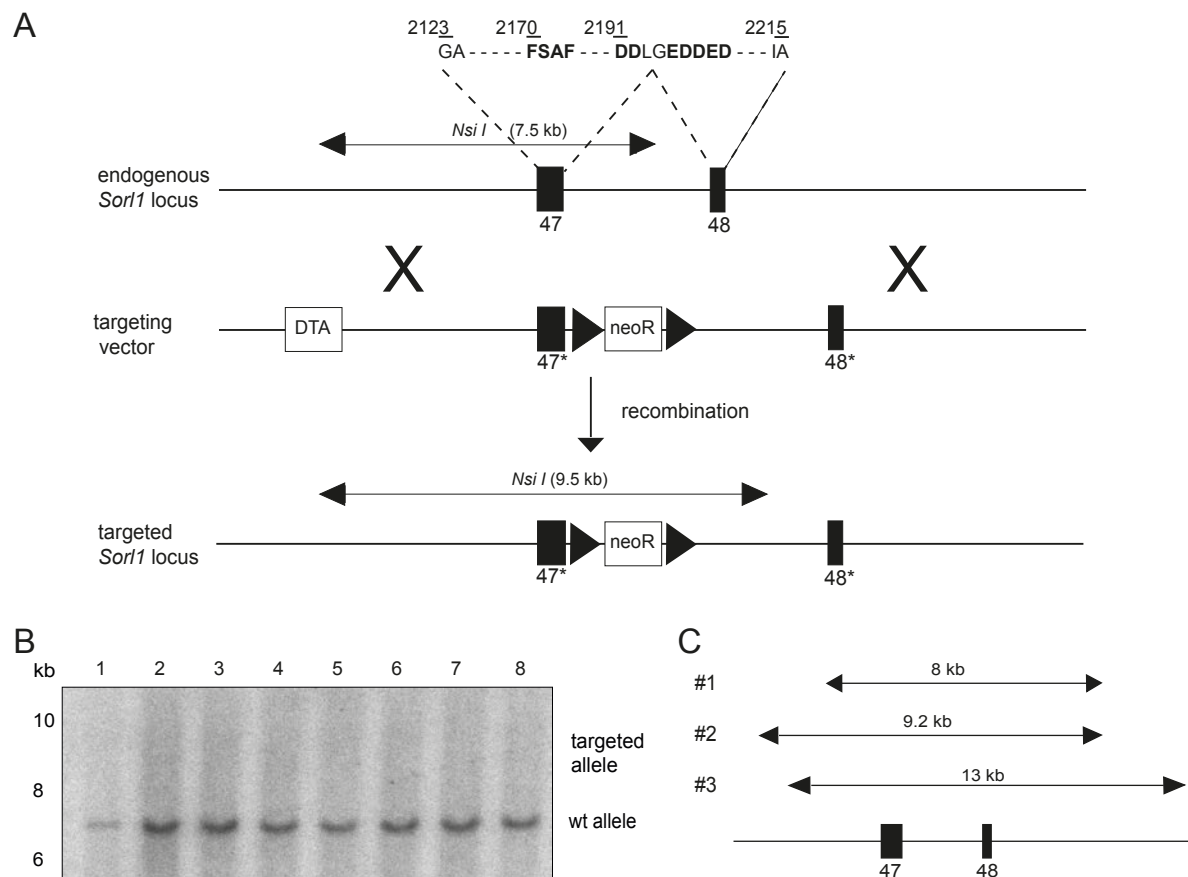


Figure 11: Targeting of the *Sorl1* locus.

(A) Targeting approach to knock-in mutations in exon 47 and 48 (black squares) of the *Sorl1* locus. Amino acids modified by site-directed mutagenesis are shown above and depicted in bold. Organization of the targeting vector and the wild-type *Sorl1* locus is indicated. A diphtheria toxin A expression cassette (DTA) and a neomycin-conferring resistance cassette (neoR) permit negative and positive selection of targeted embryonic stem cell clones. Black triangles represent loxP recombination sites. Arrows indicate the size of DNA fragments upon *Nsi* I digest.

(B) Genomic DNA of individual embryonic stem cell clones (1-8) from an embryonic stem cell targeting (with vector variant #1) were digested with *Nsi* I and analyzed by southern blot. A 7.5 kb DNA fragment is characteristic for a (non targeted) wild-type allele whereas a 9.5 kb DNA fragment would indicate a targeted allele and thereby homologous recombination.

(C) Different targeting vector variants (#1 - #3) carrying either 8 kb, 9.2 kb or 13 kb of homologous genomic DNA.

Targeting of the Rosa26 locus to knock-in cDNA expressing human SORLA trafficking adaptor binding-defective mutants

Since targeting of the endogenous *Sor11* locus could not be achieved, I decided to knock-in human SORLA cDNAs defective in binding PACS1 (acidic) or the retromer complex (FSAF) into the *Rosa26* locus using homologous recombination in embryonic stem cells.

The *Rosa26* locus was identified in a gene-trap study in 1991 (Friedrich and Soriano 1991). Although the function of *Rosa26* remains unknown, the locus is widely used for the insertion of cDNA by homologous recombination enabling *Rosa26* promoter-controlled cDNA expression in various tissues (Zambrowicz, Imamoto et al. 1997).

To target the *Rosa26* locus for homologous recombination, I used a vector that enables a cre-inducible expression of the human SORLA cDNA variants under control of the endogenous *Rosa26* promoter (referred to as SORLA^{acidic} and SORLA^{FSAF}) (Hohenstein, Slight et al. 2008). In detail, the vector carries a DTA cassette and a neomycin-conferring resistance cassette (neoR) to select targeted embryonic stem cell clones. Since neoR blocks transcription of the SORLA cDNA, expression of SORLA^{acidic} or SORLA^{FSAF} is only facilitated upon cre-mediated removal of neoR (Fig. 12A). A transcriptional stop is facilitated by a polyadenylation signal (polyA). Previously, a mouse model expressing the wild-type human SORLA cDNA (referred to as SORLA^{wt}) was generated in the same way and serves as a control strain (Fuyu Lin, Aarhus University, Denmark).

Homologous recombination at the *Rosa26* locus is preferred over a pronuclear injection, which results in random integration of the cDNA into the genome potentially leading to unpredictable expression profiles and variable copy numbers. In contrast, targeting the *Rosa26* locus theoretically leads to equal transgene expression levels and therefore enables the comparison between mouse lines or, more specifically, between different SORLA variants.

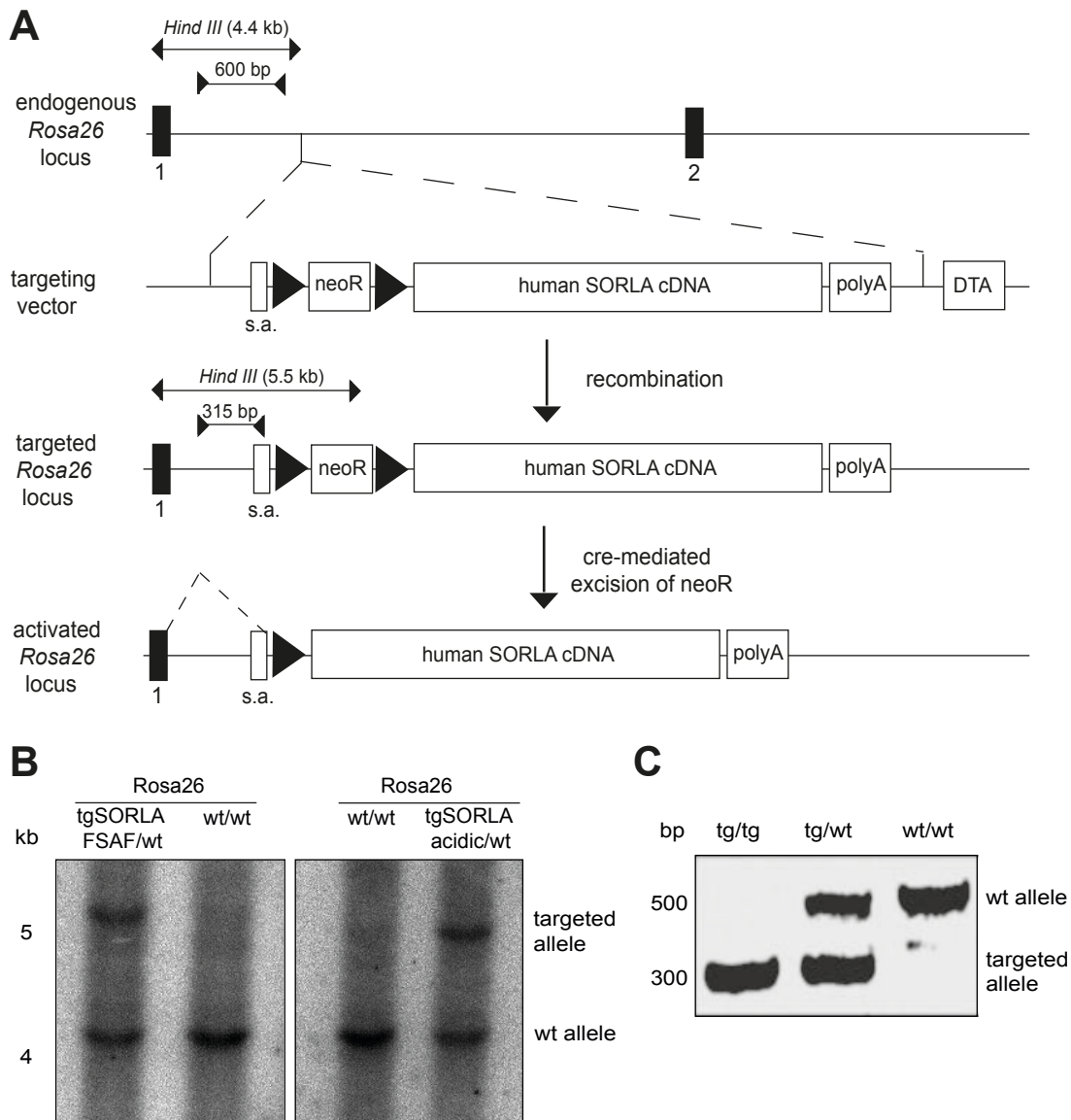


Figure 12: Generation of transgenic mice expressing human SORLA mutants.

(A) Targeting strategy describing homologous recombination at the *Rosa26* locus for the expression of human cDNA that encodes SORLA receptor variants lacking the binding site for PACS1 (SORLA^{acidic}) or the retromer complex (SORLA^{FSAF}).

The cDNA is inserted upon homologous recombination in embryonic stem cells between exons 1 and 2 of the *Rosa26* locus (black squares). A diptheria toxin A expression cassette (DTA) and a neomycin-conferring resistance cassette (neoR) allow for negative and positive selection of targeted embryonic stem cell clones, respectively. Upon cre recombinase-mediated excision of neoR, a splice acceptor site (s.a.) directs cDNA expression from the *Rosa26* promoter. A polyadenylation signal (polyA) serves as a transcriptional stop signal. Black triangles indicate loxP recombination sites. Arrows indicate DNA fragments resulting from genomic DNA digest by Hind III. Inverse arrows mark PCR products to discriminate targeted (tg) and non-targeted (wt) allele.

(B) Genomic DNA of embryonic stem cells of the indicated genotype was subjected to a Hind III digest and analysis by southern blotting. The 4.4 kb DNA fragment corresponds to the non-targeted allele. An additional 5.5 kb DNA fragment is indicative of the targeted allele confirming homologous recombination in embryonic stem cells of Rosa26^{tgSORLA^{acidic}} and Rosa26^{tgSORLA^{FSAF}}, respectively.

(C) PCR fragments indicate targeting of the endogenous *Rosa26* locus (wt/wt) on both alleles (tg/tg) or on one allele (wt/tg), respectively.

Expression controlled by the endogenous *Rosa26* promoter is supposed to be ubiquitous but rather low. To generate an alternative model with higher transgene expression, the targeting construct in Fig. 12A was modified by introducing a cytomegalovirus early enhancer element in combination with a chicken beta-actin promoter (CAG) upstream of the SORLA cDNA (Richard Mort, University of Edinburgh, Scotland) (Fig. 13A) (mice are named CAG-SORLA^{acidic} and CAG-SORLA^{FSAF}, respectively). In principle, this modification is supposed to also drive ubiquitous but stronger expression of the inserted SORLA cDNA variants compared to the *Rosa26* promoter. A mouse model expressing wild-type human SORLA cDNA (referred to as CAG-SORLA^{wt}) was generated in the same way (and kindly provided by Safak Caglayan, Max Delbrueck Centrum, Berlin).

Embryonic stem cells were electroporated with the different targeting vectors to allow for homologous recombination at the *Rosa26* locus (Figs. 12A and 13A). DNA of isolated embryonic stem cell clones was extracted, digested with Hind III, and screened for a targeting event using southern blot analysis. In non-targeted embryonic stem cells, a radioactively labeled DNA probe hybridizes with a DNA fragment in the size of 4.4 kb. Upon homologous recombination, embryonic stem cells reveal another fragment of 5.5 kb or 7.5 kb in size, respectively (Figs. 12B and 13B). Successfully targeted embryonic stem cells were injected into blastocysts by Drs. Ernst-Martin and Annette Fuechtbauer (Aarhus University, Denmark) to generate chimeras. Targeting in the obtained chimeric animals was confirmed by southern blot (as described above).

Germ line transmission was obtained for the above constructs from now on referred to as SORLA^{wt}, SORLA^{acidic} or SORLA^{FSAF} and CAG-SORLA^{wt}, CAG-SORLA^{acidic} or CAG-SORLA^{FSAF}, respectively.

Mice were bred with the cre deleter strain of mice (Schwenk, Baron et al. 1995), expressing cre-recombinase ubiquitously, thereby removing neoR and facilitating expression of human SORLA cDNA variants in all cells. To eliminate expression of endogenous murine SORLA, mice were crossed with animals carrying a targeted disruption of the endogenous SORLA gene locus (*Sorl1*^{-/-}) (Andersen, Reiche et al. 2005) and kept homozygous for the targeted *Rosa26* locus.

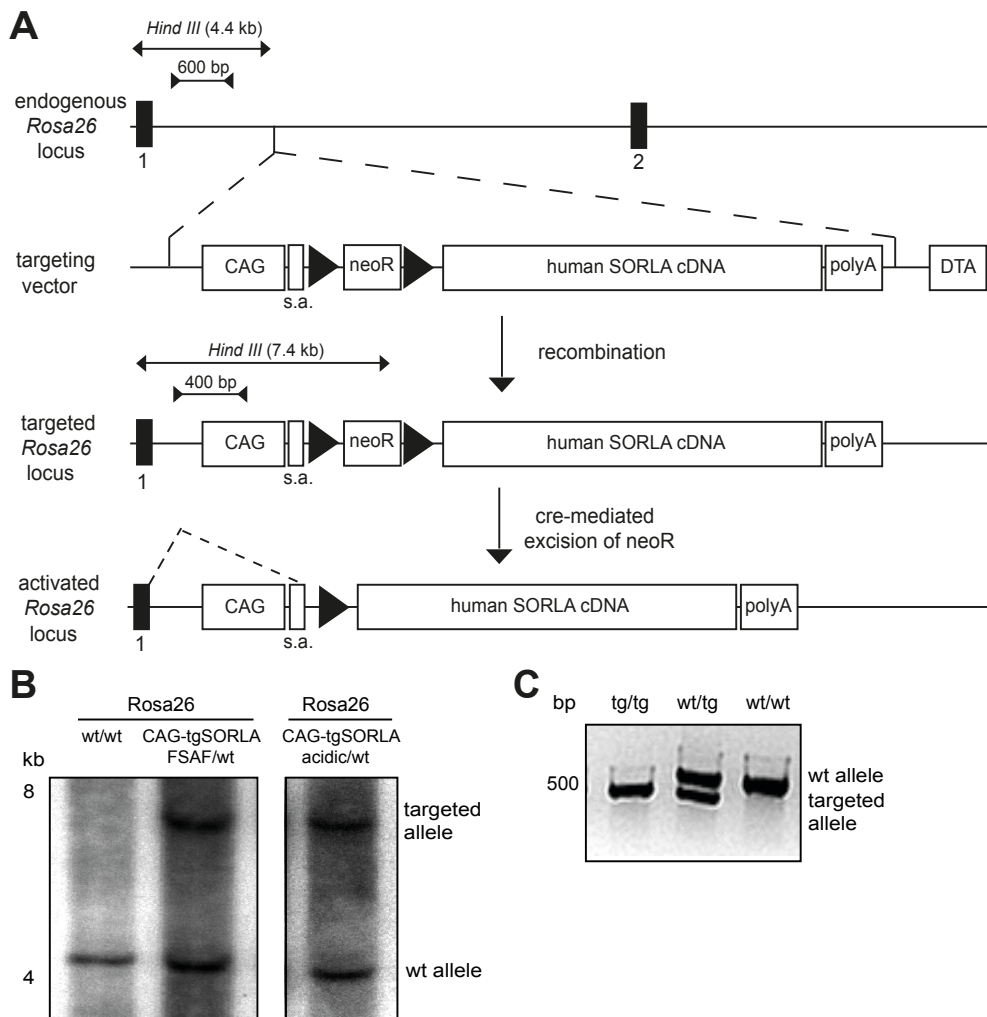


Figure 13: Generation of transgenic mice expressing human SORLA mutants controlled by the CAG promoter.

(A) Targeting of the *Rosa26* locus for the expression of human cDNA encoding SORLA receptor variants that lack the binding site for PACS1 (SORLA^{acidic}) or the retromer complex (SORLA^{FSAF}). Expression is directed from the endogenous *Rosa26* promoter and, additionally, from an artificial, ubiquitously active promoter/enhancer element.

Homologous recombination is used to insert cDNA in embryonic stem cells between exons 1 and 2 of the *Rosa26* locus (black squares). A diphtheria toxin A expression cassette (DTA) and a neomycin-conferring resistance cassette (neoR) allow for negative and positive selection of targeted embryonic stem cell clones, respectively. Expression of cre recombinase facilitates excision of neoR, thereby activating the locus and allowing for cDNA expression. A splice acceptor site (s.a.) facilitates *Rosa26* promoter-mediated cDNA expression. Additionally, a cytomegalovirus early enhancer element in combination with a chicken beta-actin promoter (CAG) was inserted upstream of the s.a. site and thereby allows for a *Rosa26*-independent expression of the cDNA. A polyadenylation signal (polyA) prevents downstream transcription. Black triangles mark loxP recombination sites. Arrows indicate DNA fragments resulting upon genomic DNA digest by Hind III. Inverse arrows mark PCR products to discriminate targeted (tg) and non-targeted (wt) allele.

(B) Genomic DNA of embryonic stem cells of the indicated genotype was subjected to a Hind III digest and analysis by southern blotting. The 4.4 kb DNA fragment corresponds to a non-targeted allele. An additional 7.5 kb DNA fragment is indicative of a targeted allele confirming homologous recombination in embryonic stem cells of *Rosa26*^{CAG-tgSORLA^{acidic}} and *Rosa26*^{CAG-tgSORLA^{FSAF}}, respectively.

(C) PCR fragments indicate targeting of the endogenous *Rosa26* locus (wt/wt) on both alleles (tg/tg) or on one allele (wt/tg), respectively.

Since breedings hardly gave rise to homozygous CAG-SORLA^{wt} animals, (CAG-) mice were bred to heterozygosity in respect to *Rosa26* locus.

Breedings were carefully monitored using PCR based analysis of offspring (Figs. 12C and 13C).

3.1.2. In vivo characterization of the generated mouse models

SORLA protein expression levels in various brain regions

Having established the various mouse models, I first analyzed the protein levels of the human SORLA variants in major brain regions by western blot (Fig. 14).

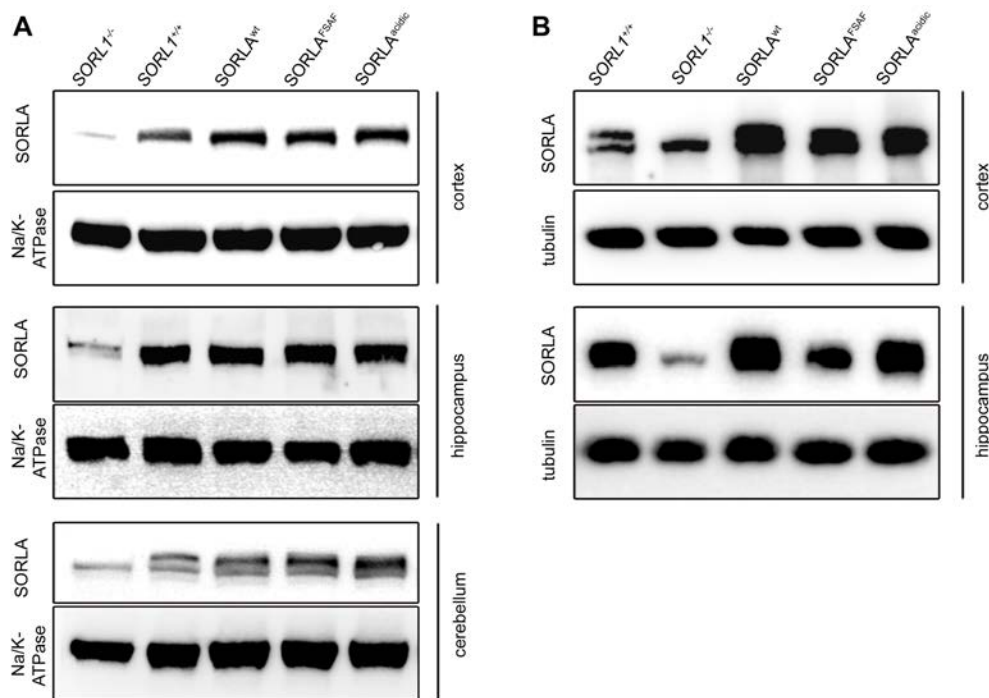


Figure 14: Expression levels of SORLA^{wt}, SORLA^{FSAF} and SORLA^{acidic} in the mouse brain.

Membrane extracts of cortex, hippocampus and cerebellum were analysed for SORLA expression by western blot. Extracts from animals being SORLA-deficient (*Sorli*^{-/-}) or expressing endogenous receptor (*Sorli*^{+/+}) were used as negative or positive control, respectively. Detection of Na/K-ATPase or tubulin served as a loading control.

(A) Mice being deficient for endogenous SORLA expression but homozygous for SORLA^{wt}, SORLA^{FSAF} and SORLA^{acidic} cDNA in the *Rosa26* locus. SORLA expression is driven by the endogenous *Rosa26* promoter. Expression levels between endogenous SORLA (*Sorli*^{+/+}) and the cDNA variants in cortex and hippocampus are comparable. Protein levels of receptor variants SORLA^{FSAF} and SORLA^{acidic} in the cerebellum are mildly increased compared to SORLA^{wt}.

(B) Mice being heterozygous for CAG-SORLA^{wt}, CAG-SORLA^{FSAF} and CAG-SORLA^{acidic} cDNA in the *Rosa26* locus but lacking endogenous SORLA expression. SORLA protein levels are increased in comparison to animals expressing the receptor endogenously (*Sorli*^{+/+}). Of note, SORLA expression in CAG-SORLA^{FSAF} and CAG-SORLA^{acidic} does not equal those in CAG-SORLA^{wt} indicating a heterogenous expression between the variants.

To draw conclusions from the influence of the mutations in the cytoplasmic tail of the receptor on trafficking and amyloidogenic processing, SORLA needs to be comparably expressed.

Sorl1^{-/-} mice serve as negative control, only showing a faint background band or a immunoreactive unspecific band that is clearly distinguishable from the corresponding SORLA band.

As seen in Fig. 14A, expression of SORLA from the *Rosa26* promoter resulted in protein levels for SORLA^{FSAF}, and SORLA^{acidic} that equaled SORLA^{wt} levels in hippocampus and cortex. In contrast, protein levels of receptor variants SORLA^{FSAF} and SORLA^{acidic} in the cerebellum were mildly increased compared to SORLA^{wt}. All in all, expression of the SORLA variants controlled by *Rosa26* promoter activity reached levels comparable to those seen in mice expressing the endogenous murine SORLA receptor (*Sorl1*^{+/+}).

Remarkably, additional activity of the CAG enhancer/promoter lead to increased cortical and hippocampal levels of CAG-SORLA^{wt} that mainly exceeded endogenous murine SORLA levels (*Sorl1*^{+/+}) (Fig. 14B). Interestingly, western blots suggest differences in the expression of CAG-SORLA^{acidic}, CAG-SORLA^{FSAF} and CAG-SORLA^{wt}. In detail, cortical lysates exhibited higher CAG-SORLA^{wt} protein levels compared to CAG-SORLA^{acidic} or CAG-SORLA^{FSAF}. Furthermore, whereas CAG-SORLA^{wt} equals CAG-SORLA^{acidic} expression in hippocampal extracts, the CAG-SORLA^{FSAF} protein amount is prominently decreased and reaches levels of endogenous SORLA expression (*Sorl1*^{+/+}).

Taken together, the generated mouse models show a robust expression of SORLA cDNA. Interestingly, additional activity of the CAG enhancer/promoter resulted in a heterogenous expression of the human SORLA variants that differ from endogenous murine SORLA protein levels.

On the other hand, in hippocampus and cortex, brain areas that are vulnerable to Alzheimer's disease, protein levels of SORLA^{wt}, SORLA^{FSAF}, and SORLA^{acidic} reach comparable levels that also equal expression of endogenous, murine SORLA suggesting the validity of the mouse models for studying Alzheimer's disease-related processes.

Phenotypic characterization of the generated mouse models

Offspring from breedings of mice heterozygous for SORLA^{wt}, SORLA^{FSAF}, and SORLA^{acidic} cDNA in the *Rosa26* locus occur in an expected mendelian ratio (wt/wt, tg/wt, tg/tg in respect

Results

to the *Rosa26* locus) of 1:2:1 (data not shown), indicating no obvious differences in reproduction or viability between the variants. Furthermore, Nissl staining revealed no alterations in the overall architecture of the cortex, hippocampus or cerebellum of the various strains (Fig. 15).

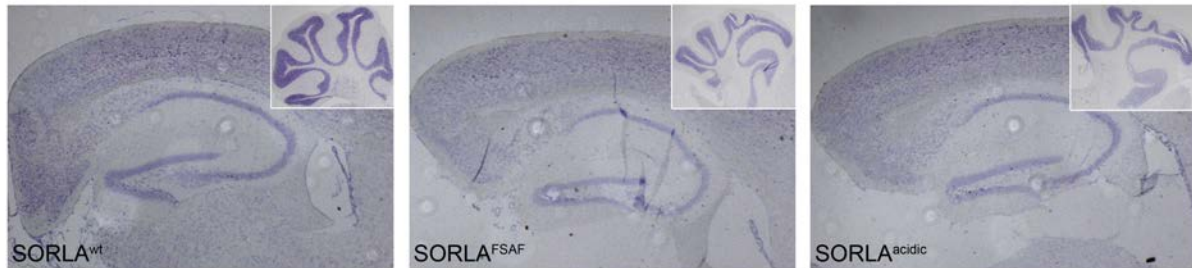


Figure 15: Brain architecture in mice expressing SORLA^{wt}, SORLA^{FSAF}, and SORLA^{acidic}. Nissl-stained sagittal brain sections of SORLA^{wt}, SORLA^{FSAF}, and SORLA^{acidic} mice. Hippocampus, parts of the cortex and the cerebellum (inset) are depicted, showing no obvious differences between the genotypes.

In contrast to the generated mouse lines, whose SORLA cDNA expression solely depends on the endogenous *Rosa26* promoter, breedings of mice heterozygous for CAG-SORLA^{wt} resulted in a reduced number of offspring homozygous for the targeted *Rosa26* locus (tg/tg) (5.9 % compared to expected 25 %) (Table 1). Surprisingly, the effect seems to be specific for the SORLA^{wt} variant, since offsprings from SORLA^{FSAF}- and SORLA^{acidic}-expressing mice occurred in the expected Mendelian ratio (Table 1).

Table 1: Viability in transgenic mice expressing SORLA variants.

Offspring (n = 43–97 animals) from breedings of mice being *Sor11*^{-/-} and heterozygous for CAG-SORLA^{wt}, CAG-SORLA^{FSAF}, or CAG-SORLA^{acidic} cDNA in the *Rosa26* locus were genotyped at 4 weeks of age. The allele ratio of newborn mice of the respective genotypes are given. Offspring of mice expressing SORLA^{FSAF} and SORLA^{acidic} variants show the expected Mendelian ratio of 25% : 50% : 25%. In contrast, the Mendelian ratio of offsprings of CAG-SORLA^{wt} is altered, suggesting embryonic or postnatal lethality upon massively increased human wild-type SORLA expression levels.

	expected Mendelian ratio	genotype		
		SORLA ^{wt}	SORLA ^{FSAF}	SORLA ^{acidic}
tg/tg	25 %	5.9 %	26.8 %	27.9 %
tg/wt	50 %	58.8 %	52.6 %	48.9 %
wt/wt	25 %	35.3 %	20.6 %	23.3 %

Non-comparable expression levels of the CAG-SORLA variants (Fig. 14B) as well as potential lethality of CAG-SORLA^{wt} overexpressing mice (tg/tg) (Table 1) may complicate conclusions from experiments using these mouse strains. For this reason, I decided to conduct further studies in animals expressing the SORLA variants under control of the endogenous *Rosa26* promoter. In these animals, expression of the SORLA variants is comparable in cortex and hippocampus and equals endogenous murine SORLA levels (Fig. 14A).

3.1.3. Intracellular trafficking of the SORLA variants in the brain

Western blot analyses revealed an equal expression of the human SORLA variants in cortex and hippocampus (Fig. 14). To more specifically characterize the cell-specific expression of SORLA^{wt}, SORLA^{FSAF}, and SORLA^{acidic}, I performed immunohistological analyses on sagittal brain sections of the respective mouse strains. Co-staining of SORLA and NeuN, a neuron-specific protein, substantiated SORLA expression to be mainly restricted to neurons in cortex and hippocampus (Fig. 16). No SORLA immunoreactivity was detectable in mice deficient for SORLA expression (*Sor11*^{-/-}) demonstrating the specificity of the SORLA antibody. Interestingly, whereas SORLA^{wt} and SORLA^{FSAF} showed a perinuclear staining comparable to that seen for murine SORLA (*Sor11*^{+/+}), the SORLA^{acidic} protein was more dispersed localized throughout the soma of the neurons (insets in Fig. 16).

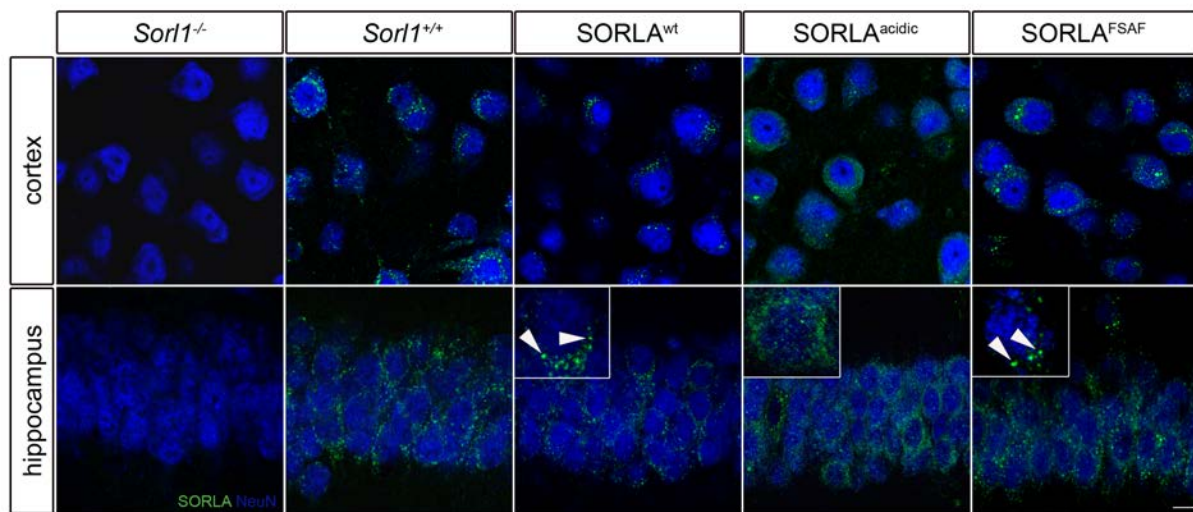


Figure 16: Immunohistological detection of SORLA in cortex and hippocampus of mice expressing SORLA^{wt}, SORLA^{FSAF}, or SORLA^{acidic}.

Immunodetection of SORLA (green) and neuronal marker NeuN (blue) on free-floating sagittal sections of cortex and hippocampus.

Mice were either wild-type for the murine *Sorl1* locus (*Sorl1*^{+/+}) or deficient for *Sorl1* (*Sorl1*^{-/-}) but homozygous for the SORLA^{wt}, SORLA^{FSAF} and SORLA^{acidic} cDNA inserted into *Rosa26*. Insets in the merged micrographs pinpoint genotype specific observations regarding the localization of SORLA.

Whereas SORLA^{wt} and SORLA^{FSAF} localize predominantly to intracellular vesicles (arrowheads) comparable to *Sorl1*^{+/+}, SORLA^{acidic} shows a dispersed subcellular pattern. No SORLA immunoreactivity is seen in *Sorl1*^{-/-} mice. Scale bar: 10 μ m.

Immunocytochemical analysis of the subcellular localization of SORLA variants in primary neurons

To dissect the subcellular localization of the SORLA variants in more detail, I conducted immunocytochemistry experiments in hippocampal primary neurons. In detail, overlap of SORLA and various proteins characteristic for cellular substructures was assessed quantitatively using two different methods. Whereas the Pearson's correlation coefficient (r) measures the correlation of two signals, thresholded Manders' values (tM) denote the overlap, and thereby colocalization, of the signal in one channel with a signal in the other channel (Manders, Verbeek et al. 1993).

In Figs. 17 and 18, co-staining of SORLA and trans-Golgi network (TGN) markers Vti1b and γ -adaptin revealed a distinct reduction in the overlap with SORLA^{FSAF} and SORLA^{acidic} when compared to SORLA^{wt}.

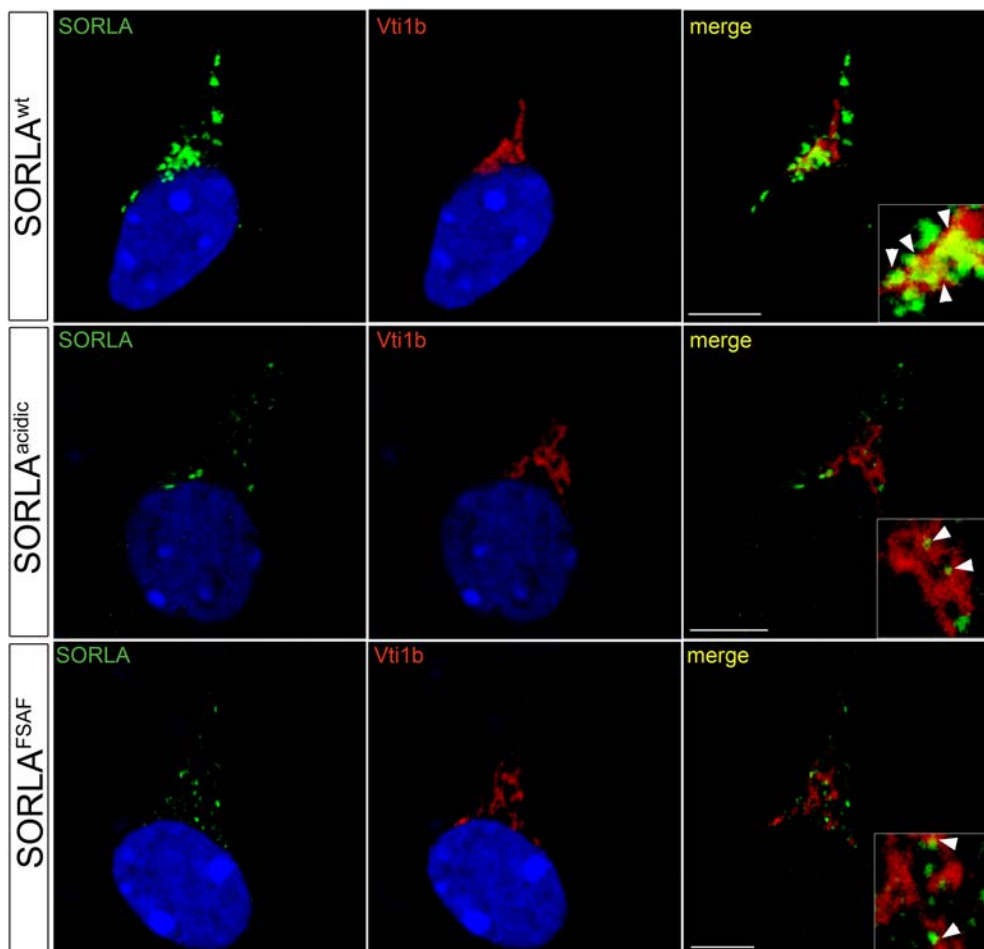


Figure 17: Trans-Golgi network localization (Vti1b) of SORLA^{wt}, SORLA^{FSAF}, and SORLA^{acidic} in primary neurons.

Localization of SORLA (green) and the trans-Golgi network marker Vti1b (red) in primary hippocampal neurons of mice of the indicated genotypes was assessed using confocal immunofluorescence microscopy. DAPI was used to stain nuclei (blue). The arrowheads in the inset indicate colocalization of the SORLA variants with Vti1b. Scale bar: 5 μ m.

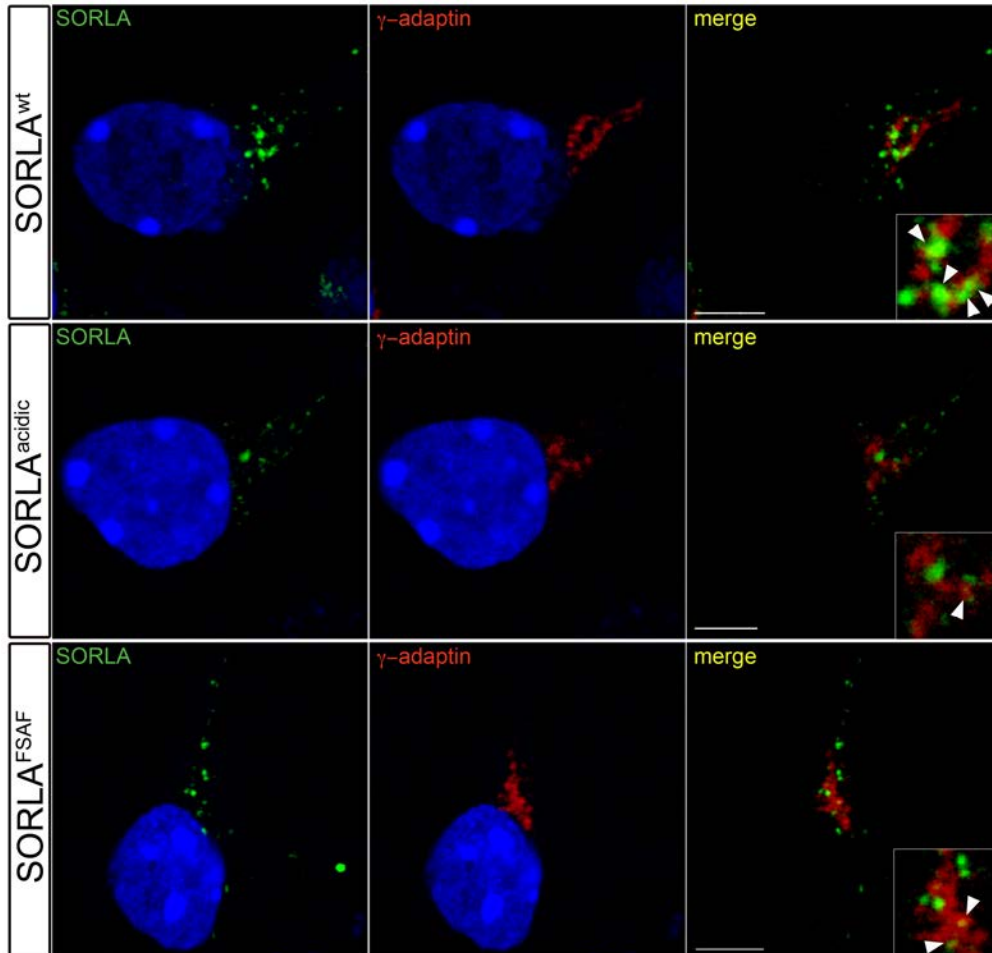


Figure 18: Trans-Golgi network localization (γ -adaptin) of SORLA^{wt}, SORLA^{FSAF}, and SORLA^{acidic} in primary neurons.

Localization of SORLA (green) and the trans-Golgi network marker γ -adaptin (red) in primary hippocampal neurons of mice of the indicated genotypes was assessed using confocal immunofluorescence microscopy. DAPI was used to stain nuclei (blue). The arrowheads in the inset indicate colocalization of the SORLA variants with γ -adaptin. Scale bar: 5 μ m.

Qualitative differences were substantiated by a significant decrease ($p < 0.001$) in Pearson's correlation coefficient (r) for SORLA and Vti1b or γ -adaptin, respectively (Table 2). Furthermore, both tM-values in the SORLA^{FSAF} and SORLA^{acidic} variants were significantly reduced ($p < 0.001$) suggesting loss of SORLA from the TGN.

Table 2: Quantification of the trans-Golgi network localization of SORLA^{wt}, SORLA^{FSAF}, and SORLA^{acidic} in primary neurons.

Thresholded Manders' colocalization coefficients (tM), indicating the degree of overlap between Vti1b or γ -adaptin and SORLA (tM1) or vice versa (tM2), and the Pearson's correlation coefficient (r) of Vti1b or γ -adaptin with SORLA are given.

Values are the mean \pm standard error of the mean (n = 22 - 23 cells). According to Student's *t*-test, r- and tM-values of SORLA^{FSAF} and SORLA^{acidic} were significantly decreased compared to SORLA^{wt} (p<0.001) suggesting SORLA^{FSAF} and SORLA^{acidic} being less abundant in the trans-Golgi network than SORLA^{wt}.

	SORLA ^{wt}	SORLA ^{acidic}	SORLA ^{FSAF}	p value
SORLA and Vti1b				
tM1 (Vti1b overlap with SORLA)	0.279 \pm 0.020	0.174 \pm 0.011	0.144 \pm 0.008	<0.001
tM2 (SORLA overlap with Vti1b)	0.685 \pm 0.021	0.388 \pm 0.025	0.54 \pm 0.022	<0.001
r (correlation SORLA and Vti1b)	0.207 \pm 0.02	0.075 \pm 0.011	0.122 \pm 0.009	<0.001
SORLA and γ-adaptin				
tM1 (γ -adaptin overlap with SORLA)	0.376 \pm 0.033	0.163 \pm 0.016	0.199 \pm 0.015	<0.001
tM2 (SORLA overlap with γ -adaptin)	0.405 \pm 0.027	0.215 \pm 0.017	0.251 \pm 0.013	<0.001
r (correlation SORLA and γ -adaptin)	0.084 \pm 0.024	0.028 \pm 0.009	-0.02 \pm 0.01	<0.001

SORLA shuttles proteins between the TGN and endosomes. Since PACS1 and the retromer complex are important for retrograde trafficking of target proteins, I hypothesized a defect in endosome-to-TGN retrieval of SORLA to be causative for the loss of TGN localization of the SORLA^{FSAF} and SORLA^{acidic} variants.

To test this hypothesis, I performed co-stainings of SORLA and the early endosome marker Rab5. In support of my model, the overlap between Rab5 and SORLA^{wt} was decreased compared to the overlap between Rab5 and SORLA^{FSAF} or SORLA^{acidic} (arrowheads in the insets of Fig 19).

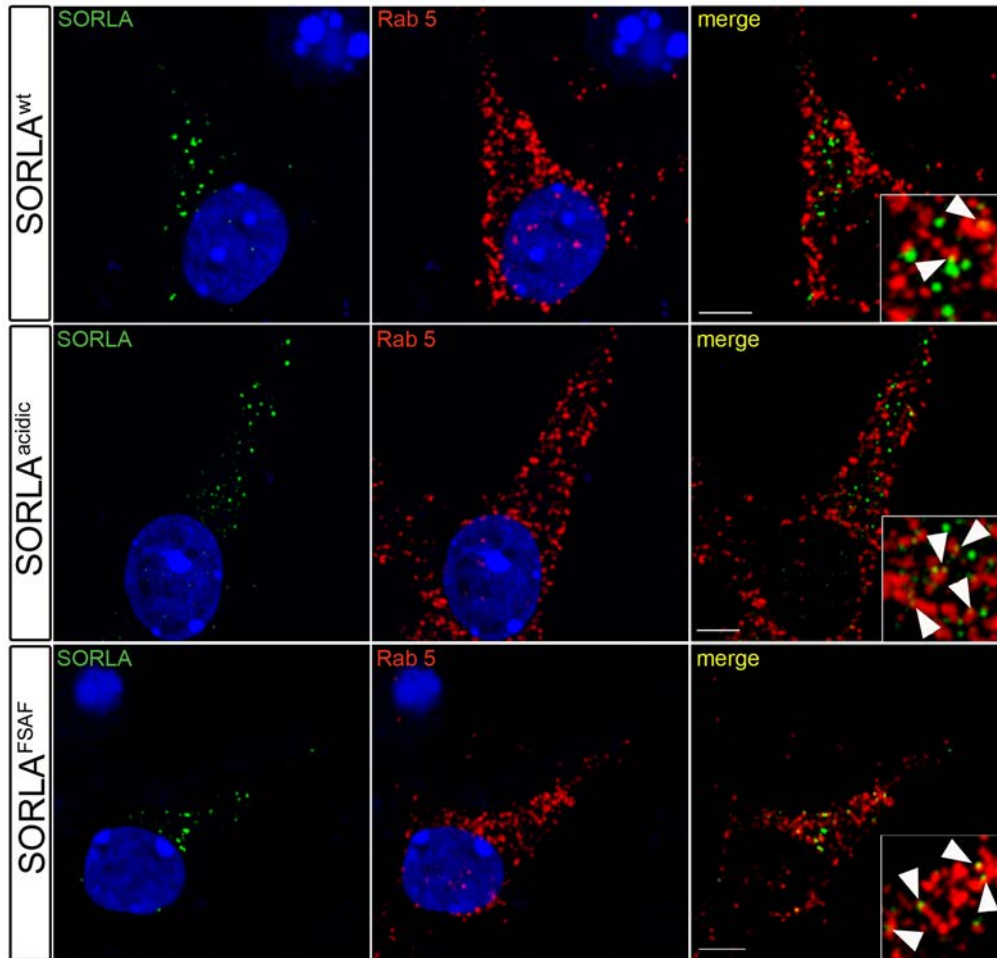


Figure 19: Endosomal localization of SORLA^{wt}, SORLA^{FSAF}, and SORLA^{acidic} in primary neurons.

Localization of SORLA (green) and the early endosome marker Rab5 (red) in primary hippocampal neurons of mice of the indicated genotypes was assessed using confocal immunofluorescence microscopy. DAPI was used to stain nuclei (blue). The arrowheads in the inset indicate colocalization of the SORLA variants with Rab5. Scale bar: 5 μ m.

This qualitative assumption was strengthened by documenting a significant reduction in signal correlation (r) of SORLA and Rab5 in SORLA^{wt} (Table 3). While similar changes in Pearson's correlation coefficient (r) as compared to SORLA^{wt} pointed towards an equal trafficking behaviour of SORLA^{FSAF} and SORLA^{acidic}, the analysis of tM values suggest subtle differences between the two mutants. Thus, SORLA^{FSAF} revealed significant differences in both tM1 and tM2 as compared to SORLA^{wt}. In contrast, in SORLA^{acidic} expressing neurons, only tM1 was significantly elevated as compared to SORLA^{wt} indicating an increased overlap of Rab5 with SORLA (Table 3).

Table 3: Quantification of the endosomal localization of SORLA^{wt}, SORLA^{FSAF}, and SORLA^{acidic} in primary neurons.

Thresholded Manders' colocalization coefficients (tM) indicating the degree of overlap between Rab5 and SORLA (tM1) or vice versa (tM2) and the Pearson's correlation coefficient (r) of Rab5 with SORLA are given.

Values are the mean \pm standard error of the mean (n = 21 - 22 cells). According to Student's *t*-test, r- and tM1-values of SORLA^{FSAF} or SORLA^{acidic} were significantly increased compared to SORLA^{wt} (p<0.01; p<0.001) suggesting SORLA^{FSAF} and SORLA^{acidic} being more abundant in endosomes than SORLA^{wt}.

	SORLA ^{wt}	SORLA ^{mutant}	p value
SORLA^{acidic} and Rab5			
tM1 (Rab5 overlap with SORLA)	0.099 \pm 0.007	0.18 \pm 0.006	<0.001
tM2 (SORLA overlap with Rab5)	0.444 \pm 0.029	0.521 \pm 0.033	>0.05
r (correlation SORLA and Rab5)	0.061 \pm 0.008	0.104 \pm 0.011	<0.01
SORLA^{FSAF} and Rab5			
tM1 (Rab5 overlap with SORLA)	0.099 \pm 0.007	0.135 \pm 0.009	<0.01
tM2 (SORLA overlap with Rab5)	0.444 \pm 0.029	0.63 \pm 0.032	<0.001
r (correlation SORLA and Rab5)	0.061 \pm 0.008	0.14 \pm 0.013	<0.001

The tM values suggest an interpretation whereby SORLA^{acidic} localizes to more dispersed vesicles (as seen in Fig. 16), leading to an increased number of SORLA^{acidic}-positive vesicles as compared to SORLA^{FSAF} and SORLA^{wt}. Assuming no alteration in the number of Rab5-positive vesicles when comparing genotypes, more Rab5-positive vesicles overlap with SORLA^{acidic}-positive vesicles resulting in an increase in tM1. SORLA^{acidic}-containing vesicles exceed the number of those being positive for SORLA^{wt}, leading to a nominally unchanged overlap with Rab5-containing vesicles and thereby explaining no alterations of tM2.

To narrow down the fate of SORLA^{FSAF} and SORLA^{acidic}, I conducted co-stainings of SORLA and Lamp1, a protein enriched in lysosomes (Fig. 20).

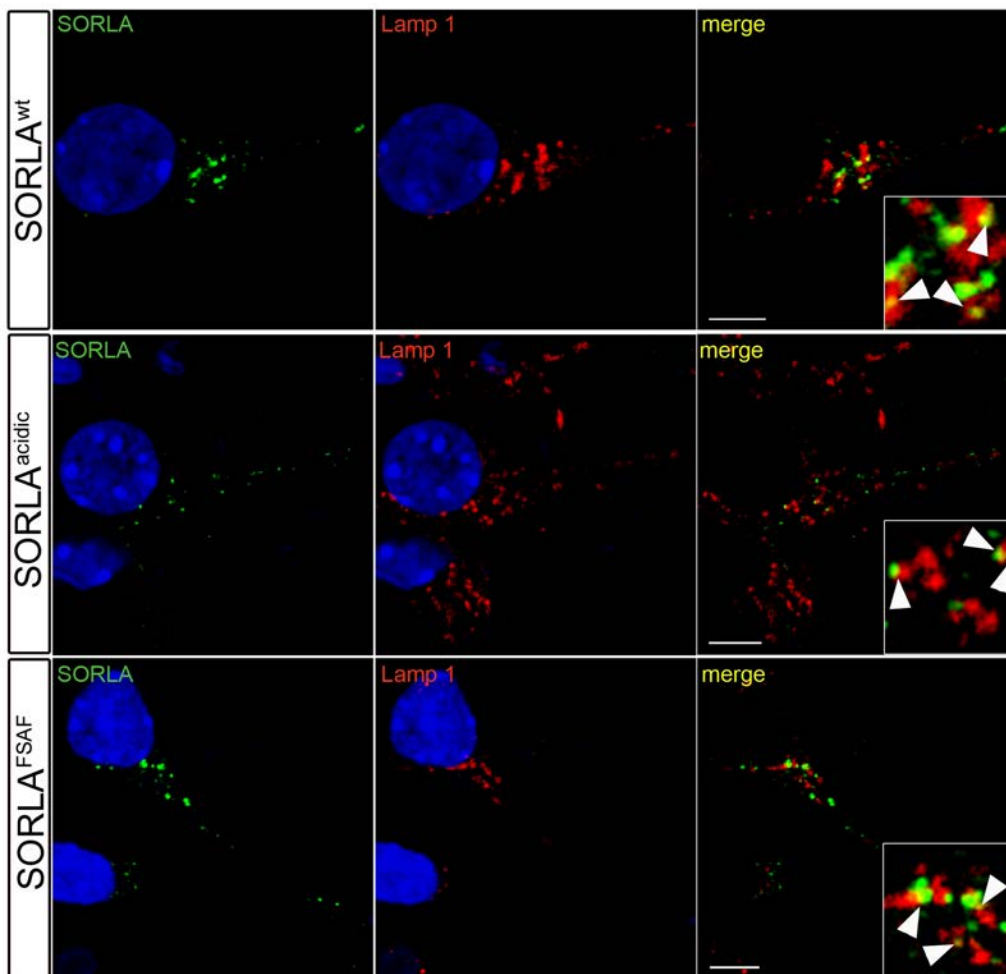


Figure 20: Lysosomal localization of SORLA^{wt}, SORLA^{FSAF}, and SORLA^{acidic} in primary neurons.

Localization of SORLA (green) and the lysosomal marker Lamp1 (red) in primary hippocampal neurons of mice of the indicated genotypes was assessed using confocal immunofluorescence microscopy. DAPI was used to stain nuclei (blue). The arrowheads in the inset indicate colocalization of the SORLA variants with Lamp1. Scale bar: 5 μ m.

Mutation of the binding sites for the retromer complex or PACS1 in SORLA^{FSAF} or SORLA^{acidic} respectively, did not cause a shift into lysosomal compartments as Pearson's correlation coefficient and thresholded Manders' values were unchanged comparing the SORLA variants ($p > 0.05$) (Table 4).

Table 4: Quantification of the lysosomal localization of SORLA^{wt}, SORLA^{FSAF}, and SORLA^{acidic} in primary neurons.

Thresholded Manders' colocalization coefficients (tM) indicating the degree of overlap between Lamp1 and SORLA (tM1) or vice versa (tM2) and the Pearson's correlation coefficient (r) of Lamp1 with SORLA are given.

Values are the mean \pm standard error of the mean (n = 16 - 20 cells). Differences in r- and tM-values between the genotypes were not significantly altered (p>0.05, Student's *t*-test) suggesting no differences in lysosomal localization between SORLA^{wt} and SORLA^{FSAF} or SORLA^{acidic}.

	SORLA ^{wt}	SORLA ^{mutant}	p value
SORLA^{acidic} and Lamp1			
tM1 (Lamp1 overlap with SORLA)	0.146 \pm 0.015	0.141 \pm 0.012	>0.05
tM2 (SORLA overlap with Lamp1)	0.416 \pm 0.022	0.377 \pm 0.028	>0.05
r (correlation SORLA and Lamp1)	0.047 \pm 0.012	0.047 \pm 0.011	>0.05
SORLA^{FSAF} and Lamp1			
tM1 (Lamp1 overlap with SORLA)	0.103 \pm 0.001	0.110 \pm 0.007	>0.05
tM2 (SORLA overlap with Lamp1)	0.433 \pm 0.026	0.492 \pm 0.020	>0.05
r (correlation SORLA and Lamp1)	0.076 \pm 0.015	0.090 \pm 0.012	>0.05

Taken together, confocal immunofluorescence microscopy of primary neurons from mice expressing SORLA mutants SORLA^{FSAF} or SORLA^{acidic} suggest a shift of these receptor variants from the TGN into endosomal compartments as compared to SORLA^{wt}. tM-values indicating the overlap of SORLA and Rab5 (Table 3) served as an explanation for the dispersed pattern of SORLA^{acidic} seen in the immunohistological analysis (Fig. 16), and thereby propose a difference in the trafficking behaviour of SORLA^{acidic} and SORLA^{FSAF}.

Expression of trafficking adaptor proteins in the brain

The trafficking of SORLA between subcellular compartments is regulated by various adaptor proteins. Since SORLA^{FSAF} and SORLA^{acidic} exhibit an altered trafficking behaviour compared to SORLA^{wt}, I performed western blot analysis and quantified levels of adaptor proteins that are known to interact with SORLA (Nielsen, Gustafsen et al. 2007; Schmidt, Sporbert et al. 2007; Fjorback, Seaman et al. 2012). Levels of PACS1, AP1 (γ -adaptin subunit), AP2 (μ subunit) and components of the retromer complex (VPS35) were unchanged between the genotypes (Fig. 21) excluding altered expression of trafficking adaptors in the receptor variants as the reason for the observed differences in sorting.

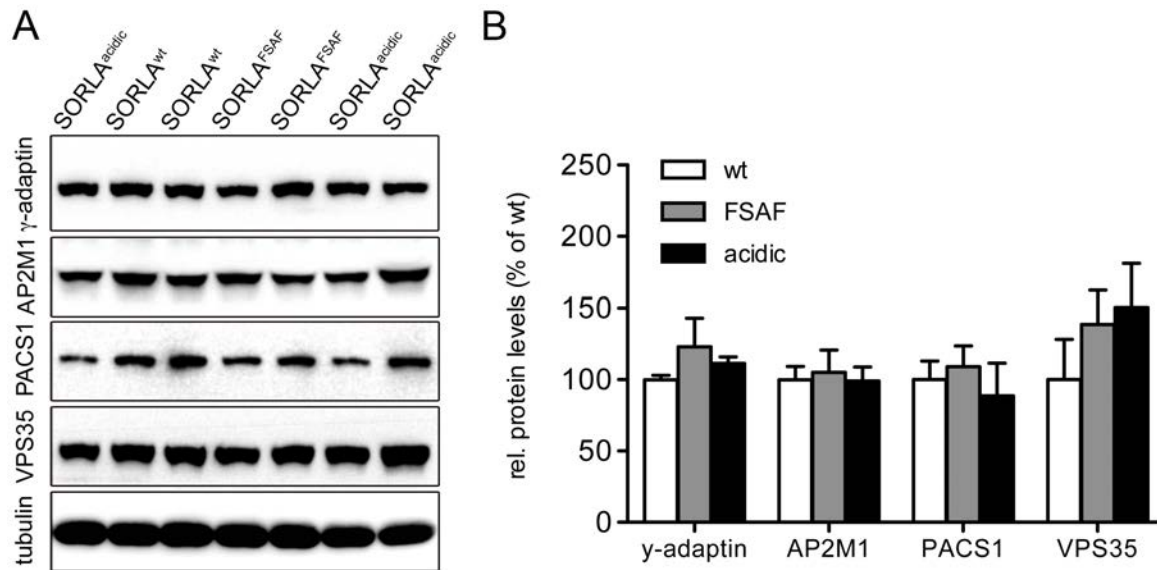


Figure 21: Expression of trafficking adaptor proteins in the brain of $SORLA^{wt}$, $SORLA^{FSAF}$, and $SORLA^{acidic}$ mice.

(A) Protein expression of trafficking adaptors binding to SORLA were determined in cortical extracts of mice expressing $SORLA^{wt}$, $SORLA^{FSAF}$, and $SORLA^{acidic}$ using western blot analyses.

(B) Protein levels of AP1 (γ -adaptin subunit), AP2 (μ subunit), PACS1 and VPS35 were quantified by densitometric scanning of replicate experiments ($n = 4$ animals). Values are given as the mean \pm standard error of the mean. For all analyzed adaptor proteins, no statistical significant difference ($p > 0.05$, Student's t -test) between mice expressing $SORLA^{wt}$ and $SORLA^{FSAF}$ or $SORLA^{acidic}$ was determined. Detection of tubulin served as a loading control.

SORLA expression in purified synaptosomes

As a TGN retrieval defect seen in $SORLA^{FSAF}$ or $SORLA^{acidic}$ may interfere with long-range retrograde trafficking of this receptor (and of APP), I focused next on the abundance of SORLA at the synapse. To that end, I performed an ultracentrifugation-based subcellular fractionation to separate cortical synaptosomes (P2 fraction) from all other membrane associated proteins (P3 fraction) (Fig. 22A). The presence of the synaptic-membrane protein PSD95 in the P2 fraction as well as its absence in the P3 fraction indicated an enrichment of synaptosomes in P2 (Fig. 22B). In line with a previous study on SORLA in rat brain localizing the receptor mainly to the cell body (Posse De Chaves, Vance et al. 2000), subcellular fractionation of the cortex revealed a predominant localization of $SORLA^{wt}$ to non-synaptosome associated membranes (P3) but not to synaptosomes (P2). $SORLA^{FSAF}$ is also less abundant in synaptosomes illustrating no overt differences in the synaptosomal localization of $SORLA^{wt}$ and $SORLA^{FSAF}$.

However, mutation of the acidic cluster shifted the SORLA^{acidic} variant into synaptosomes. This shift was likely caused by a defective re-routing of the SORLA^{acidic} mutant from the synapse and is not resulting from a secondary effect on the trafficking machinery since localization of sortilin, a member of the VPS10p receptor family, showed the same subcellular distribution between the genotypes (Fig. 22B).

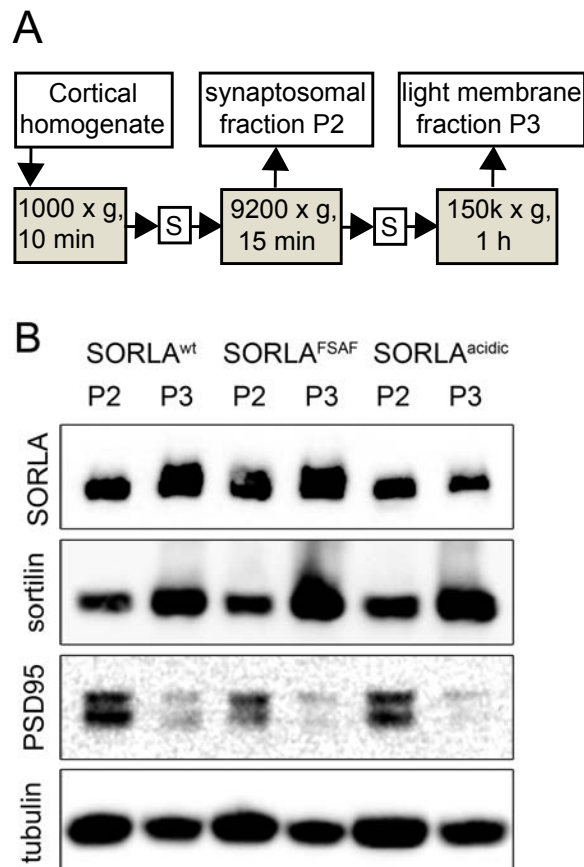


Figure 22: Subcellular protein separation of cortical extracts of mice expressing SORLA^{wt}, SORLA^{FSAF}, and SORLA^{acidic}.

(A) Cortex proteins of mice expressing SORLA^{wt}, SORLA^{FSAF}, and SORLA^{acidic} were biochemically separated yielding pelleted fractions containing synaptosomes (P2) and light membranes (P3). Whereas P2 only contains proteins of the synapse, P3 comprises all residual membrane proteins. S, supernatant.

(B) Fractions were analyzed by western blot. Detection of the synaptic membrane protein PSD95 indicates specific enrichment of synaptosomes in P2. SORLA^{wt} and SORLA^{FSAF} predominantly localize to the P3 fraction whereas SORLA^{acidic} is more abundant in P2. Localization of the VPS10p receptor family protein sortilin is not altered between the genotypes. Detection of tubulin served as a loading control.

3.1.4. Analysis of the mitogen-activated protein kinase pathway in the brain of mice expressing SORLA variants

Recently, a study revealed a role of SORLA in the metabolism of the glial cell line-derived neurotrophic factor (GDNF) (Glerup, Lume et al. 2013). Neurotrophic signaling activates a phosphorylation-triggered signaling cascade, resulting in a variety of effects on downstream targets. Since activation of elements in the signaling cascade correlate with phosphorylation, I determined phosphorylated forms of ERK and AKT, two key components in the mitogen-activated protein kinase pathway.

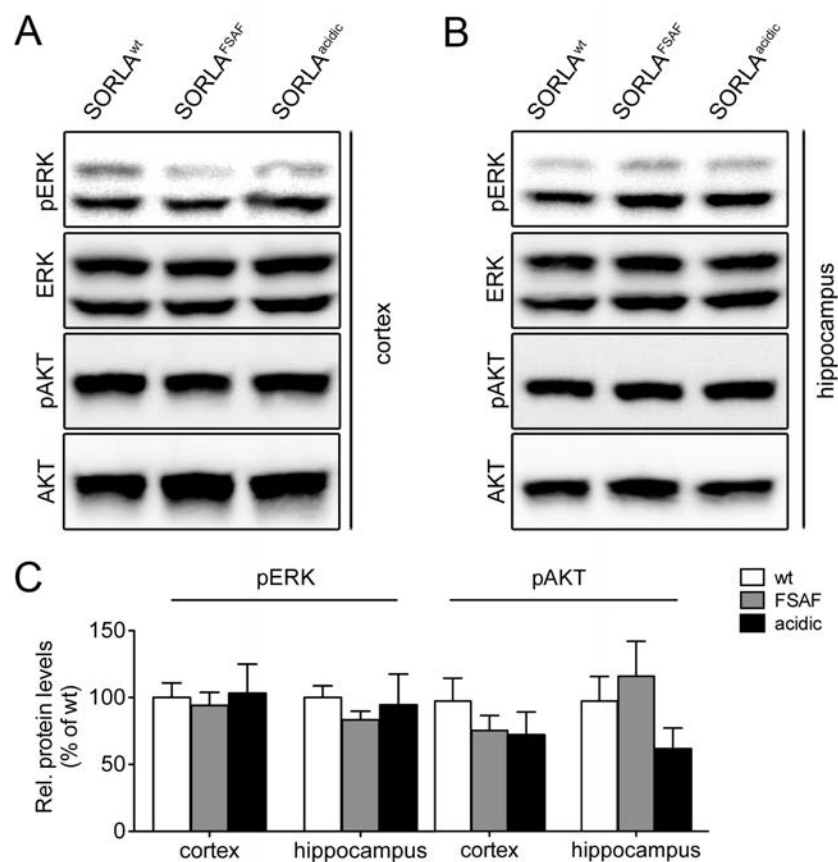


Figure 23: Protein expression of components of the mitogen-activated protein kinase pathway in mice expressing SORLA^{wt}, SORLA^{FSAF}, and SORLA^{acidic}.

(A, B) Cortical and hippocampal brain extracts of mice expressing SORLA^{wt}, SORLA^{FSAF}, and SORLA^{acidic} were analyzed for expression (and phosphorylation) of mitogen-activated protein kinase pathway key components AKT and ERK (pAKT, pERK) using western blot analysis.

(C) Western blots were quantified by densitometric scanning (n = 6 - 7 animals per genotype). All values are given as the mean \pm standard error of the mean. Quantification was evaluated using Student's *t*-test. Differences in AKT/ERK phosphorylation (pAKT, pERK) between SORLA^{wt}- and SORLA^{FSAF}- or SORLA^{acidic}-expressing mice were not significantly altered ($p > 0.05$). Detection of tubulin served as a loading control.

Supprisingly, mutating the binding site for PACS1 or the retromer complex in the cytoplasmic tail of SORLA did not significantly alter phosphorylation levels of ERK and AKT as compared to SORLA^{wt} suggesting no influence on major signaling cascades (Fig. 23).

3.1.5. Influence of SORLA variants on the localization and processing of APP in the brain

According to current concepts, SORLA interacts with APP and traps the molecule in the TGN circumventing its trafficking to compartments where secretases reside. The model was refined by revealing that altered trafficking of SORLA provokes a change in APP trafficking and, consequently, processing (Schmidt, Sporbert et al. 2007; Herskowitz, Offe et al. 2012). Notably, mutating the binding site for PACS1 or the retromer complex resulted in faulty SORLA trafficking and increased APP processing (Schmidt, Sporbert et al. 2007; Fjorback, Seaman et al. 2012). However, these studies were carried out in cell lines, and their relevance for the situation in neurons *in vivo* remained unclear.

Initial studies documenting altered trafficking of SORLA^{acidic} and SORLA^{FSAF} in primary neurons discussed above, provided first conclusive evidence for a role of SORLA-adaptor interactions. Next, I extended these studies to the characterization of APP transport and processing in the brain of SORLA^{acidic}- and SORLA^{FSAF}-expressing mice.

Amyloidogenic processing in an Alzheimer's disease mouse model expressing human SORLA^{wt}, SORLA^{FSAF}, and SORLA^{acidic}

To study the functional consequences of altered SORLA trafficking on APP processing, I crossed animals expressing the different SORLA variants with the 5xFAD line of mice, a well established Alzheimer's disease model. 5xFAD mice overexpress human APP695 carrying the Swedish, Florida, and London EOAD mutation as well as human Presenilin 1 harbouring two EOAD mutations. The neural-specific *Thy1* promoter controls expression of the transgenes, thereby ensuring a specific overexpression in the brain (Oakley, Cole et al. 2006). To test the suitability of the model for studying the influence of SORLA on amyloid processes, I also crossed *Sor11*-deficient animals with 5xFAD mice.

In line with the effect of the loss of SORLA on processing of murine APP (Andersen, Reiche et al. 2005) and human APP695 harbouring the Indiana EOAD mutation in the PDAPP line of

Results

mice (Rohe, Carlo et al. 2008), 5xFAD/*Sor11*^{-/-} mice showed elevated A β ₄₀ and A β ₄₂ levels as well as an increase in sAPP α and sAPP β compared to 5xFAD/SORLA^{wt} suggesting 5xFAD as a suitable model to analyze the influence of SORLA trafficking on APP processing (Fig. 24).

I next determined the levels of APP metabolites in the cytosolic fraction of cortical protein lysates of mice expressing SORLA^{FSAF} or SORLA^{acidic} on the 5xFAD background. In the brain of 5xFAD/SORLA^{FSAF} and 5xFAD/SORLA^{acidic} mice, APP processing products sAPP α , sAPP β , A β ₄₀, and A β ₄₂ were all increased compared to 5xFAD/SORLA^{wt} mice (Fig. 24). Remarkably, an increase in all APP processing products had been demonstrated before in CHO cells upon expression of SORLA^{acidic} or in SH-SY5Y cells upon SORLA^{FSAF} expression (Schmidt, Sporbert et al. 2007; Fjorback, Seaman et al. 2012). Hence, findings in SORLA^{acidic}- and SORLA^{FSAF}-overexpressing mice recapitulate said *in vitro* studies and support a role for SORLA in APP processing in the brain *in vivo*.

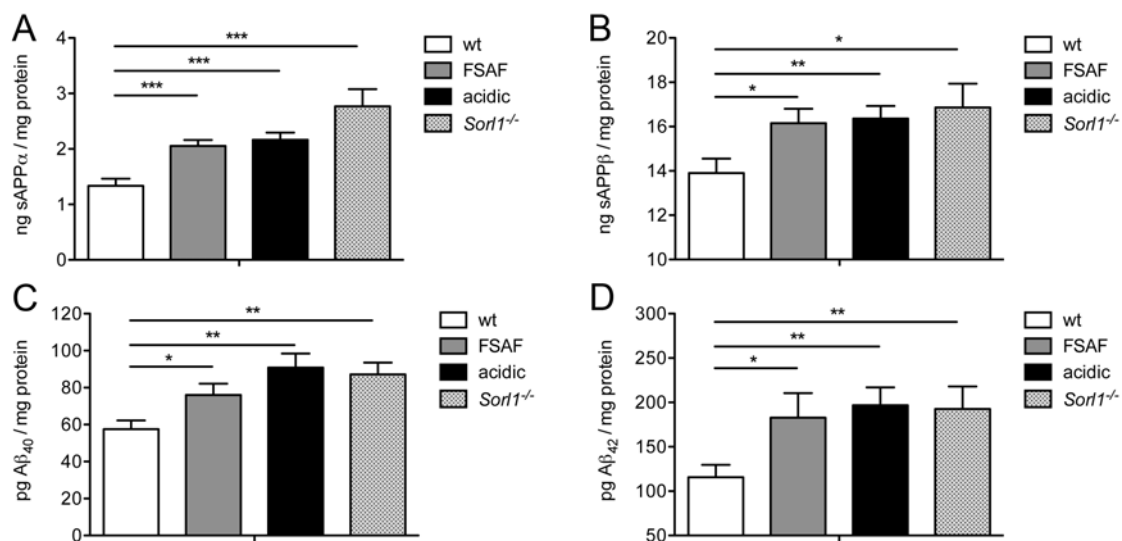


Figure 24: APP metabolites in the brain of an Alzheimer's disease mouse model (5xFAD) expressing SORLA^{wt}, SORLA^{FSAF}, and SORLA^{acidic}.

Mice expressing SORLA^{wt}, SORLA^{FSAF}, or SORLA^{acidic} were crossed with 5xFAD animals, a well-characterized mouse model for Alzheimer's disease.

APP processing in the cytoplasmic fraction of cortical brain extracts of mice of the indicated genotypes was determined using an immunobased biological assay (Meso Scale Discovery). Levels of soluble (s) APP α (A), sAPP β (B), A β ₄₀ (C), and A β ₄₂ (D) are depicted. Values are given as the mean \pm standard error of the mean (duplicate measurements in 14 - 15 animals per genotype (*Sor11*^{-/-}, n = 8 animals)). Statistical significant differences between SORLA^{wt} and the other genotypes were determined using Student's *t*-test. In mice expressing SORLA^{FSAF} or SORLA^{acidic} or in mice deficient for endogenous SORLA expression (*Sor11*^{-/-}), all APP processing products are significantly increased compared to mice expressing SORLA^{wt} (*, p<0.05, **, p<0.01; ***, p<0.001).

Alteration in SORLA trafficking due to mutations or complete loss of the receptor did not alter total APP levels in the brain of 5xFAD/*Sor11*^{-/-}, 5xFAD/SORLA^{FSAF}, and 5xFAD/SORLA^{acidic} mice compared to 5xFAD/SORLA^{wt} (Fig. 25) excluding the possibility of increased APP levels as the cause for elevated concentrations of APP processing products.

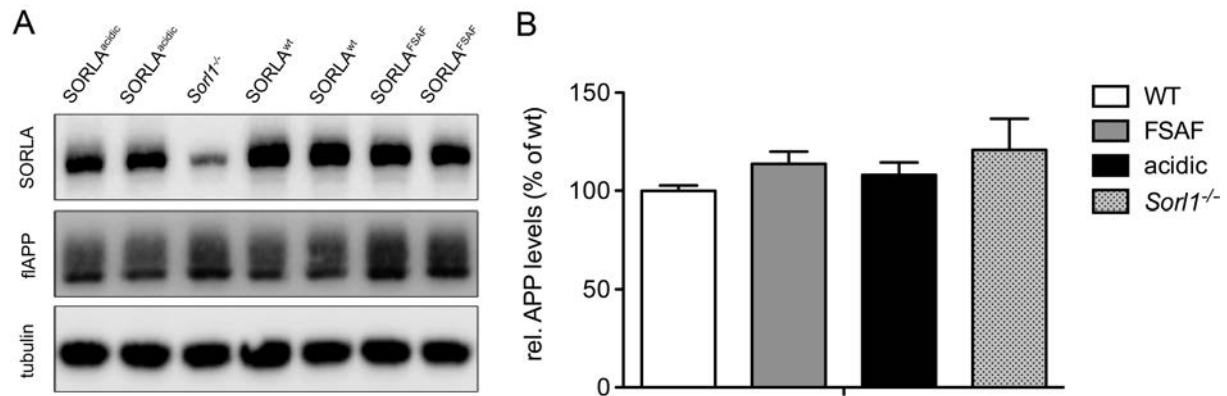


Figure 25: APP expression levels in cortical brain lysates of 5xFAD mice expressing SORLA^{wt}, SORLA^{FSAF} and SORLA^{acidic}.

Mice expressing SORLA^{wt}, SORLA^{FSAF} or SORLA^{acidic} were crossed with 5xFAD animals.

(A) The membrane fractions of cortical brain extracts of mice of the indicated genotype were analyzed for SORLA and APP by western blot.

(B) APP levels were quantified by densitometric scanning of replicate blots (n = 14 animals; for *Sor11*^{-/-}: n = 8 animals). Values are given as the mean ± standard error of the mean. Student's *t*-test revealed no statistical significant differences in APP protein expression between SORLA^{wt} and the other genotypes (p>0.05). Detection of tubulin served as a loading control.

Synaptosomal localization of APP in 5xFAD mice expressing SORLA trafficking mutants

Neurons are highly polarized cells subdivided into axon, soma and dendrites. Protein sorting between the various cellular compartments is tightly regulated and disturbances in this complex sorting system may affect APP trafficking and processing. Although the neuronal site of APP cleavage still warrants clarification, A β exerts its toxic effects at the synapse (Shankar, Li et al. 2008) suggesting APP trafficking to and from the synapse as an important factor for APP processing. Since APP transport in neurons is not entirely depending on the cytoplasmic tail of APP (Back, Haas et al. 2007), a sorting receptor like SORLA may play a role in the neuronal trafficking of APP to the synaptic membranes.

To shed light on APP trafficking in neurons, I performed synaptosomal fractionation in 5xFAD mice expressing human SORLA variants. As seen before (Fig. 22B), SORLA^{wt} and

Results

SORLA^{FSAF} localize predominantly to non-synaptosomal membranes (P3), whereas SORLA^{acidic} shows an equal distribution between synaptosomal (P2) and non-synaptosomal membranes, suggesting an increase in synaptic localization compared to SORLA^{wt} and SORLA^{FSAF} (Fig. 26A).

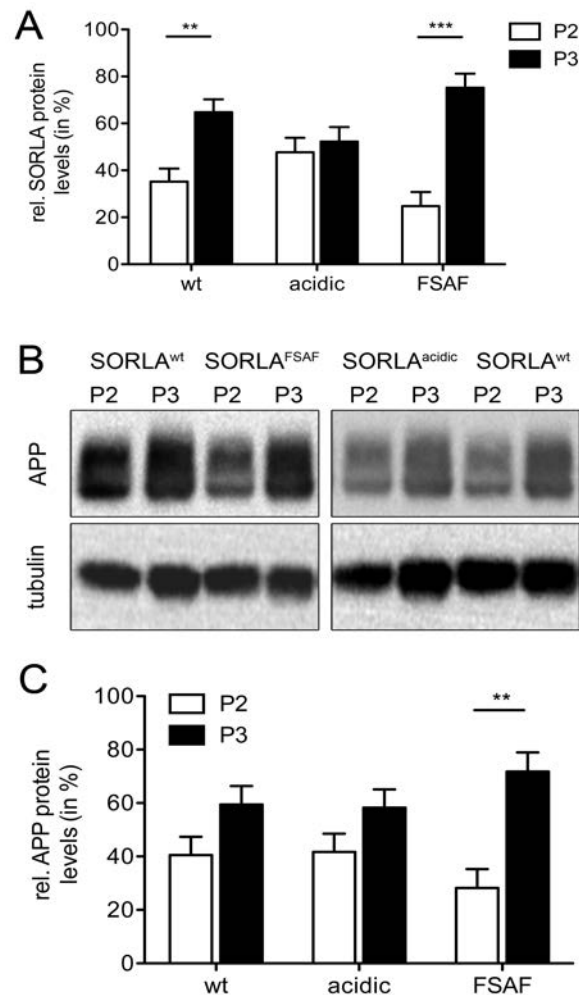


Figure 26: APP and SORLA localization in subcellular fractions of 5xFAD mice expressing SORLA^{wt}, SORLA^{FSAF}, and SORLA^{acidic}.

Cortical extracts of mice of the indicated genotypes were biochemically separated (see Fig. 22A). Pelleted fractions containing synaptosomes (P2) or all residual membrane proteins (P3) were analyzed for SORLA and APP protein expression.

(A) Densitometric scanning of replicate western blots (5-6 animals per genotype) reveal a predominant localization of SORLA^{wt} and SORLA^{FSAF} to light membranes (P3) (**, $p < 0.01$; ***, $p < 0.001$) whereas SORLA^{acidic} is equally distributed between synaptosomes (P2) and P3.

(B, C) In SORLA^{wt}- and SORLA^{acidic}-expressing animals, APP distributes equally between P2 and P3. In contrast, mice expressing the SORLA^{FSAF} variant exhibit a prominent shift of APP from P2 to P3 as substantiated by densitometric scanning of replicate blots (5-6 animals per genotype) (**, $p < 0.01$).

Values are the mean \pm standard error of the mean. Differences in SORLA and APP protein levels in P2 and P3 were evaluated using Student's *t*-test. Detection of tubulin served as a loading control.

However, despite a higher abundance of SORLA^{acidic} at the synapse in 5xFAD/SORLA^{acidic} mice, APP in these mice showed an equal distribution between P2 and P3. In contrast,

mutation of the retromer binding site in 5xFAD/SORLA^{FSAF} mutant mice shifted APP away from the synapse as compared to 5xFAD/SORLA^{wt} animals (Fig. 26B and C).

Phosphorylation of APP at Thr⁶⁶⁸ in 5xFAD mice expressing human SORLA variants

APP processing and neuronal trafficking is, in part, dependent on the phosphorylation at Thr⁶⁶⁸ in the cytoplasmic tail of APP. In detail, phosphorylation diminishes the interaction of APP and Fe65 and, consequently, affects amyloidogenic processing (Ando, Iijima et al. 2001). Furthermore, phosphorylation facilitates interaction with JIP-1, a protein regulating axonal transport of APP (Muresan and Muresan 2005). I determined phosphorylation of APP in the cortex of 5xFAD mice expressing human SORLA variants using an antibody detecting only APP phosphorylated at Thr⁶⁶⁸ (Fig. 27). Dephosphorylated protein lysate was used to confirm the phosphospecificity of the antibody (Fig. 27A). Phosphorylation at Thr⁶⁶⁸ was not altered between the various SORLA variants (Fig. 27B), excluding a role for APP phosphorylation in SORLA-dependent pathways of neuronal APP transport and processing.

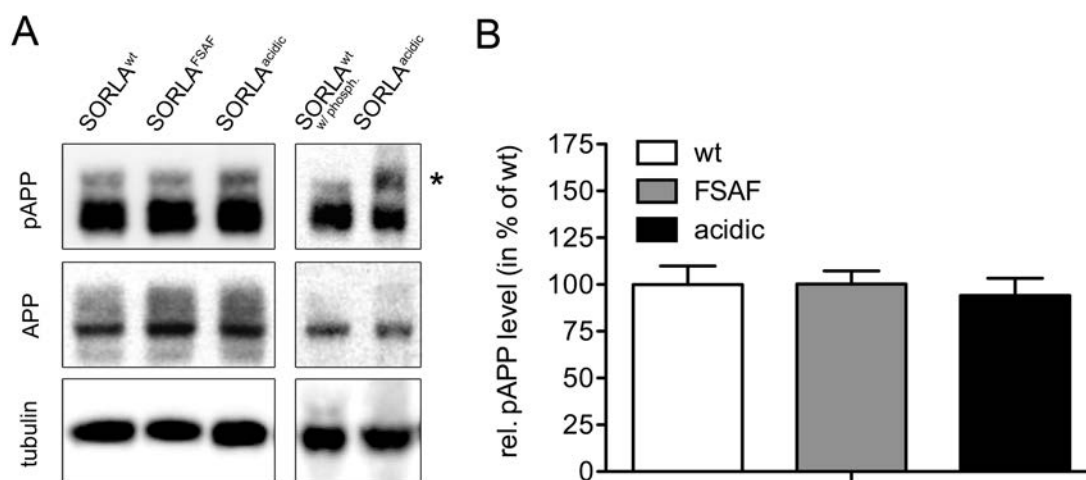


Figure 27: APP phosphorylation levels in cortical brain lysates of 5xFAD mice expressing SORLA^{wt}, SORLA^{FSAF}, and SORLA^{acidic}.

(A) Phosphorylation levels of APP at Thr⁶⁶⁸ (pAPP) in cortical membrane extracts of the indicated genotypes were determined by western blot. The corresponding band is indicated (*). Pretreatment of protein lysate with phosphatase (w/ phosph.) confirmed the phosphospecificity of the antibody. APP levels were not altered comparing genotypes.

(B) Densitometric scanning of replicate blots (10 animals per genotype) documented no significant differences ($p > 0.05$, Student's *t*-test) in APP phosphorylation levels of mice expressing SORLA^{FSAF} or SORLA^{acidic} compared to SORLA^{wt}-expressing animals. Values are the mean \pm standard error of the mean. Detection of tubulin served as a loading control.

Taken together, my data substantiated a role for SORLA trafficking in APP processing *in vivo*. Immunocytochemical studies, revealing a TGN-retrieval defect of SORLA^{FSAF} and SORLA^{acidic} were complemented with biochemical studies, suggesting malfunctions in retrograde trafficking of SORLA and/or APP from the synapse in 5xFAD/SORLA^{FSAF} or 5xFAD/SORLA^{acidic} mice compared to 5xFAD/SORLA^{wt} animals. Furthermore, my findings rule out secondary effects of receptor missorting on major signaling cascades or phosphorylation of APP, pinpointing changes in the trafficking behaviour of SORLA^{FSAF} and SORLA^{acidic} as the underlying mechanism explaining increased APP processing in the brain of the respective mouse models.

3.2. ROLE OF PACS1 FOR SORLA TRAFFICKING AND APP PROCESSING IN THE NEURONAL CELL LINE SH-SY5Y

Mice expressing a SORLA variant harbouring disruptions in the acidic cluster (SORLA^{acidic}) exhibit defects in TGN retrieval, suggesting loss of interaction between SORLA and PACS1 as causative for the malfunctions in receptor trafficking. However, the acidic cluster motif not only mediates binding of PACS1 but also overlaps with the binding site for the adaptor complex (AP) 2, a protein complex which is crucial for endocytosis. Conceptually, data obtained in SORLA^{acidic} mice cannot distinguish between sorting defects caused by loss of PACS1 or AP2 interaction. To dissect the role of PACS1 for SORLA transport and APP processing in neurons, I performed PACS1 knockdown studies in the neuroblastoma cell line SH-SY5Y stably overexpressing human SORLA and APP695 transgenes (SY5Y-S/A).

3.2.1. Trafficking of SORLA in PACS1-deficient SY5Y-S/A cells

Initially, I established a protocol to erase endogenous PACS1 expression in cells using siRNA knockdown approaches. Treatment of SY5Y-S/A cells with a siRNA directed against PACS1-mRNA (w/o PACS1) resulted in substantially reduced PACS1 protein levels compared to cells treated with a scrambled control siRNA (w/ PACS1). In contrast, protein expression of SORLA and APP was not changed upon knockdown of PACS1 (Fig. 28).

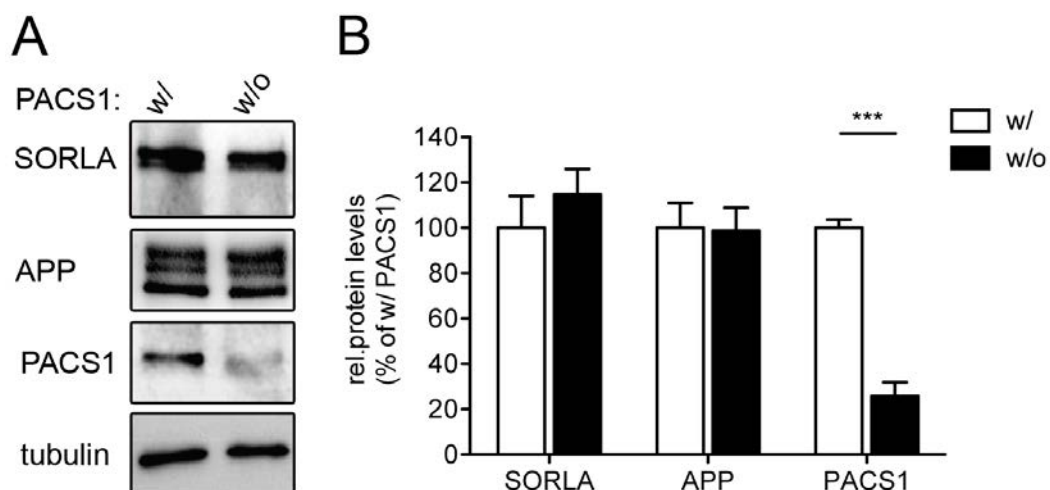


Figure 28: Knockdown of PACS1 in SY5Y-S/A cells.

SH-SY5Y cells stably overexpressing human cDNAs encoding SORLA and APP695 (SY5Y-S/A) were treated with siRNA against endogenous PACS1 (w/o PACS1) or with a scrambled control siRNA (w/ PACS1).

(A) The effect of siRNA treatment on protein levels of SORLA, APP, and PACS1 was monitored by western blot. (*Figure legend continues.*)

Results

(Figure legend continued.)

(B) Densitometric scanning of replicate blots (number of samples per condition: 12). Whereas PACS1 expression is significantly reduced in siRNA-treated cells (***, $p < 0.001$), levels of SORLA and APP are not affected ($p > 0.05$).

Values are given as the mean \pm standard error of the mean. Detection of tubulin served as a loading control. Statistical differences in SORLA, APP, and PACS1 protein levels were evaluated using Student's *t*-test.

Since PACS1 plays a role in shuttling of proteins between TGN and endosomes, I analyzed the subcellular localization of SORLA upon loss of PACS1 in SY5Y-S/A cells using confocal immunofluorescence microscopy. In Fig. 29, co-staining of SORLA and the TGN marker Vti1b revealed a distinct overlap between the two proteins in the presence of PACS1 (w/ PACS1). This assumption was substantiated by a strong correlation of the signals in both channels ($r = 0.4 \pm 0.01$) (Table 5). In contrast, loss of PACS1 (w/o PACS1) resulted in a more dispersed localization of SORLA leading to a significant reduction in signal correlation ($r = 0.3 \pm 0.02$; $p < 0.001$). The significant reduction in the overlap between SORLA and Vti1b in PACS1-knockdown cells (tM1, $p < 0.01$; tM2, $p < 0.001$) suggested a loss of the receptor from the TGN and a concomitant shift into another subcellular compartment (Table 5).

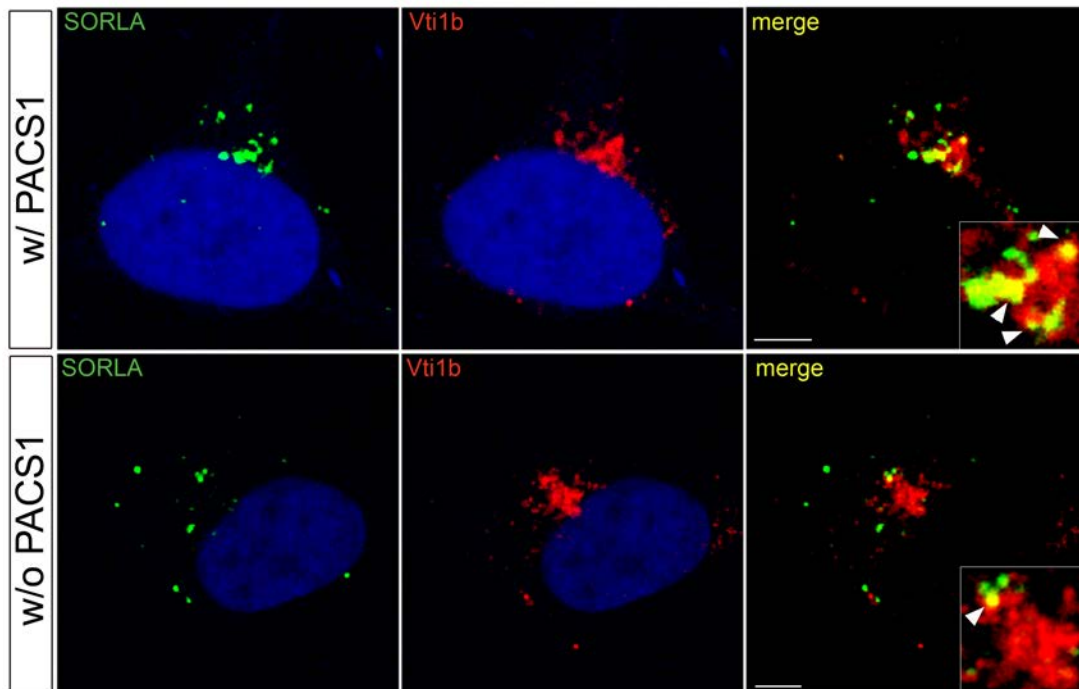


Figure 29: Effect of PACS1 knockdown on the trans-Golgi network localization of SORLA in SY5Y-S/A cells.

SY5Y-S/A cells were treated with a siRNA against PACS1 (w/o PACS1) or with a scrambled control siRNA (w/ PACS1). Localization of SORLA (green) and the trans-Golgi network marker Vti1b (red) was assessed using confocal microscopy. DAPI was used to stain nuclei (blue). Arrowheads in the insets indicate colocalization of the two proteins. Scale bar: 5 μ m.

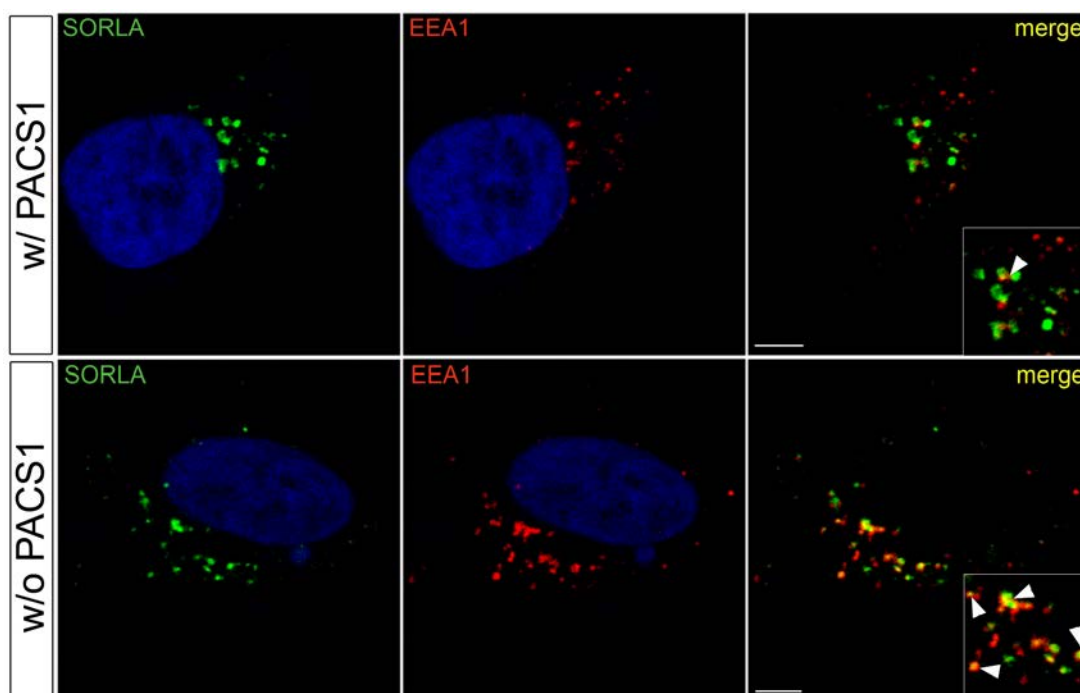
Table 5: Quantification of the trans-Golgi network localization of SORLA in SY5Y-S/A cells.

SY5Y-S/A cells were treated with a siRNA against PACS1 (w/o PACS1) or with a scrambled control siRNA (w/ PACS1). Thresholded Manders' colocalization coefficients (tM), indicating the degree of overlap between Vti1b and SORLA (tM1) or vice versa (tM2), and the Pearson's correlation coefficient (r) of Vti1b with SORLA are given.

Values are the mean \pm standard error of the mean of 20 – 22 cells. A loss in trans-Golgi network localization of SORLA upon knockdown of PACS1 (w/o PACS1) results in significantly decreased r- and tM-values compared to scrambled siRNA treated cells (w/ PACS1) ($p < 0.01$; $p < 0.001$, Student's *t*-test).

	w/ PACS1	w/o PACS1	p value
SORLA and Vti1b			
tM1 (Vti1b overlap with SORLA)	0.254 \pm 0.017	0.186 \pm 0.015	<0.01
tM2 (SORLA overlap with Vti1b)	0.586 \pm 0.023	0.430 \pm 0.014	<0.001
r (correlation SORLA and Vti1b)	0.397 \pm 0.012	0.301 \pm 0.017	<0.001

In line with more distally localized SORLA-positive vesicles in cells lacking PACS1 (w/o PACS1), compared to the perinuclear pattern in cells expressing PACS1 (w/ PACS1), a significantly increased colocalization with EEA1 resulted in elevated tM values (tM1, $p < 0.001$; tM2, $p < 0.01$) (Fig. 30) (Table 6). A significant increase in signal correlation in PACS1 siRNA-treated cells confirmed this conclusion ($p < 0.001$).

**Figure 30: PACS1 knockdown alters the endosomal localization of SORLA in SY5Y-S/A cells.**

SY5Y-S/A cells were treated with a siRNA against PACS1 (w/o PACS1) or with a scrambled control siRNA (w/ PACS1). Localization of SORLA (green) and the early endosome marker EEA1 (red) was assessed using confocal microscopy. DAPI was used to stain nuclei (blue). Arrowheads in the inset indicate colocalization of the two proteins. Scale bar: 5 μ m.

Table 6: Quantification of the endosomal localization of SORLA in SY5Y-S/A cells.

SY5Y-S/A cells were treated with a siRNA against PACS1 (w/o PACS1) or with a scrambled control siRNA (w/ PACS1). Thresholded Manders' colocalization coefficients (tM), indicating the degree of overlap between Vti1b and SORLA (tM1) or vice versa (tM2), and the Pearson's correlation coefficient (r) of Vti1b with SORLA are given.

Values are the mean \pm standard error of the mean of 22 cells. Treatment of SY5Y-S/A cells with a siRNA against PACS1 (w/o PACS1) results in an accumulation of SORLA in endosomal vesicles explaining significantly increased r- and tM-values compared to scrambled siRNA treated cells (w/ PACS1) ($p < 0.01$; $p < 0.001$, Student's *t*-test).

	w/ PACS1	w/o PACS1	p value
SORLA and EEA1			
tM1 (EEA1 overlap with SORLA)	0.072 \pm 0.004	0.117 \pm 0.009	<0.01
tM2 (SORLA overlap with EEA1)	0.152 \pm 0.017	0.220 \pm 0.017	<0.001
r (correlation SORLA and EEA1)	0.099 \pm 0.008	0.176 \pm 0.014	<0.001

In conclusion, evaluation of quantitative confocal microscopy-based measurements documented a shift of SORLA from the TGN into early endosomes in the absence of PACS1 in the neuronal cell line SY5Y-S/A.

3.2.2. SORLA-dependent function for PACS1 in APP trafficking and amyloidogenic processing

Loss of PACS1 affects TGN localization of SORLA. Since APP parallels SORLA trafficking (Schmidt, Sporbart et al. 2007; Herskowitz, Offe et al. 2012), I expected that altered trafficking of SORLA upon loss of PACS1 results in changes in APP localization.

In line with the hypothesis, knockdown of PACS1 (w/o PACS1) did not influence colocalization of SORLA and APP (Fig. 31A) as tM1- and tM2-values were not altered as compared to control siRNA-treated cells ($p > 0.05$) (Table 7). Also, the signal correlation (r) in both channels was unchanged, indicating that APP parallels SORLA trafficking in the presence and absence of PACS1.

These findings were confirmed upon colocalization analysis of APP and Vti1b. In the presence of PACS1 (w/ PACS1) APP showed a perinuclear staining with a distinct overlap with Vti1b (inset in Fig. 31B). In contrast, treatment with a siRNA targeting PACS1 (w/o PACS1) resulted in a significant decrease in signal correlation (r) compared to cells treated with a scrambled siRNA (w/ PACS1) ($p < 0.001$) (Table 8); resembling the findings in colocalization experiments of SORLA and Vti1b (Fig. 29).

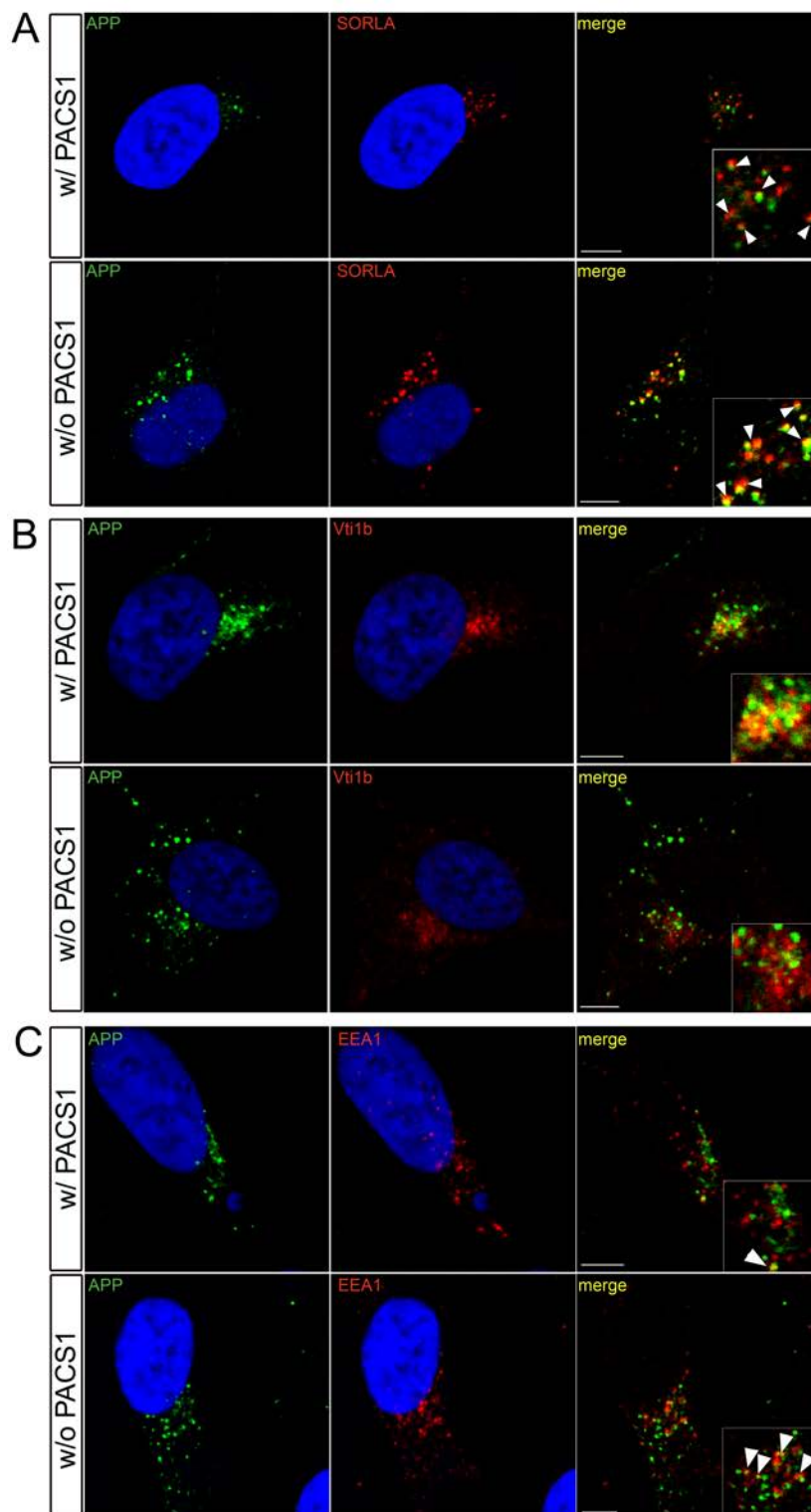


Figure 31: Effect of PACS1 knockdown on the subcellular trafficking of APP in SY5Y-S/A cells. SY5Y-S/A cells were treated with a siRNA against PACS1 (w/o PACS1) or with a scrambled control siRNA (w/ PACS1). Localization of APP (green) and SORLA (red) (A) or marker proteins (red) for the trans-Golgi network (Vti1b) (B) or for early endosomes (EEA1) (C) was assessed using confocal microscopy. DAPI was used to stain nuclei (blue). Arrowheads in the insets indicate colocalization of APP with SORLA, Vti1b or EEA1, respectively. Scale bar: 5 μ m.

Results

As expected, APP localized to more distal vesicles in the absence of PACS1 (w/o PACS1) (Fig. 31C), resulting in an elevated overlap of APP and EEA1 (tM1, $p < 0.001$; tM2, $p < 0.01$) paralleled by an increase in signal correlation ($p < 0.01$) (Table 7) as compared to cells treated with a scrambled siRNA.

Table 7: Quantification of the subcellular localization of APP in SY5Y-S/A cells.

SY5Y-S/A cells were treated with a siRNA against PACS1 (w/o PACS1) or with a scrambled control siRNA (w/ PACS1). Localization of APP and SORLA, Vti1b or EEA1 was assessed using confocal immunofluorescence microscopy.

19 - 29 cells per condition were analyzed to determine the Pearson's correlation coefficient (r) of SORLA/Vti1b/EEA1 with APP as well as the thresholded Manders' colocalization coefficients (tM) that indicate the degree of overlap of SORLA/Vti1b/EEA1 with APP (tM1) or vice versa (tM2). All values are the mean \pm standard error of the mean. Differences between the conditions were assessed using Student's t -test.

tM-values suggest lack of alteration in the overlap of APP and SORLA ($p > 0.05$), but an increase in the overlap of APP with the early endosome marker EEA1 and a concomitant decrease in the overlap of APP with the trans-Golgi network marker Vti1b upon knockdown of PACS1 (w/o PACS1). Thus, statistical differences in r suggest that APP parallels SORLA trafficking (SORLA, $p > 0.05$) ultimately resulting in a shift of APP from the TGN ($p < 0.001$) into early endosomes ($p < 0.01$).

	w/ PACS1	w/o PACS1	p value
APP and SORLA			
tM1 (SORLA overlap with APP)	0,504 \pm 0,038	0,457 \pm 0,039	>0.05
tM2 (APP overlap with SORLA)	0,233 \pm 0,018	0,251 \pm 0,002	>0.05
r (correlation APP and SORLA)	0,367 \pm 0,021	0,378 \pm 0,029	>0.05
APP and Vti1b			
tM1 (Vti1b overlap with APP)	0,134 \pm 0,01	0,118 \pm 0,007	>0.05
tM2 (APP overlap with Vti1b)	0,84 \pm 0,016	0,611 \pm 0,028	<0.001
r (correlation APP and Vti1b)	0,348 \pm 0,018	0,266 \pm 0,015	<0.001
APP and EEA1			
tM1 (EEA1 overlap with APP)	0,059 \pm 0,004	0,081 \pm 0,004	<0.001
tM2 (APP overlap with EEA1)	0,448 \pm 0,026	0,559 \pm 0,027	<0.01
r (correlation APP and EEA1)	0,145 \pm 0,011	0,189 \pm 0,009	<0.01

Taken together, in SY5Y-S/A cells treated with a siRNA against PACS1, APP depicts an altered trafficking behaviour resembling that of SORLA. In detail, depletion of PACS1 localizes APP away from TGN compartments and into EEA1-positive vesicles strongly suggesting the hypothesized role of SORLA as a trafficking receptor for APP.

3.2.3. Knockdown of PACS1 affects APP processing in SY5Y-S/A cells

Intracellular APP routing is a tightly regulated process. Subtle differences in the trafficking routes may cause an altered processing of the protein. A defect in retrograde TGN-retrieval results in an accumulation of APP in endosomes where amyloidogenic processing is supposed to be initiated (Soriano, Chyung et al. 1999) (Kinoshita, Fukumoto et al. 2003). On the other hand, less abundance of SORLA in the TGN may correlate with increased release of APP to the cell surface where α -secretases reside (Lammich, Kojro et al. 1999).

Since PACS1 knockdown in SY5Y-S/A cells shifted SORLA and APP from the TGN into endosomal compartments, I determined levels of APP metabolites in the supernatant of SY5Y-S/A cells treated with a siRNA against PACS1. In line with my assumption of altered trafficking influencing APP processing, loss of PACS1 coincided with an increase in sAPP α , sAPP β , A β ₄₀ and A β ₄₂ levels (Fig. 32).

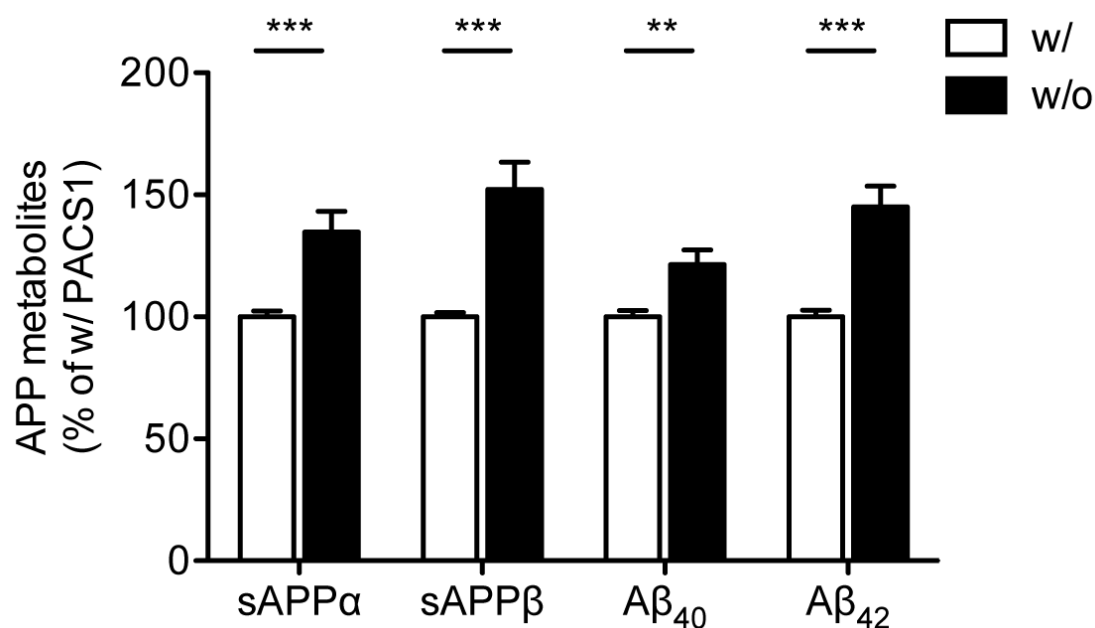


Figure 32: Loss of PACS1 enhances APP processing in SY5Y-S/A cells.

APP processing products in the supernatant of SY5Y-S/A cells treated with a siRNA against PACS1 (w/o PACS1) or with a scrambled control siRNA (w/ PACS1) were determined using an immunobased biological assay (Meso Scale Discovery). Levels of soluble (s) APP α , sAPP β , A β ₄₀, and A β ₄₂ are depicted. Values are given as the mean \pm standard error of the mean and were calculated as % of w/ PACS1 (set to 100%) (triplicate measurements of five experiments for each condition).

Levels of sAPP α , sAPP β , A β ₄₀, and A β ₄₂ in the supernatant of cells treated with siRNA against PACS1 (w/o PACS1) were significantly increased compared to scrambled siRNA treated cells (w/ PACS1) as evaluated by Student's *t*-test (**, $p < 0.01$; ***, $p < 0.001$).

3.2.4. Effects of siRNA-mediated PACS1 knockdown on β -secretase (BACE1) activity

Being a trafficking adaptor for various proteins, PACS1 may influence the catabolism of APP independent of SORLA sorting. For example, PACS1 is implicated in the trafficking of furin, a protease that regulates the maturation of BACE1, the secretase catalyzing the first step in amyloidogenic processing (Wan, Molloy et al. 1998; Creemers, Ines Dominguez et al. 2001). Furthermore, GGA3 acts as an adaptor protein in a complex together with PACS1 potentially resulting in an impaired GGA3 stability upon loss of PACS1 (Scott, Fei et al. 2006). GGA3, on the other hand, facilitates degradation of BACE1 (Tesco, Koh et al. 2007). All together, the aforementioned facts suggest a potential role for PACS1 in the metabolism of BACE1.

To further explore this concept, I measured GGA3 and BACE1 protein levels. Since maturation of BACE1 may influence its catalytic function, I also determined enzymatic activity of this secretase.

Knockdown of PACS1 in SY5Y-S/A cells revealed no influence of loss of PACS1 on GGA3 expression (Fig. 33A and B). Analysis of cellular extracts by western blot revealed three distinct bands corresponding to various glycosylation forms of BACE1. Of those, the 75kDa species (Fig. 33C, 1*) denotes the fully matured BACE1 protein. Notably, loss of PACS1 did not affect BACE1 protein levels (Fig. 33C). To ultimately test the influence of PACS1 knockdown on BACE1 activity, I performed a BACE1 activity assay. In detail, a secretase substrate is tagged with two fluorophores, a donor and an acceptor. The donor emits fluorescent energy upon light excitation that is quenched by the acceptor. Upon enzymatic cleavage by BACE1, the quenching is released and thereby the substrate starts emitting fluorescent signals. Thus, the read-out of fluorescence over time allows conclusions regarding the cleavage rate and activity of the secretase.

In this assay, loss of PACS1 did not interfere with BACE1 activity (Fig. 33D) indicating, all in all, a negligible effect of PACS1 knockdown on BACE1 function.

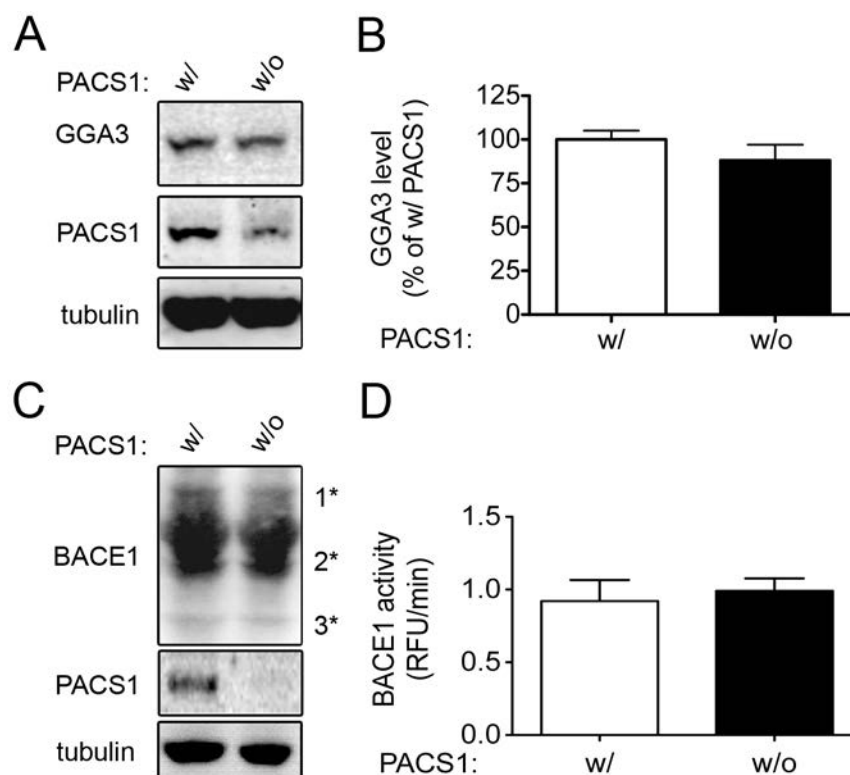


Figure 33: Effect of PACS1 knockdown on GGA3 and BACE1 expression and activity in SY5Y-S/A cells.

SY5Y-S/A cells were treated with a siRNA against PACS1 (w/o PACS1) or with a scrambled control siRNA (w/ PACS1) to elucidate the influence of PACS1 on protein levels of GGA3 and BACE1 and on BACE1 activity.

(A, B) Western blot analysis and densitometric scanning of replicate blots revealed unchanged GGA3 expression upon loss of PACS1 (C) as well as unchanged protein levels of fully glycosylated, mature, BACE1 (1*), N-linked oligosaccharides modified BACE1 (2*), or unglycosylated BACE1 precursor (3*).

(D) *In vitro* assay to measure catalytic activity of BACE1 based on processing of a secretase substrate tagged with two fluorophores. Fluorescent energy upon light excitation of one fluorophore is quenched by an acceptor fluorophore. Enzymatic cleavage by BACE1 disrupts resonance energy transfer between the fluorophores, thus, leading to an increase in fluorescence. Relative fluorescence units (RFU) per minute are measured to assess BACE1 activity. Enzymatic activity of BACE1 in SY5Y-S/A cells is not affected upon loss of PACS1.

Values are given as the mean \pm standard error of the mean (number of samples per condition: 9 - 13). Differences between the conditions in the experiments were tested for statistical significance using Student's *t*-test ($p > 0.05$).

3.2.5. SORLA-independent function for PACS1 in amyloidogenic processes

Influence of PACS1 deficiency on APP processing in SY5Y cells expressing a SORLA mutant lacking the cytoplasmic domain

To ultimately prove the involvement of SORLA in PACS1-mediated effect on APP processing, I performed knockdown of PACS1 in SH-SY5Y cells, stably overexpressing APP695 and a SORLA variant that lacks the cytoplasmic tail and is therefore not affected by PACS1-mediated sorting (SY5Y-S^{ΔCD}/A) (Schmidt, Sporbert et al. 2007). Similar to SY5Y-S/A cells, loss of PACS1 did not affect expression levels of APP and SORLA in SY5Y-S^{ΔCD}/A cells (Fig. 34A and B).

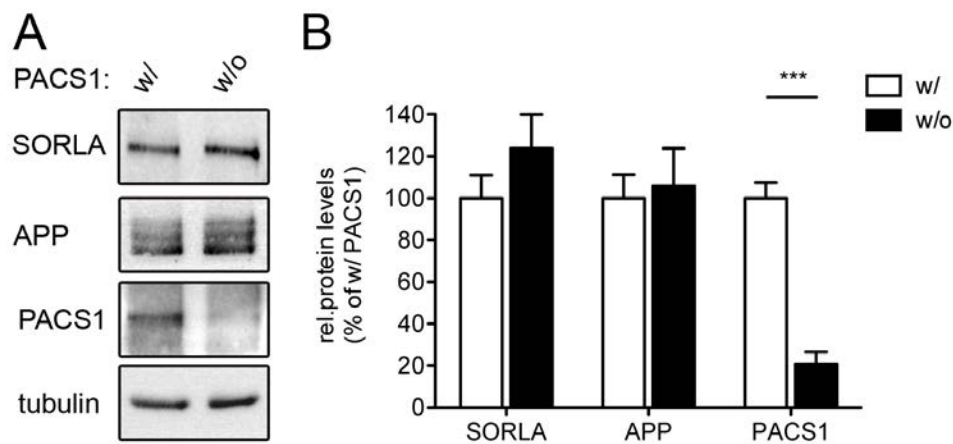


Figure 34: Knockdown of PACS1 in SY5Y cells expressing a tailless SORLA mutant.

SH-SY5Y cells stably overexpressing human APP695 and a SORLA variant lacking the cytoplasmic tail (SORLA^{ΔCD}) were treated with siRNA against endogenous PACS1 (w/o PACS1) or with a scrambled control siRNA (w/ PACS1).

(A) Effect of siRNA treatment on protein levels of SORLA, APP, and PACS1 was monitored by western blotting.

(B) Quantification of replicate blots by densitometric scanning (number of samples per condition: 7) revealed a significant reduction in PACS1 expression in siRNA-treated cells (***, $p < 0.001$). In contrast, SORLA and APP protein levels were not affected ($p > 0.05$).

Values are given as the mean \pm standard error of the mean. Statistical differences in SORLA, APP, and PACS1 protein levels were evaluated using Student's *t*-test. Detection of tubulin served as a loading control.

Although PACS1 levels are strongly downregulated upon siRNA mediated knockdown (w/o PACS1), sAPP α , sAPP β , and, A β ₄₀ levels were unaffected in SY5Y-S^{ΔCD}/A cells arguing against a change in amyloidogenic and non-amyloidogenic processing (Fig. 35). Surprisingly,

$A\beta_{42}$ levels were increased upon loss of PACS1 suggesting a specific, SORLA-independent effect of PACS1 on the metabolism of $A\beta_{42}$.

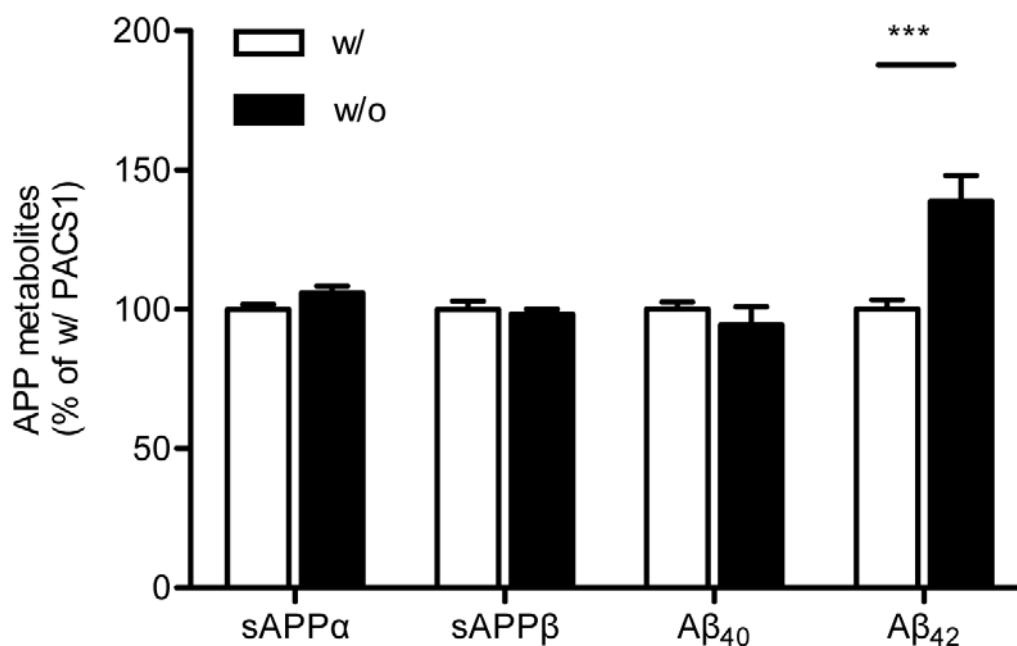


Figure 35: Effect of PACS1 knockdown on APP processing in SY5Y cells expressing a tailless SORLA mutant.

APP processing products in the supernatant of SY5Y-S^{CD}/A cells treated with a siRNA against PACS1 (w/o PACS1) or with a scrambled control siRNA (w/ PACS1) were determined using an immunobased biological assay (Meso Scale Discovery). Levels of soluble (s) APP α , sAPP β , A β_{40} , and A β_{42} are depicted. Values are given as the mean \pm standard error of the mean and were calculated as % of w/ PACS1 (set to 100%) (triplicate measurements of five experiments for each condition). According to Student's *t*-test, sAPP α , sAPP β , and A β_{40} levels were unchanged upon knockdown of PACS1 ($p > 0.05$). However, levels of A β_{42} are significantly increased in cells treated with siRNA against PACS1 (w/o PACS1) compared to scrambled siRNA-treated cells (w/ PACS1) (***, $p < 0.001$).

SORLA-independent function for PACS1 in the catabolism of A β_{42}

PACS1 regulates the intracellular trafficking of various proteins, including the cation-independent mannose-6-phosphate receptor (CI-MPR). This sorting receptor acts by shuttling mannose-6-phosphate containing cargo to endosomal compartments. Rerouting of the receptor to the TGN requires the action of PACS1 (Scott, Fei et al. 2006).

Amongst its multiple cargos, CI-MPR targets the zymogene cathepsin B to the lysosome where it is proteolytically activated. Being a cysteine protease, mature cathepsin B degrades various substrates in the lysosome or, upon secretion, in the extracellular space (Fig. 36) (Roshy, Sloane et al. 2003). Notably, cathepsin B specifically degrades A β_{42} over other A β forms, such as A β_{40} (Mueller-Steiner, Zhou et al. 2006). Hence, I reasoned that the SORLA-

independent mechanism of PACS1 on $A\beta_{42}$ catabolism may be based on alterations in the CI-MPR-cathepsin B system.

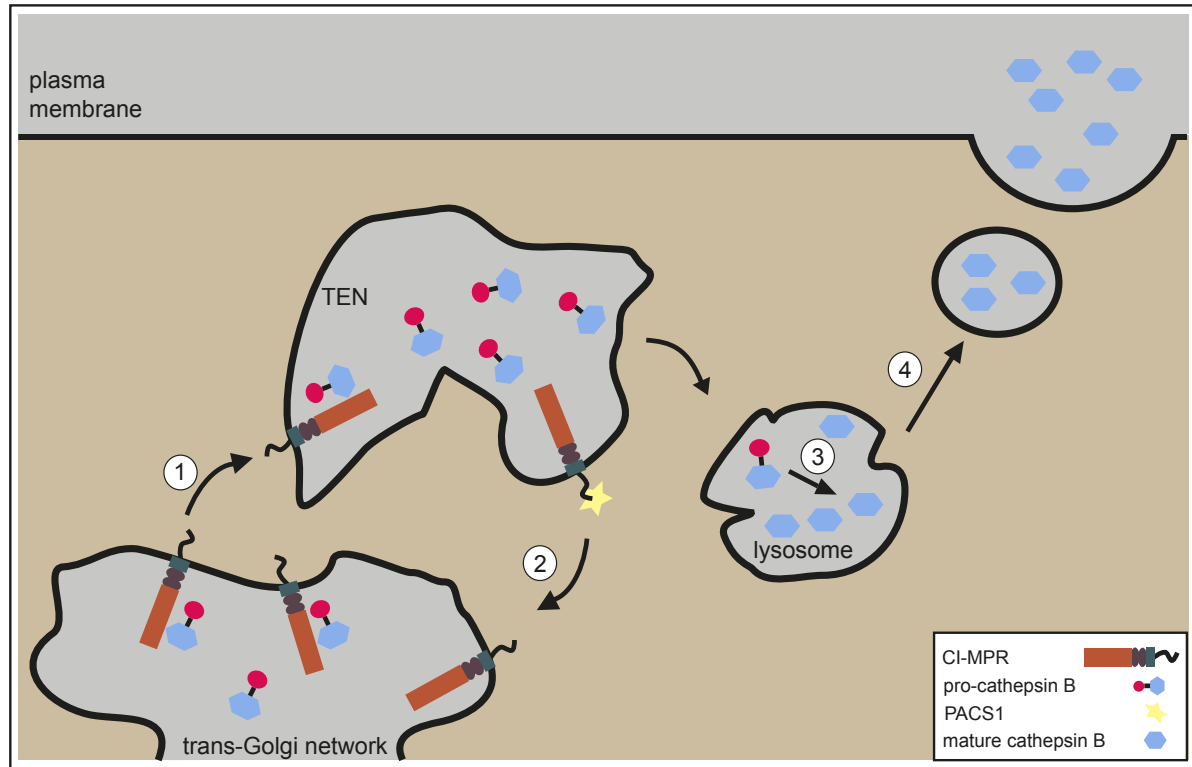


Figure 36: Model for PACS1-dependent sorting of the CI-MPR.

The cation-independent mannose-6-phosphate receptor (CI-MPR) targets the proenzyme cathepsin B (pro-cathepsin B) to the tubular endosomal network (TEN) (1). Upon release of its cargo, CI-MPR is re-routed to the trans-Golgi network (TGN) and recycled for another round of sorting. The TGN retrieval depends on the interaction with PACS1 (Scott, Fei et al. 2006) (2).

Reaching the endosomal network in its inactive state, pro-cathepsin B traffics to lysosomal compartments where it is processed into its active form (mature cathepsin B) (3). The cysteine protease cathepsin B exerts its action in degrading peptides in the endo-lysosomal system and, upon secretion (4), in the extracellular space (Roshy, Sloane et al. 2003). Among the various substrates, cathepsin B degrades specifically $A\beta_{42}$ over other $A\beta$ forms (Mueller-Steiner, Zhou et al. 2006).

To that end, I determined cathepsin B and CI-MPR protein levels in SY5Y-S/A cells treated with a siRNA against PACS1 or a scrambled control siRNA (w/ PACS1). Knockdown of PACS1 (w/o PACS1) revealed significantly decreased levels of the CI-MPR ($p < 0.001$) compared to controls (w/ PACS1) suggesting improper routing of this receptor (Fig. 37A and B). In line with an aberrant trafficking of CI-MPR as a consequence of a loss of PACS1, mature cathepsin B levels are decreased in cell lysate and cell supernatant (Fig. 37C and D).

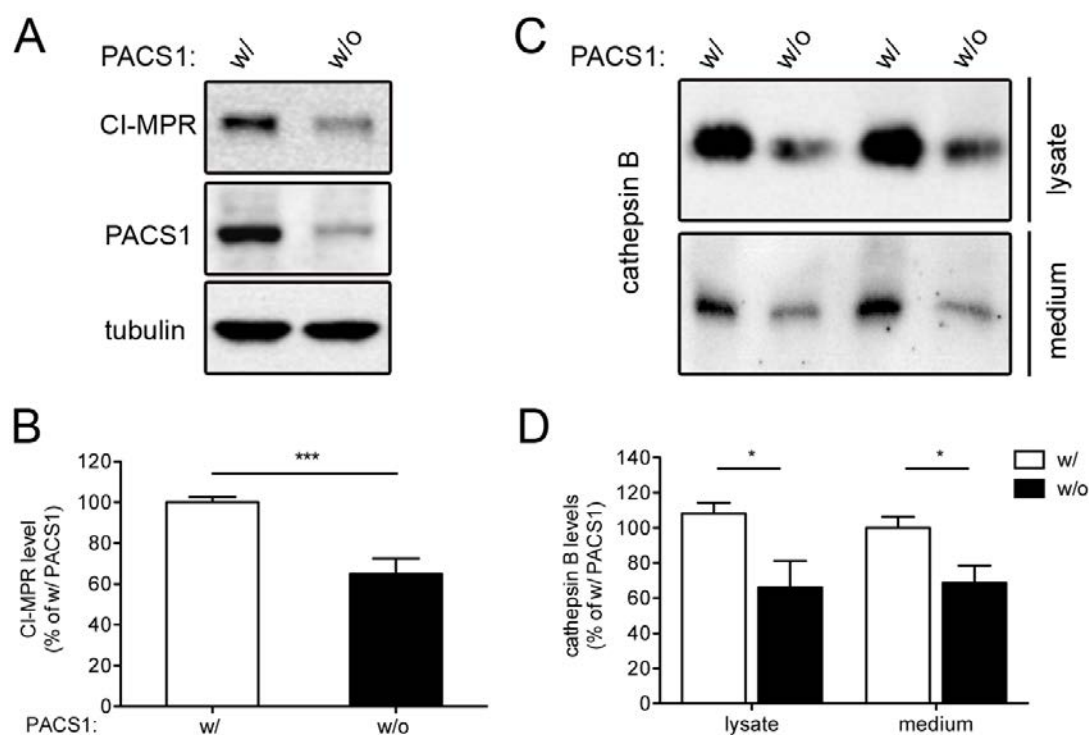


Figure 37: Knockdown of PACS1 affects protein levels of the cation-independent mannose-6 phosphate receptor and of cathepsin B in SY5Y-S/A cells.

SY5Y-S/A cells were treated with a siRNA against PACS1 (w/o PACS1) or with a scrambled control siRNA (w/ PACS1).

(A, C) Levels of the cation-independent mannose-6-phosphate receptor (CI-MPR) in the lysate and cathepsin B in lysate and supernatant of cells were analyzed by western blotting.

(B, D) Densitometric scanning of replicate blots (number of samples per condition: 9 - 13) show a significantly reduced expression of the CI-MPR in the cell lysate and of cathepsin B in cell lysate and medium upon loss of PACS1 (w/o PACS1) (*, $p < 0.05$; ***, $p < 0.001$). Values are given as the mean \pm standard error of the mean. Differences in protein levels between the conditions were evaluated by Student's *t*-test.

The cation-dependent mannose-6-phosphate receptor (CD-MPR) is also involved in the trafficking of cathepsin B. To exclude potential effects of PACS1 knockdown on CD-MPR expression, I determined CD-MPR protein levels in SY5Y-S/A cells treated with PACS1 siRNA. Knockdown of PACS1 failed to influence CD-MPR expression levels pointing towards alterations in CI-MPR protein levels as the cause for changes in mature cathepsin B levels in these cells (Fig. 38).

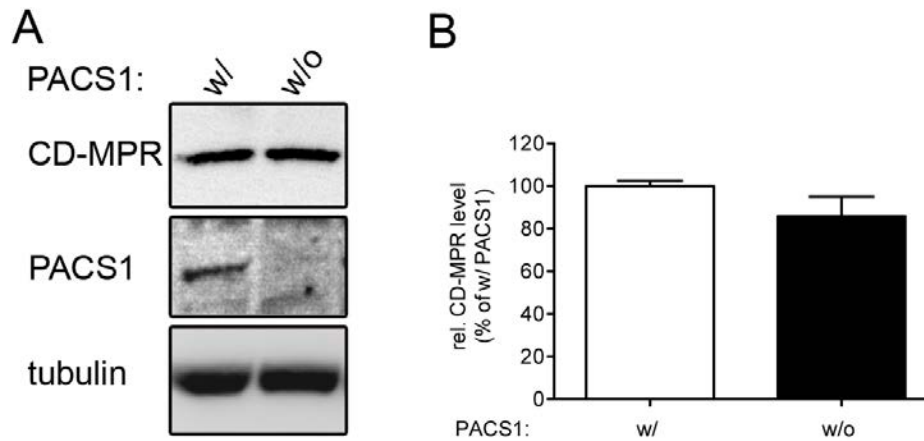


Figure 38: Loss of PACS1 does not impair CD-MPR expression levels in SY5Y-S/A cells.

SY5Y-S/A cells were treated with a siRNA against PACS1 (w/o PACS1) or with a scrambled control siRNA (w/ PACS1).

(A) Protein levels of the cation-dependent mannose-6-phosphate receptor (CD-MPR) were monitored by western blotting.

(B) Densitometric scanning of replicate blots (number of samples: 10) indicate no influence of PACS1 knockdown on CD-MPR expression ($p > 0.05$). Values are given as the mean \pm standard error of the mean. Differences in protein levels between the conditions were evaluated by Student's *t*-test.

In line with lower protein levels of CI-MPR following knockdown of PACS1, I propose a mechanism whereby loss of PACS1 leads to an altered trafficking of CI-MPR which, in turn, causes an aberrant transport of cathepsin B to the endosomal/lysosomal system leading to decreased mature cathepsin B protein levels and, consequently, an increase in $A\beta_{42}$.

4. DISCUSSION

My investigations substantiated the relevance of intracellular sorting of SORLA for APP trafficking and processing in neuronal cell lines as well as in the brain of mice *in vivo*. In detail, these findings pinpoint three underlying concepts concerning neuronal transport and catabolism of APP and its cleavage products.

Firstly, experiments in mice uncovered a role for adaptor protein mediated sorting of SORLA for APP routing and amyloidogenic processing *in vivo*. Secondly, findings in neuronal cells shed light on the molecular mechanism of PACS1-regulated retrograde sorting of SORLA and APP. Thirdly, my findings elucidated the importance of PACS1 for the generation of catalytically active cathepsin B, a major A β ₄₂-degrading enzyme.

4.1. IMPLICATION OF SORLA FOR ALZHEIMER'S DISEASE

SORLA is a 250 kDa type-I transmembrane protein highly expressed in the brain that mainly localizes to the TGN of cells, and, with lesser extent also to endosomes and the plasma membrane (Hermans-Borgmeyer, Hampe et al. 1998; Nielsen, Gustafsen et al. 2007).

The receptor's implication in Alzheimer's disease was suggested based on the low expression levels of SORLA seen in Alzheimer's disease patients (Scherzer, Offe et al. 2004). Although several members of the LRP- and VPS10p receptor family are implicated in Alzheimer's disease-related processes, unambiguous genetic evidences for involvement of most of these receptors in late-onset Alzheimer's disease are missing. In contrast, meta-analyses (Reitz, Cheng et al. 2011) and genome-wide association studies (Meng, Lee et al. 2007; Naj, Jun et al. 2011) confirmed the association of several single nucleotide polymorphisms (SNPs) in *Sorll* with Alzheimer's disease. In line with low SORLA protein levels in a subgroup of Alzheimer's disease patients (Andersen, Reiche et al. 2005), two closely linked SNPs were identified to cause a decrease in SORLA expression, suggesting low SORLA levels as risk factor in Alzheimer's disease (Caglayan, Bauerfeind et al. 2012).

Follow-up studies showed that SORLA directly interacts with APP, ascribing a role to this receptor as a negative regulator of APP processing (Andersen, Reiche et al. 2005; Andersen, Schmidt et al. 2006; Schmidt, Sporbert et al. 2007). According to current concepts, SORLA mainly localizes to the TGN, where it binds APP and prevents the exit of this precursor into secretory compartments where processing occurs.

Consequently, aberrant intracellular routing of SORLA affects APP localization and cleavage. To elucidate the trafficking behaviour of SORLA, receptor variants lacking binding sites for PACS1 or the retromer complex, adaptor proteins implicated in subcellular trafficking of target proteins between the TGN and endosomes (Schmidt, Sporbert et al. 2007; Fjorback, Seaman et al. 2012) were expressed in established cell lines.

These receptor mutants failed to localize to the TGN and caused increased processing of APP, suggesting a shift of SORLA/APP complexes into endosomal compartments and to the plasma membrane where amyloidogenic- and non-amyloidogenic processing happen, respectively.

However, Alzheimer's disease is a multifactorial disease in the brain that involves a complex interplay between neurons, glia, and immunoreactive cells. Therefore, molecular concepts gained in non-neuronal cell lines discussed above do not necessarily reflect the *in vivo* situation in the diseased brain.

4.2. ROLE OF SORLA IN ALZHEIMER'S DISEASE *IN VIVO*

Studies in *Sor11* null mice reported elevated levels of amyloidogenic and non-amyloidogenic processing products and an increased amyloid plaque burden, supporting a role for SORLA in regulating APP processing *in vivo* as well (Andersen, Reiche et al. 2005; Rohe, Carlo et al. 2008). However, whether increased processing originates from abnormal APP routing or from a so far unknown function of SORLA remained unanswered. To ultimately confirm faulty trafficking of SORLA as the underlying cause of increased APP processing *in vivo*, I generated mouse models expressing SORLA mutants that are unable to interact with the trafficking adaptors PACS1 (SORLA^{acidic}) or the retromer complex (SORLA^{FSAF}).

4.2.1. Generation of novel mouse models to study SORLA function in Alzheimer's disease processes *in vivo*

I conducted several attempts to introduce mutations in the *Sor11* locus that lead to the expression of SORLA variants unable to bind PACS1 or the retromer complex (Fig. 8). Since I was not able to accomplish successful targeting of the *Sor11* locus, I knocked-in cDNAs encoding human SORLA variants into the *Rosa26* locus using homologous recombination in embryonic stem cells (Fig. 12). This approach is favoured over pronuclear injection of

transgenes since it enables expression of the cDNA under control of the endogenous *Rosa26* promoter resulting in similar expression levels of the different SORLA variants and allowing for direct comparison between the various mouse lines.

Nevertheless, there are several concerns in respect to the chosen approach. The expression pattern as well as the expression level of *Rosa26* may be different compared to endogenous *Sorll* potentially leading to a loss of the receptor's ability to influence Alzheimer's disease-related processes. To exclude such confounding issues, I always compared mice expressing SORLA^{FSAF} or SORLA^{acidic} with animals expressing human wild-type SORLA cDNA (SORLA^{wt}) but not with *Sorll*^{+/+} mice, expressing endogenous, murine SORLA.

Mice deficient for endogenous murine SORLA (*Sorll*^{-/-}) but homologous for the SORLA cDNA in the *Rosa26* locus, express the receptor in comparable levels in cortex and hippocampus (Fig. 14), brain areas that are severely affected in Alzheimer's disease (Armstrong 2011). Remarkably, transgene protein levels equal that of endogenous murine SORLA documenting suitability of the generated model to study the effect of SORLA variants on APP processing. Although I cannot exclude with certainty that the expression of murine SORLA and SORLA^{wt}, SORLA^{FSAF}, and SORLA^{acidic} may differ in some cell populations in the brain, the overall expression pattern of human and murine SORLA in cortex and hippocampus is comparable with the receptor being mainly confined to neurons (Fig. 16).

4.2.2. Human SORLA^{wt} cDNA expression protects APP from processing in a mouse model of Alzheimer's disease

Initially, I crossed the SORLA^{wt} animals with the 5xFAD line of mice, an established Alzheimer's disease mouse model (Oakley, Cole et al. 2006). 5xFAD mice express transgenes for both a mutant human APP695 carrying the Swedish, the Florida, and the London EOAD mutation and for a protein in the γ -secretase complex, human Presenilin 1, harboring two EOAD mutations. The expression of both transgenes is driven by the neural-specific *Thy1* promoter to achieve overexpression in the brain. I focused on the analysis of the cortex, a part of the brain that is particularly vulnerable to neurodegeneration (Armstrong 2011).

Previously, loss of endogenous SORLA was shown to increase processing of murine APP (Andersen, Reiche et al. 2005) as well as human APP in two mouse models of Alzheimer's disease (Dodson, Andersen et al. 2008; Rohe, Carlo et al. 2008). To further substantiate the

hypothesis of SORLA being a negative regulator of APP processing and to, more importantly, confirm the functionality of human wild-type SORLA expressed in the *Rosa26* locus, I determined the levels of APP processing products in 5xFAD/*Sor11*^{-/-} and 5xFAD/SORLA^{wt} mice (Fig. 24).

Analysis of cortical brain extracts of 5xFAD/*Sor11*^{-/-} mice revealed an increase by 106 % in the non-amyloidogenic processing product sAPP α . Elevated sAPP α levels support a model whereby loss of SORLA allows for more efficient exit of APP from the TGN to the cell surface, where non-amyloidogenic processing occurs (Sisodia 1992). APP that escapes α -secretase processing at the plasma membrane, is internalized and reaches endosomal compartments where β - and γ -secretases reside. In line with this assumption, levels of sAPP β (21 %), A β ₄₀ (51 %), and A β ₄₂ (66 %) were also increased in *Sor11*^{-/-} mice as compared to SORLA^{wt} animals. As levels of full-length APP were not changed in *Sor11* null mice, increased APP expression as a result of elevated APP processing products can be excluded (Fig. 25).

SORLA is supposed to act as a retention factor for APP in the TGN. Conceptually, a decrease in SORLA expression is expected to result in an equal increase of sAPP α and sAPP β as seen in cell lines, in mice, or in primary neurons derived thereof (Schmidt, Sporbert et al. 2007; Rohe, Carlo et al. 2008). This effect, however, was not seen in my 5xFAD model wherein sAPP α and sAPP β levels in *Sor11* null mice were increased to a different extent (106 % vs. 21 %) compared to SORLA^{wt}. The most likely explanation for this discrepancy lies in the peculiarity of the Swedish EOAD mutation in APP695 in the 5xFAD model that allows better accessibility of the β -secretase (Haass, Lemere et al. 1995), resulting in higher basal levels of sAPP β generation and a concomitant decrease in sAPP α production (Oakley, Cole et al. 2006). Hence, quantitatively equal changes in amyloidogenic and non-amyloidogenic processing cannot be appreciated by increases in sAPP α and sAPP β production in this mouse line. In support of this assumption, measurements of cortical extracts of SORLA-deficient mice expressing APP695 with the Swedish EOAD mutation in another mouse model in a previous study revealed subtle differences in sAPP β but a strong increase in sAPP α levels compared to control animals (Dodson, Andersen et al. 2008).

Following β -secretase cleavage, the remaining β -CTF is processed by the γ -secretase resulting in A β peptides of various lengths, which should, consequently, lead to a proportional increase in sAPP β and A β . However, *Sor11* null mice crossed with 5xFAD animals show a 21 %

increase in sAPP β but increases of 51 % and 66 % for A β ₄₀ and A β ₄₂, respectively (Fig. 24). This discrepancy may be explained by two different mechanisms.

Firstly, sAPP β and A β strongly differ in molecular weight and, therefore, may be differently affected by unspecific proteolytic degradation resulting in non-equimolar levels in the cell medium.

Secondly, SORLA also plays a role in the catabolism of A β . Recent findings suggest, that SORLA binds and internalizes extracellular A β and, thereby, mediates the transport of the peptide into lysosomes where proteolytic breakdown occurs (Safak Caglayan, PhD thesis, 2013). In line with these data, loss of SORLA would result in a decreased degradation of A β and, consequently, an increased A β abundance in brain lysates of *Sor11* null mice.

All in all, investigations in SORLA-deficient 5xFAD mice revealed two important findings. Firstly, analyses of APP metabolites substantiated the molecular function of SORLA as a negative regulator of APP processing and corroborate 5xFAD as a suitable model to study the influence of SORLA on APP processing. Secondly, and more importantly for my thesis project, my experiments confirmed the functionality of human wild-type SORLA cDNA knocked-in into the *Rosa26* locus in modulating APP processing. Hence, SORLA expression controlled by the *Rosa26* promoter protects APP from amyloidogenic- and non-amyloidogenic processing comparable to the situation seen with the endogenously expressed, murine receptor. Thus, a knock-in of SORLA cDNA variants into the *Rosa26* locus turned out to be a suitable approach to study the consequence of mutations in the cytoplasmic tail of SORLA for the processing of APP *in vivo*.

4.2.3. SORLA^{FSAF} and SORLA^{acidic} variants exhibit an altered subcellular localization and cause increased processing of APP in 5xFAD mice

To test the consequence of mutated binding sites for PACS1 or for the retromer complex in the cytoplasmic tail of SORLA on the processing of APP in the brain *in vivo*, I also crossed the SORLA^{FSAF} and SORLA^{acidic} animals with the 5xFAD line of mice and compared them to the prior established 5xFAD/SORLA^{wt} line.

Remarkably, 5xFAD/SORLA^{acidic} and 5xFAD/SORLA^{FSAF} mice showed increased levels of sAPP α , sAPP β , A β ₄₀, and A β ₄₂ as compared to 5xFAD/SORLA^{wt} animals (Fig. 24). Total APP levels were not altered comparing 5xFAD/SORLA^{acidic} and 5xFAD/SORLA^{FSAF} with

5xFAD/SORLA^{wt} mice (Fig. 25). Thus, changes in levels of APP cleavage products in the trafficking mutant lines are likely caused by altered APP processing rates. Studies showing that SORLA binds and traffics APP strongly suggest that altered APP routing is the underlying molecular cause for this imbalance in processing in the mutant mice (Schmidt, Sporbert et al. 2007; Herskowitz, Offe et al. 2012). This hypothesis was confirmed by my analyses of SORLA transport in primary neurons from the various mouse lines (Fig. 17 - 20). Mutations in SORLA^{acidic} and SORLA^{FSAF} disrupt binding sites for PACS1 or the retromer complex, adaptors that are implicated in endosome-to-TGN trafficking. In line with a proposed TGN-retrieval defect, SORLA^{acidic} and SORLA^{FSAF} accumulate in endosomes of primary neurons (Fig. 19). The fate of the accumulating SORLA molecules is unclear at present. Lysosomal localization of SORLA^{acidic} and SORLA^{FSAF} is not altered (Fig. 20), arguing against an aberrant shunt of the molecules into late endosomal/lysosomal degradation pathways. In the most obvious scenario, retrieval of SORLA^{acidic} and SORLA^{FSAF} from endosomes to the TGN may simply be delayed, resulting in a prolonged residence time of SORLA^{acidic} and SORLA^{FSAF} molecules in endosomes. Although both PACS1 and the retromer complex are implicated in TGN-retrieval (Bonifacino and Hurley 2008; Youker, Shinde et al. 2009), they seem to adopt non-redundant functions in the intracellular sorting of SORLA since mutation of one binding site cannot be compensated completely by the action of the other adaptor. Still, a SORLA mutant line lacking binding sites for both PACS1 and the retromer complex may show more severe defects.

Since amyloidogenic processing predominantly occurs in the endosomal compartment (Soriano, Chyung et al. 1999; Kinoshita, Fukumoto et al. 2003), a delayed retrieval of SORLA from endosomes may explain the increased production of sAPP β in SORLA^{FSAF} (16 %) and in SORLA^{acidic} (18 %) expressing mice (Fig. 24). The remaining CTF is further subjected to γ -secretase cleavage yielding A β peptides (De Strooper 2003). Consequently, in SORLA^{FSAF} or SORLA^{acidic} mice, levels of A β ₄₀ (32 % and 58 %) and A β ₄₂ (57 % and 70 %) are also increased. A model how faulty trafficking of SORLA^{FSAF} and SORLA^{acidic} causes increased amyloidogenic processing as compared to the normal situation is discussed in Fig. 39A and B.

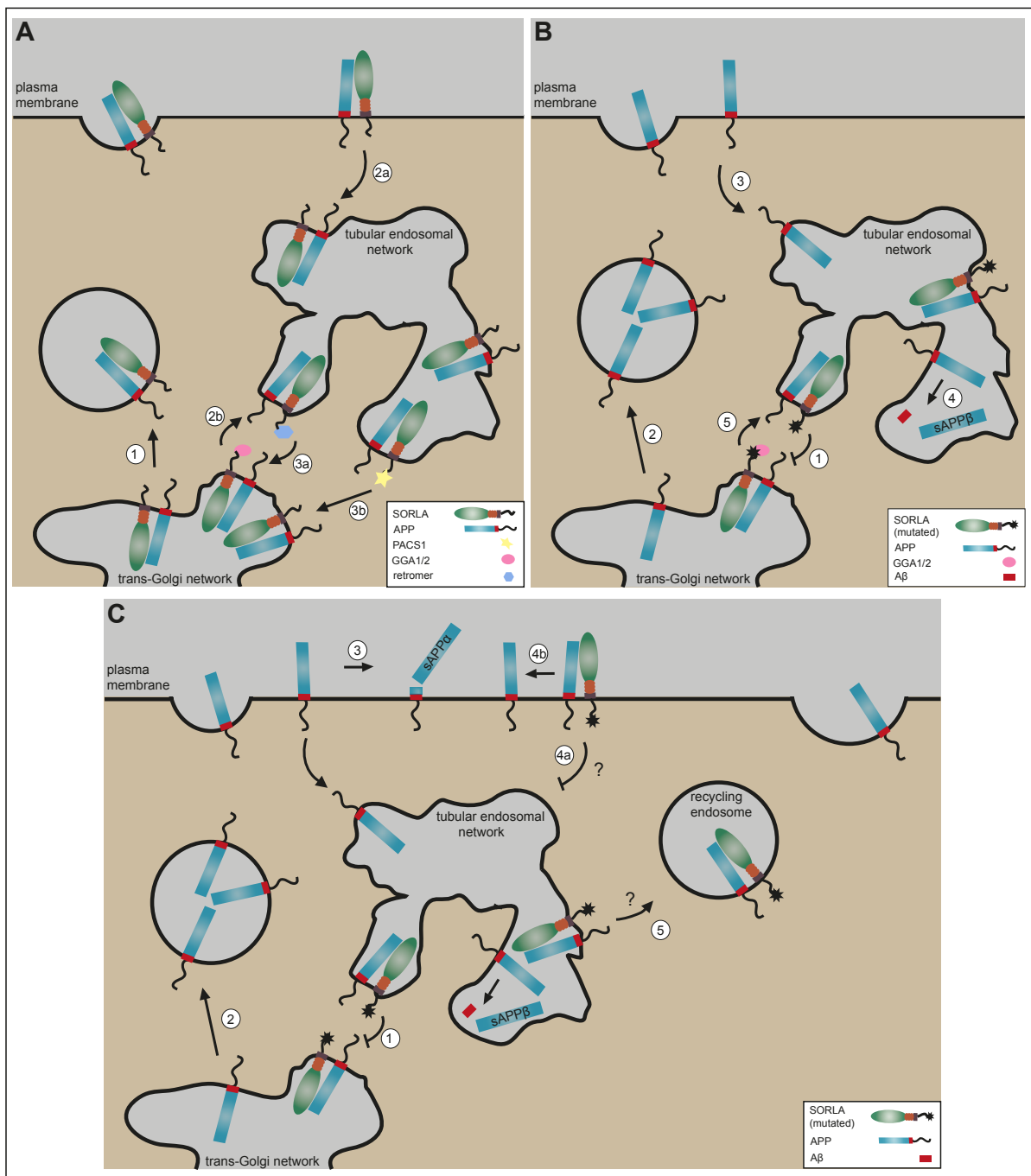


Figure 39: Model for the role of the interaction between SORLA and PACS1 or the retromer complex in trafficking and processing of APP.

(A) APP trafficking and processing in normal neurons: Wild-type SORLA interacts with APP in the trans-Golgi network (TGN) in neurons and reduces the release of APP to the cell surface (1) where non-amyloidogenic cleavage occurs. SORLA/APP complexes enter the tubular endosomal network (TEN) either via endocytosis from the plasma membrane (2a) or via GGA1/2-dependent anterograde transport from the TGN (2b). SORLA protects APP from cleavage by β - and γ -secretase in endosomes via retrograde routing of the receptor to the TGN involving interaction of SORLA with the retromer complex (3a) and PACS1 (3b). (*Figure legend continues.*)

(Figure legend continued.)

(B) Amyloidogenic processing in cells expressing SORLA trafficking mutants: Expression of SORLA mutants lacking the PACS1 (SORLA^{acidic}) or retromer (SORLA^{FSAF}) binding motif in neurons impairs endosome-to-TGN sorting of SORLA and APP (1), resulting in an increased residence time of APP in the TEN. Additionally, lack of SORLA in the TGN allows APP to exit to the cell surface (2) and, upon internalization (3), to be converted into sAPP β and A β (4). Alternatively, APP may reach endosomal compartments via anterograde transport, involving the interaction of SORLA with GGA1/2 (5).

(C) Non-amyloidogenic processing in cells expressing SORLA trafficking mutants: As a consequence of a defective retrograde sorting of SORLA^{FSAF} and SORLA^{acidic} (1), receptor levels in the TGN are decreased, resulting in an inability to retain APP in the TGN, thus, leading to the escape of APP to the cell surface (2) where non-amyloidogenic processing occurs (3).

The PACS1-binding site in SORLA overlaps with an interaction motif for AP2, a protein important for the internalization of receptors from the cell surface. Impaired internalization of SORLA^{acidic}/APP complexes (4a) may result in increased sAPP α levels (4b).

Although not clarified in this study, accumulation of SORLA in endosomes may lead to an increased rerouting of SORLA^{FSAF} and/or SORLA^{acidic} to the plasma membrane via recycling endosomes (5), potentially further increasing non-amyloidogenic processing.

So far, most studies focused on the effect of SORLA on APP trafficking and disregarded sorting of the CTF of APP, the γ -secretase substrates. The cytoplasmic tail of SORLA was shown to interact with the CTF and potentially affects its trafficking (Spoelgen, von Arnim et al. 2006). Thus, improper TGN-rerouting of SORLA^{FSAF} and SORLA^{acidic} compared to SORLA^{wt} would increase the time span of the CTF in compartments where the γ -secretase reside, ultimately resulting in an elevated processing into A β . Hence, aberrant CTF routing may serve as an explanation for non-equimolar concentrations of sAPP β and A β seen in SORLA^{FSAF} and SORLA^{acidic} mice.

Compared to SORLA^{wt}, non-amyloidogenic processing in animals expressing SORLA^{acidic} (62 %) is also increased.

The PACS1-binding site mutated in the cytoplasmic tail of SORLA^{acidic} also overlaps with an interaction motif of AP2, important for internalization of transmembrane proteins from the plasma membrane (Nielsen, Gustafsen et al. 2007). Thus, SORLA^{acidic} may be less efficiently internalized and resides at the cell surface, resulting in an increased non-amyloidogenic APP cleavage (see model in Fig. 39C).

As seen in SORLA^{acidic}-expressing mice, non-amyloidogenic processing in animals expressing SORLA^{FSAF} (53 %) is also elevated as compared to SORLA^{wt}. Since the mutated retromer binding site in SORLA^{FSAF} was not reported to interfere with internalization, an increased transport of SORLA^{FSAF} via recycling endosomes to the cell surface (Hopkins, Gibson et al. 1994) may cause elevated non-amyloidogenic processing in SORLA^{FSAF} mice compared to SORLA^{wt} (see model in Fig. 39C).

But, since I was not able to detect a difference in plasma membrane localization between SORLA^{wt} and SORLA^{FSAF} or SORLA^{acidic} in confocal immunofluorescence microscopy (data not shown), I favour a different explanation for the elevated sAPP α levels in the two mutant mouse models. Non-amyloidogenic processing in SORLA-deficient animals is supposed to be caused by an increased release of APP from the TGN (Andersen, Reiche et al. 2005; Schmidt, Sporbert et al. 2007). In line with an elevated abundance of SORLA in endosomes, localization of SORLA^{FSAF} and SORLA^{acidic} in the TGN is decreased (Figs. 17 and 18). Hence, less SORLA in the TGN and a concomitant increased exit of APP via secretory vesicles to the cell surface may serve as an explanation for increased non-amyloidogenic processing in animals expressing SORLA^{FSAF} and SORLA^{acidic} (Fig. 39C).

Compared to 5xFAD/SORLA^{wt}, the increase in sAPP α in 5xFAD/*Sor11*^{-/-} animals is higher (106 %) than in 5xFAD/SORLA^{FSAF} (53 %) and 5xFAD/SORLA^{acidic} (62 %) mice. This fact may be explained by SORLA-dependent anterograde trafficking of SORLA^{FSAF}/APP and SORLA^{acidic}/APP complexes.

SORLA interacts with trafficking adaptors GGA1 and GGA2 that are implicated in TGN-to-endosomes transport of the receptor (Schmidt, Sporbert et al. 2007). Consequently, mutation of the GGA binding site in the cytoplasmic tail of SORLA affects SORLA anterograde trafficking and resulted in an increased non-amyloidogenic processing in cell lines. In SORLA^{FSAF} and SORLA^{acidic} the motif mediating interaction with GGA is intact, allowing for anterograde transport of the receptor variants to endosomal compartments in contrast to *Sor11*^{-/-}. Therefore, shuttling of APP from the TGN to endosomes in SORLA^{FSAF} and SORLA^{acidic} mice may slightly increase amyloidogenic processing at the expense of non-amyloidogenic processing, explaining higher sAPP α levels in 5xFAD/*Sor11*^{-/-} mice compared to 5xFAD/SORLA^{FSAF} and 5xFAD/SORLA^{acidic} mice (Fig. 24).

All in all, a retrograde retrieval defect of SORLA^{FSAF} and SORLA^{acidic} likely explains the increased processing of APP seen in the respective mouse models. Remarkably, similar alterations in amyloidogenic processing are seen in SORLA mutant and SORLA-deficient animals, suggesting the impact of altered trafficking of the receptor as being as deleterious as its complete loss. In contrast, non-amyloidogenic processing is more drastically increased in *Sor11*^{-/-} animals as compared to SORLA^{FSAF} and SORLA^{acidic} mice, pointing towards a more pronounced effect of complete loss of SORLA on sAPP α production as compared to SORLA^{FSAF} or SORLA^{acidic}, respectively.

4.2.4. SORLA^{FSAF} and SORLA^{acidic} differ in synaptic localization and provoke alterations in axonal transport of APP

Whereas the role of PACS1 in Alzheimer's disease-related processes is first described in this thesis, a role for the retromer complex in Alzheimer's disease-related processes emerged earlier. Mice heterozygous for a disruption of the retromer subunit *Vps26* exhibit increased levels in sAPP β , A β ₄₀, and A β ₄₂ (Muhammad, Flores et al. 2008). Furthermore, heterozygous deletion of the VPS35 ortholog in *Drosophila melanogaster* caused a 50 % reduction in VPS35 protein amount and resulted in increased A β levels compared to wild-type flies (Muhammad, Flores et al. 2008). Additionally, SNPs in genes that encode components of the retromer complex (SNX1) or regulatory co-factors (SNX3, RAB7A) were associated with an increased risk of Alzheimer's disease (Vardarajan, Bruesegem et al. 2012), providing genetic evidence for an important function of the retromer complex in controlling amyloidogenic processing. A follow-up study revealed a role for retromer in APP trafficking in neurons (Bhalla, Vetanovetz et al. 2012). In detail, shRNA-mediated silencing of VPS35 in primary neurons reduced the frequency of long-range transport of APP in neuronal processes. Furthermore, VPS35 deficiency lead to increased A β production, presumably due to alterations in APP routing in neurons.

Various studies reported colocalization of SORLA and APP in the cell body of non-neuronal cell lines and primary neurons whereby SORLA affects the trafficking of APP (Andersen, Reiche et al. 2005; Offe, Dodson et al. 2006). However, the implication of SORLA for antero- or retrograde transport of APP along the axonal path remained elusive.

That is why I also analysed subcellular localization of SORLA and APP in cortical lysates of my various mouse lines. In these studies, I uncovered that mutation of the retromer-binding site in SORLA did not alter the abundance of this receptor in synaptosomes as compared to SORLA^{wt}, suggesting normal retrograde retrieval of SORLA^{FSAF} from the synapse (Fig. 22). In 5xFAD/SORLA^{FSAF} animals, APP is less prominently present in synaptosomes as compared to SORLA^{wt} suggesting that expression of SORLA^{FSAF} impairs APP routing at the synapse (Fig. 26B and C).

In contrast to the retromer-binding defect, the PACS1-binding defective SORLA mutant is more abundant in compartments enriched for synapses, suggesting a retrograde retrieval defect of this receptor (Fig. 22). Surprisingly, APP does not parallel SORLA^{acidic} routing at the synapse as APP abundance in synaptosomes is not altered as compared to SORLA^{wt} (Fig. 26B and C).

Taken together, my findings revealed a different synaptic localization for SORLA^{FSAF} versus SORLA^{acidic}. Whereas SORLA^{acidic} exhibits a synaptic retrieval defect, SORLA^{FSAF} localizes in synaptosomes comparable to SORLA^{wt}. While interaction of SORLA with PACS1 and retromer may serve related functions in TGN/endosome sorting in the cell soma, interaction with PACS1 seems more important for SORLA routing at the synapse compared to the retromer complex.

Surprisingly, APP does not parallel SORLA trafficking at the synapse. In line with this observation, a recent finding indicated SORLA/APP interaction to be confined to distinct neuronal compartments (Gustafsen, Glerup et al. 2013). In detail, in a proximity ligation assay SORLA/APP complexes were seen in the cell body of primary neurons but not in axons and synapses. Obviously, SORLA does not directly traffic APP along axons, hence, SORLA^{FSAF} must exert its action on synaptic APP trafficking in an indirect still unknown way.

Modifications of the cytoplasmic domain of APP are known to regulate the neuronal routing of the precursor protein. Phosphorylation at Thr⁶⁶⁸ in the tail of APP is supposed to mediate axonal transport (Muresan and Muresan 2005).

The phosphorylation of Thr⁶⁶⁸ in APP is mediated by various kinases, including the glycogen-synthase kinase 3 beta (Aplin, Gibb et al. 1996), the p34cdc2 protein kinase (Suzuki, Oishi et al. 1994), the cyclin-dependent kinase 5 (Iijima, Ando et al. 2000), and the c-jun N-terminal kinases (Kimberly, Zheng et al. 2005) (Taru, Iijima et al. 2002). These kinases act upon stimulation by different signaling cascades. Since activation of elements in the signaling cascade correlate with phosphorylation, I determined phosphorylation levels of AKT and ERK, proteins involved in major signaling cascades and known to be altered upon SORLA-dependent GDNF signaling (Glerup, Lume et al. 2013). However, expression of SORLA^{FSAF} (or SORLA^{acidic}) did not alter phosphorylation levels of ERK and AKT as compared to SORLA^{wt}, suggesting no influence of cytoplasmic mutations of SORLA on these signaling cascades (Fig. 23) and presumably unchanged activity of kinases regulating phosphorylation of Thr⁶⁶⁸ in APP.

APP phosphorylation at Thr⁶⁶⁸ is not altered (Fig. 27). Thus, changes in phosphorylation of APP at Thr⁶⁶⁸ can be excluded as a cause for altered synaptic APP sorting in my 5xFAD/SORLA^{FSAF} mice.

Taken together, mouse models expressing human SORLA variants defective in binding the retromer complex or PACS1, showed an altered receptor trafficking in neurons. In these mice, the expression levels for major adaptor proteins are unchanged (Fig. 21), suggesting the loss of interaction with the retromer complex (SORLA^{FSAF}) or PACS1 (SORLA^{acidic}) as underlying cause for altered routing of the receptor. Crossing these animals with an Alzheimer's disease mouse model resulted in aberrant trafficking and increased processing of APP. Based on my findings, I propose a model whereby SORLA co-traffics APP in the neuronal cell body and thereby influences the catabolism of APP. SORLA mutants non-responsive to PACS1- or retromer-mediated sorting accumulate in endosomes and are likely unable to re-route APP back to the TGN, provoking an increased proteolytic processing fate (Fig. 39B and C).

4.3. THE ROLE OF PACS1 IN ALZHEIMER'S DISEASE-RELATED PROCESSES

My studies *in vivo* substantiated the importance of SORLA for APP processing, focusing on the loss of binding sites conveying the interaction of SORLA with PACS1 or the retromer complex.

Whereas a stretch of aromatic amino acids in the cytoplasmic tail of SORLA is supposed to solely mediate binding to the retromer complex, the acidic cluster in the receptor (that is mutated in SORLA^{acidic}) serves not only as a binding site for PACS1, but also for AP2 and AP1 and thereby potentially mediates both internalization as well as antero- and retrograde transport of the receptor (Nielsen, Gustafsen et al. 2007; Schmidt, Sporbert et al. 2007). Hence, defects in the trafficking of SORLA^{acidic} cannot formally be excluded to arise from disrupted AP1- and/or AP2 binding (rather than defective PACS1 binding). In order to substantiate the function of PACS1 for amyloidogenic processes, I carried out studies in the neuroblastoma cell line SH-SY5Y. In these studies, knockdown of PACS1 expression confirmed a SORLA-dependent role for this adaptor in Alzheimer's disease-related processes. In addition, my experiments also identified a novel function for PACS1 in control of A β levels independent of SORLA activity as discussed in the following.

4.3.1. SORLA-dependent function for PACS1 in APP processing in SY5Y cells

In line with findings obtained in SORLA^{acidic}-expressing mice, I observed a shift of SORLA from the TGN into endosomes upon knockdown of PACS1 in the neuroblastoma cell line SH-SY5Y stably overexpressing SORLA and APP (Figs. 29 and 30). SORLA protein levels were not altered upon PACS1 knockdown (Fig. 28), paralleling normal protein levels (Fig. 14A) seen in SORLA^{acidic} mice. These experiments in a neuronal cell line confirmed a function for PACS1 in retrograde sorting of SORLA and suggest a loss of the PACS1/SORLA interaction as a major cause for aberrant trafficking of SORLA^{acidic} *in vivo*.

Altered routing of SORLA provokes a co-trafficking of APP in various cell lines (Schmidt, Sporbert et al. 2007; Herskowitz, Offe et al. 2012). In agreement with these findings, knockdown of PACS1 resulted in an accumulation of APP in endosomes and a concomitant loss from the TGN (Fig. 31). In contrast, loss of PACS1 did not affect the degree of colocalization between SORLA and APP, documenting co-trafficking of the two molecules in the presence and absence of PACS1 (Fig. 31). As a consequence of altered trafficking of SORLA and APP both amyloidogenic and non-amyloidogenic processing rates were increased in cells lacking PACS1 (Fig. 32).

Normal SORLA and APP protein levels following PACS1 knockdown (Fig. 28) exclude an increase in lysosomal shuttling (and degradation) but rather suggest delayed rerouting to the TGN as the reason for accumulation of SORLA and APP in endosomes. According to my working model (Fig. 40), an extended time-span of APP in endosomal compartments is the major cause of increased amyloidogenic processing as a consequence of PACS1 knockdown.

Although I was not able to detect an increase of SORLA levels at the cell surface by confocal immunofluorescence microscopy upon knockdown of PACS1 (data not shown), I cannot exclude enhanced recycling of SORLA/APP to the plasma membrane or a delayed internalization of SORLA/APP from the cell surface as further consequences of PACS1 loss (Fig. 40).

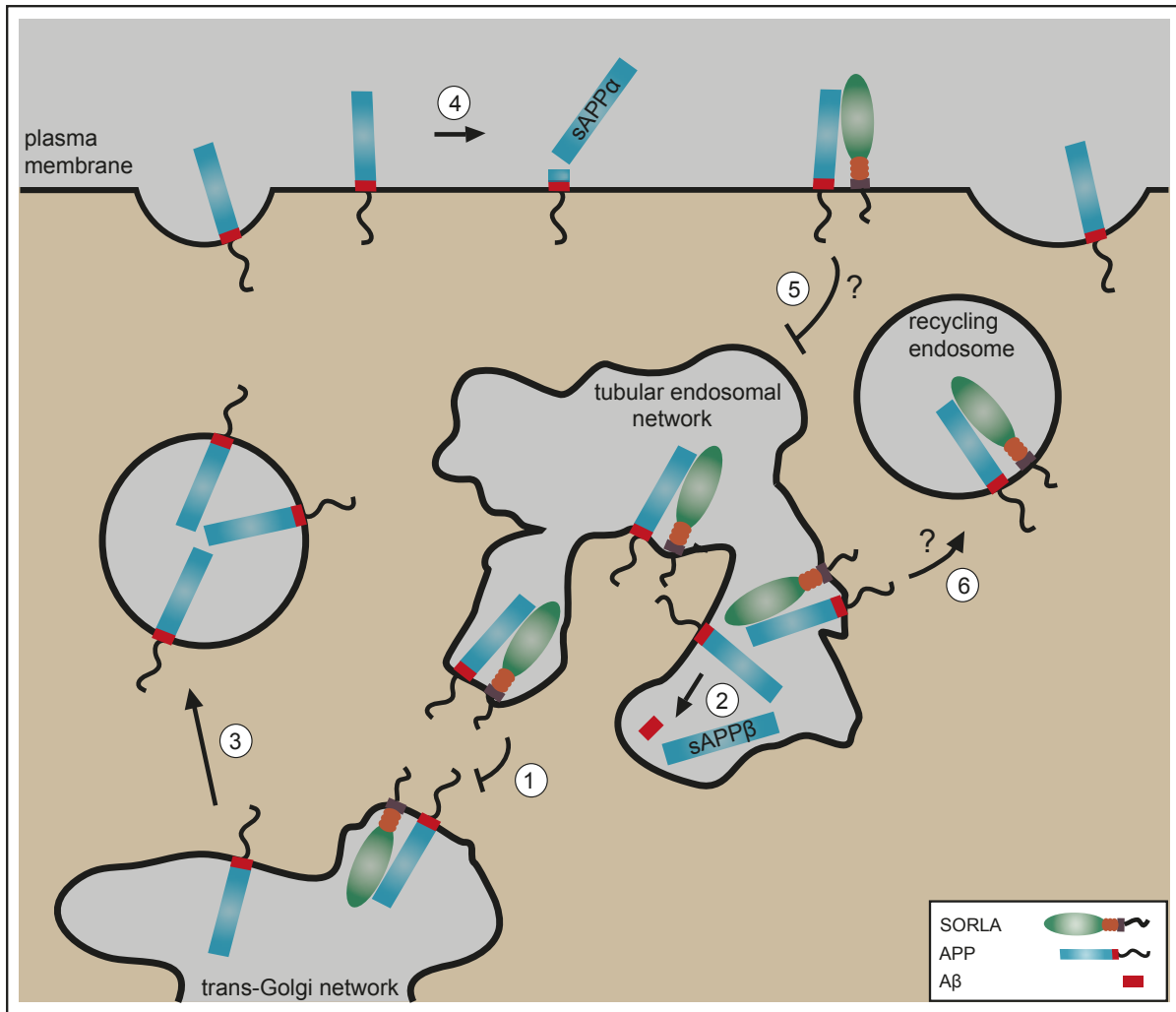


Figure 40: Role of PACS1 in SORLA transport and APP processing.

In wild type neurons, SORLA interacts with APP in the trans-Golgi network (TGN) and prevents APP from reaching the plasma membrane or the tubular endosomal network (TEN), compartments where non-amyloidogenic and amyloidogenic processing occurs, respectively.

Knockdown of PACS1 in SH-SY5Y cells disrupts retrograde sorting of SORLA/APP complexes (1), leading to the depletion of SORLA from the TGN and a concomitant accumulation of SORLA and APP in endosomes where amyloidogenic processing into sAPP β and A β occurs (2).

Loss of SORLA from the TGN may allow exit of APP to the cell surface (3), where APP is non-amyloidogenically processed into sAPP α (4). Alternatively, loss of PACS1 may also affect internalization from (5) or recycling of (6) SORLA/APP complexes to the plasma membrane, explaining accelerated sAPP α production upon PACS1 knockdown.

Interplay between PACS1 and GGA3 regulates trafficking of CI-MPR between the TGN and endosomes (Scott, Fei et al. 2006). Loss of proteins, acting together in a trafficking complex may affect levels of other proteins in this complex. For example, decreased expression of the

retromer component VPS26 in a mouse model resulted in a lower abundance of VPS35 (Muhammad, Flores et al. 2008). In cell lines, knockdown of VPS26 resulted in lower protein levels of VPS35 and VPS29 (Arighi, Hartnell et al. 2004). Hence, loss of PACS1 may also affect GGA3 stability. Since GGA3 is implicated in the degradation of BACE1 (Tesco, Koh et al. 2007), alterations in the GGA3 protein levels may thus affect BACE1 expression. Contrary to these considerations, knockdown of PACS1 in SY5Y-S/A cells in my hands did neither change GGA3 (Fig. 33A and B) nor BACE1 protein levels (Fig. 33C) indicating a lack of influence (direct or indirect) of PACS1 on BACE1 expression.

Remarkably, PACS1 is also implicated in the trafficking of furin, a protease that regulates the maturation of BACE1 (Wan, Molloy et al. 1998; Creemers, Ines Dominguez et al. 2001). Hence, loss of PACS1 may affect enzymatic activity of BACE1. To clarify this issue, I determined the enzymatic activity of endogenous BACE1 in SY5Y cells, but did not observe any alterations in β -secretase activity upon loss of PACS1 (Fig. 33D).

Although I cannot exclude a change in the subcellular localization of BACE1, knockdown of PACS1 did not affect β -secretase expression or activity, pointing towards altered subcellular trafficking of APP as the underlying cause for increased processing of APP in neuronal cells lacking PACS1.

Alterations in APP processing in 5xFAD/SORLA^{acidic} mice qualitatively resemble changes seen in SY5Y cells upon loss of PACS1 expression. However, processing data differ in the relative levels of sAPP α and sAPP β . In detail, whereas sAPP α is more increased than sAPP β *in vivo*, the situation is vice versa in SY5Y cells (increase of 34 % in sAPP α and 52 % in sAPP β). As discussed above, a strong increase in sAPP α and a minor, yet significant, difference in sAPP β in the 5xFAD model may be due to the Swedish EOAD mutation in APP695 that allows better accessibility of the β -secretase (Haass, Lemere et al. 1995), thus, shifting the balance between sAPP β - and sAPP α production. In contrast, SY5Y cells used in this study express the wild-type form of APP695.

On the other hand, I cannot exclude that the described discrepancy originates from a disrupted binding of an adaptor other than PACS1 that also targets the acidic cluster motif in the cytoplasmic tail of SORLA.

For example, subunits of AP1 as well as AP2 interact with the cytosolic part of SORLA. A truncated C-terminus lacking 44 % of the amino acids including the acidic cluster, is unable to bind the adaptors (Nielsen, Gustafsen et al. 2007).

Knockdown of AP2 was shown to affect internalization of SORLA in HEK293 cells, suggesting a functional relevance for the interaction of AP2 with the cytoplasmic tail of SORLA (Nielsen, Gustafsen et al. 2007). Hence, an internalization defect of SORLA^{acidic} and a concomitant shift of APP to the cell surface would ultimately lead to an increased non-amyloidogenic processing and may therefore result in the higher sAPP α /sAPP β ratio seen *in vivo* compared to the data in SY5Y cells.

AP1 is a tetrameric complex that links cargo to the clathrin-coat of endosomal- and TGN-vesicles and thereby plays a role in antero- and retrograde sorting of proteins. I cannot exclude a direct role for AP1 in anterograde trafficking of SORLA as well, however, AP1 also facilitates PACS1-mediated sorting of receptors (Crump, Xiang et al. 2001). Therefore, an indirect binding of AP1 to SORLA (via PACS1) may also explain the reported co-immunoprecipitation of SORLA and the γ -subunit of AP1 (Nielsen, Gustafsen et al. 2007).

To substantiate faulty SORLA trafficking as a cause for increased APP processing, I performed knockdown experiments for PACS1 in SY5Y-S ^{Δ CD}/A cells, overexpressing APP and a SORLA mutant (SORLA ^{Δ CD}) that lacks the cytoplasmic tail, and is, therefore, insensitive to adaptor-mediated trafficking. As seen in SY5Y-S/A cells, loss of PACS1 does not alter protein levels of SORLA ^{Δ CD} and APP (Fig. 34). To test for effects of PACS1 knockdown on APP processing independent of SORLA activity, I determined levels of APP metabolites in SY5Y-S ^{Δ CD}/A cells lacking PACS1. Absence of alterations in levels of sAPP α , sAPP β , and A β ₄₀ confirmed the necessity for functional SORLA in PACS1-regulated APP processing (Fig. 35).

In conclusion, knockdown of PACS1 results in an accumulation of SORLA and APP in endosomes, resulting in an increased processing of APP (Fig. 32). However, PACS1 only exerted its action on APP processing when a fully functional receptor was expressed in cells pointing towards a crucial role for a PACS1/SORLA interplay in Alzheimer's disease-related processes.

4.3.2. SORLA-independent function for PACS1 in amyloid processes

While levels of sAPP α , sAPP β , and A β ₄₀ were unchanged in SY5Y-S^{ACD}/A cells upon loss of PACS1, A β ₄₂ levels were still significantly increased (Fig. 35). Due to the lack of the cytoplasmic tail of SORLA in SY5Y-S^{CD}, aberrant SORLA/APP trafficking can be excluded as the reason for increased levels of A β ₄₂ in those cells upon loss of PACS1. Thus, I propose a model whereby PACS1 fulfills a SORLA-independent function in the catabolism of A β ₄₂ (Fig. 41).

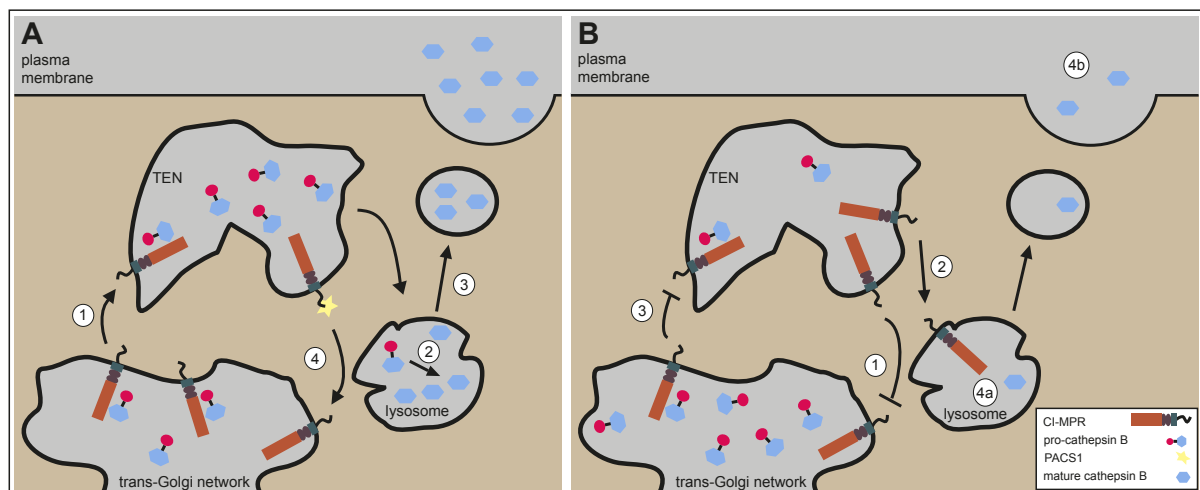


Figure 41: Model for PACS1-dependent sorting of the CI-MPR.

(A) In wild-type cells, the cation-independent mannose-6-phosphate receptor (CI-MPR) targets the proenzyme cathepsin B (pro-cathepsin B) to the tubular endosomal network (TEN) (1). Upon maturation in acidic compartments like the lysosome (2), mature cathepsin B is secreted (3) and the CI-MPR is, upon interaction with PACS1, rerouted to the trans-Golgi network (TGN) (4) and recycled for another round of sorting (Scott, Fei et al. 2006).

(B) In the absence of PACS1, rerouting of CI-MPR from the endosomal network to the TGN is disrupted (1) leading to an increased degradation of the receptor in the lysosomal compartment (2). Improper TGN-retrieval decreases the amount of CI-MPR in the TGN and results in a defective transport of pro-cathepsin B to the TEN (3) ultimately decreasing the number of mature cathepsin B molecules inside (4a) and outside the cell (4b). Thus, loss of PACS1 causes a defect in the CI-MPR-cathepsin B system, ultimately resulting in increased A β ₄₂ levels as a consequence of the decreased amount of mature cathepsin B.

Compared to other A β -degrading enzymes, the cysteine protease cathepsin B is known to preferentially degrade A β ₄₂ over other A β isoforms (like A β ₄₀) (Mueller-Steiner, Zhou et al. 2006). Interestingly, the enzyme can be found in extracellular plaques and inactivation of the protease *in vivo* leads to increased A β ₄₂ levels (Mueller-Steiner, Zhou et al. 2006).

Furthermore, targeted disruption of the *CST3* locus (encoding cystatin C, a cathepsin B inhibitor) enhanced cathepsin B activity in mice and, consequently, lowered A β ₄₂ in the brain (Sun, Zhou et al. 2008). Genetic evidence for a functional role of cathepsin B in amyloid processes came from studies that identified polymorphisms in cystatin C in patients suffering from Alzheimer's disease (Crawford, Freeman et al. 2000; Beyer, Lao et al. 2001; Bertram, McQueen et al. 2007).

To exert its role as A β -degrading enzyme, cathepsin B needs to be converted into its active state. Therefore, cathepsin B is shuttled via the CI-MPR to endosomal compartments for activation (Roshy, Sloane et al. 2003). The CI-MPR depends on the action of PACS1 for the rerouting to the TGN (Fig. 36)(Scott, Fei et al. 2006). Upon knockdown of PACS1, CI-MPR can no longer be retrieved from endosomes and is degraded (Fig. 37A and B). Presumably, a loss of the CI-MPR from the TGN is accompanied by a decreased endosomal routing of the inactive cathepsin B precursor, thus, leading to less active, mature cathepsin B inside and outside the cell (Fig. 37C and D). Consequently, a decrease in mature cathepsin B may account for a decreased proteolytic degradation of A β ₄₂ leading to elevated A β ₄₂ levels seen in SY5Y-S^{ACD}/A cells upon loss of PACS1.

Taken together, my findings point towards a role for PACS1 in the activation of cathepsin B. In line with a specific role of mature cathepsin B in the degradation of A β ₄₂, loss of PACS1 causes a decrease in cathepsin B, thereby explaining elevated A β ₄₂ levels observed in PACS1-depleted SY5Y-S^{ACD}/A cells.

4.4. FUTURE PERSPECTIVES

Recently, several studies have highlighted a possible role for SORLA in protein sorting at the synapse and in control of synaptic plasticity. Firstly, a study identified SORLA as an interaction partner of the tropomyosin-related kinase receptor B (TrkB), a receptor mediating signaling of the neurotrophin brain-derived neurotrophic factor (BDNF) (PONE-D-13-16383 (SORLA-mediated trafficking of TrkB provides a self-potentiating activation loop to enhanced BDNF response in neurons), in press). In this study, loss of SORLA has been reported to result in an impaired neuritic transport of TrkB and in a loss of TrkB from the synapse. In a second study, loss of SORLA was shown to affect neurotransmitter release in hippocampal neurons due to a decreased degradation of phosphorylated synapsin, ultimately leading to impaired hippocampal learning and memory (Dr. Michael Rohe, personal communication). Taken together, these findings suggest a pivotal role for SORLA in neuronal function, although the underlying molecular mechanisms in control of TrkB and synapsin activities remain unclear. Also the connection of these activities with the role of SORLA in APP processing, if any, requires further investigations.

In my work, I generated mouse models expressing trafficking-defective SORLA mutants. Analysis of synaptosomal preparations of cortical extracts revealed SORLA^{acidic} being more abundant at the synapse compared to SORLA^{wt} and SORLA^{FSAF}. An altered synaptic trafficking of SORLA^{acidic} may affect TrkB axonal routing, thereby leading to an aberrant synaptic TrkB trafficking and a disturbed BDNF response.

Additionally to TrkB, SORLA also affects the intracellular trafficking of APP, a protein that, besides its role in Alzheimer's disease related processes, mediates synaptic adhesion and induces presynaptic specializations - processes that pose important steps in synaptogenesis (Wang, Wang et al. 2009). My preliminary data demonstrate that SORLA impacts APP localization to the synapse. In detail, APP is less abundant in isolated synaptosomes of 5xFAD/SORLA^{FSAF} mice compared to 5xFAD/SORLA^{wt} and 5xFAD/SORLA^{acidic} animals. Since APP at the synapse is implicated in synaptogenesis, decreased synaptic localization of APP may affect synaptic integrity and function in SORLA^{FSAF}-expressing mice.

Whereas studies suggest that SORLA parallels APP trafficking in the neuronal soma (Gustafsen, Glerup et al. 2013), my data propose a model of SORLA-indirect routing of APP along axons. In detail, although I observed an accumulation of SORLA^{acidic} in synaptosomes, localization of APP in synaptosomal fractions was unchanged comparing 5xFAD/SORLA^{acidic}

and 5xFAD/SORLA^{wt} animals.

Understanding the molecular mechanism underlying APP sorting to and/or from the synapse in the SORLA mutant mice may give insights into SORLA-dependent regulation of axonal APP trafficking and provide an explanation for the discrepancy between SORLA/APP trafficking in neuronal cell bodies and axons, respectively.

5. MATERIAL AND METHODS

5.1. MATERIAL

5.1.1. Oligonucleotides

Mouse specific primer sequences

primer denotation	DNA sequence (5' → 3')	used for
probe_N_for	GCATCCGGTTGCCATTACG	generation of the probe „N“
probe_N_rev	CCACGGGTGCTCAAGACG	
probe_HBE_for	CGGCGGGAGGGGGCGTGTC	generation of the probe „HBE“
probe_HBE_rev	TGGGCGAAAAATGAGTTGC TGGTG	
LoxP1	TAAGGGATCTGTAGGGCGCA	sequencing of the loxP site
LoxP2	TGTCTCAACCGCGAGCTGT	
acidic_mut_47	GCCATCTTCTCCTCAGGGGCTGCCCTAG GTAAGTAAGCAGG	mutation of the acidic cluster in <i>Sor11</i>
acidic_mut_48	CTGTTTTATCTTCAGGAGCGGCCGCTGC AGCTGCTCCCATGATTACTGG	
FSAF_mut	CCGTCGCTTACAAAGCAGCGCCGCCGC ACAAAGCAGCGCCGCGCTGCCGCCAA CAGCCACTATGCCGCCAACAGCCACTA CAGCTCAGCT	mutation of the FSAF motif in <i>Sor11</i>

Primer used for genotyping

primer denotation	DNA sequence (5' → 3')	final concentration
ROSA_rev_tg	GCGAAGAGTTTGTCTCAACC	0.15 µM
CAG_rev_tg	AGTCCCTATTGGCGTACT	0.1 µM
ROSA/CAG_rev_wt	GGAGCGGGAGAAATGGATATG	0.15 µM
ROSA/CAG_fw	TCGCTCTGAGTTAT	0.25 µM
cre_rev	CGCCATCCACGCTGTTTTGACC	0.2 µM
cre_fw	CAGCCCGGACCGACGATGAAG	0.2 µM
PSEN1_rev	GCCATGAGGGCACTAATCAT	0.13 µM
PSEN1_fw	AATAGAGAACGCCAGGAGCA	0.13 µM
Sor11_rev	CCCCATCCTAACCAAGCCTG	0.2 µM
Sor11_KO_fw	ATGCGGTGGGCTCTATGGCTTCTG	0.13 µM
Sor11_wt_fw	CTGCTTGTTGGGGTGAGACCTG	0.07 µM

Human specific primer sequences

primer denotation	DNA sequence (5' → 3')	used for
FSAF_mut	CACGAAGCACCGGAGGCTTCAAAG CAGCGCCGCCGCTGCCGCCAACAG CCACTACAGCT	mutation of the FSAF motif in human SORLA cDNA
acidic_mut fw	CAATCTTCTCCTCTGGGGCTGCCCT GGGGGCAGCTGCTGCAGCTGCCCC TATGATAACTGGATTTTC	mutation of the acidic cluster in human SORLA cDNA
acidic_mut rev	CAGCTGCCCCCAGGGCAGCCCCAG AGGAGAAGATTGCGGACC	
SORLA cDNA 1	TCCATAGTCGTAAGACACGTACAC	sequencing of the human SORLA cDNA
SORLA cDNA 2	AGTGATCCTTGAGGAAGTGAG	
SORLA cDNA 3	ACTTCCTGGACCTCACTACTAC	
SORLA cDNA 4	GTTCAATTCTGTATGCTGTGAGGA	
SORLA cDNA 5	TCCAAATACAGTGGGTCCCAG	
SORLA cDNA 6	TGCCAGGATGGTTCCGATGA	
SORLA cDNA 7	TGAGTTCGAATGCCACCAAC	
SORLA cDNA 8	TGCGGTGACTAGTCGTGGAATA	
SORLA cDNA 9	TCCTGACCAGGACTTGTTGTATG	
SORLA cDNA 10	GAGGAAACTCGAGTCAGGCTATC	

Human specific siRNA

siRNA targeting PACS1-mRNA (5'-UCGUCAUGC UAAAAGAAAU-3', #A006697-13) or non-targeting siRNA (#D001910-01) was purchased from Thermo Scientific.

5.1.2. Antibodies*Primary antibodies*

antigen	raised in	dilution / used for	provided by / manufacturer code
AKT	rabbit	1:1000	#9272, Cell Signaling
pAKT	rabbit	1:1000	#9271, Cell Signaling
APP	mouse	1:1000 (WB)	MAB348SP (#22C11), Millipore
	rabbit	1:1000 (WB)	J.Gliemann, University of Aarhus, Denmark (#1227)
		1:400 (ICC)	
pAPP (T ⁶⁶⁸)	rabbit	1:1000	#3823, Cell Signaling

AP2M1	chicken	1:2000	ab106542, Abcam
γ -adaplin	mouse	1:400 (ICC) 1:1000 (WB)	BD610385, BD Transduction Laboratories
BACE	rabbit	1:500	#5606, Cell Signaling
cathepsin B	mouse	1:400	C6243, Sigma-Aldrich
CD-MPR	mouse	1:1000	sc-365196, Santa Cruz Biotechnology
CIMPR/ IGF2R	rabbit	1:2000	#5230-1, Epitomics
EEA1	mouse	1:100	BD610457, BD Transduction Laboratories
ERK	rabbit	1:1000	#9102, Cell Signaling
pERK	rabbit	1:1000	#4370, Cell Signaling
furin	rabbit	1:1000	ab3467, Abcam
GGA3	mouse	1:500	BD612311, BD Transduction Laboratories
LAMP-1	rat	1:1000	BD553792, BD Transduction Laboratories
Na/K- ATPase	mouse	1:1000	#05-369, Millipore
NeuN	mouse	1:1000	MAB377, Millipore
PACS1	mouse	1:200	sc-136344, Santa Cruz Biotechnology
PSD95	mouse	1:5000	MAB1596, Millipore
Rab5	mouse	1:100	#108011, Synaptic Systems
SORLA	rabbit	1:1000 (WB of mouse protein lysate)	O. Andersen University of Aarhus, Denmark
		1:400 (IHC, ICC of primary neurons)	
	goat	1:1000 (WB of SY5Y protein lysate)	J.Gliemann, University of Aarhus, Denmark
		1:5000 (ICC, SY5Y cells)	
sortilin	goat	1:1000	AF2934, R&D Systems
β -tubulin	mouse	1:1000	MMS-435P, Covance
Vti1b	mouse	1:100	BD611405, BD Transduction Laboratories
VPS35	goat	1:1000	ab10099, Abcam

Antibodies were diluted in blocking solution (WB) (see below) or PBS (ICC, IHC).

Secondary antibodies

All peroxidase-coupled secondary antibodies used in western blotting were purchased from Sigma-Aldrich and diluted 1:2000 in blocking solution (WB).

In primary neurons, SORLA staining was enhanced using biotin-coupled secondary antibody (dilution 1:250) followed by incubation with fluorophore-coupled streptavidin (dilution 1:250). Reagents were purchased from Jackson Laboratories and diluted in PBS.

All secondary antibodies used in immunofluorescence (dilution 1:2000) and immunohistological experiments (dilution 1:250) were fluorophore-coupled (Alexa488, 555 or 647) and purchased from Invitrogen and diluted in PBS.

5.1.3. Media, buffers and solutions

Media

medium denotation	composition / manufacturer code
dissociation medium	DMEM (31966, Life Technologies), 5 % FBS (10270, Life Technologies), 100 U penicillin/ml, 0.1 mg streptomycin/ml (#15140, Life Technologies)
enzyme solution	2 mg cysteine (#1.02838.0025, Merck), 1 mM CaCl ₂ , 0.5 mM EDTA in 10 ml DMEM with 25 U/ml papain (#P3125, Sigma-Aldrich)
ES cell freezing medium	ES cell medium, FBS, DMSO (D2650, Sigma-Aldrich) (3:1:1)
ES cell medium	5.58 g DMEM (52100, Gibco), 1.0 g NaHCO ₃ , 82.5 ml FBS, 100 U penicillin/ml, 0.1 mg streptomycin/ml, 5.5 ml L-glutamine (#25030-081, Life Technologies), 5.5 ml non-essential amino acids (11140, Gibco), 3.8 µl 2-mercaptoethanol, 55 µl murine LIF (10 ⁷ units/ml) (#1107, Millipore), Geneticin (#10131, Life Technologies)
feeder cultivation medium	DMEM (#B12-604F, Life Technologies), 10 % FBS, 100 U penicillin/ml, 0.1 mg streptomycin/ml
LB agar	LB-medium, 15 g/l agar
LB medium	10 g/l bacto-tryptone, 5 g/l bacto-yeast extract, 10 g/l NaCl; pH 7.2
neuronal medium	100 ml Neurobasal A (21103, Gibco), 2 ml B27 (17505, Life Technologies), 1 ml Glutamax (31966, Gibco) 100 U penicillin/ml, 0.1 mg streptomycin/ml
preparation medium	HBSS (24020, Gibco)
siRNA medium	Accell medium (#B005000, Thermo Scientific)

SOC medium	20 g/l bacto-peptone, 5 g/l bacto-yeast extract, 0.5 g/l NaCl, 0.17 g/l KCl, 0.95 g/l MgCl ₂ , 3.6 g/l glucose; pH 7.0
stop solution	25 mg albumin (A4503, Sigma-Aldrich) + 25 mg trypsininhibitor (T9253, Sigma-Aldrich) in 10 ml dissociation solution
SY5Y cultivation medium	10 % FBS, 100 U penicillin/ml, 0.1 mg streptomycin/ ml, 5.5 ml non essential amino acids, 5.5 ml L-glutamine, 0.3 % Hygromycin (#10687, Invitrogen) and 0.1 % Zeocin (#R25005, Invitrogen) in DMEM/Ham's F12 (1:1) (#E15-012, Life Technologies)
SY5Y freezing medium	FBS, SY5Y cultivation medium, DMSO (ratio 2:2:1)

Buffers and solutions

denotation	composition
blocking solution (free-floating sections)	1 % BSA, 10 % donkey serum, 0.5 % Tween-20 in PBS
blocking solution (Western blot)	5 % milk powder dissolved in TBS-T, 5 % BSA dissolved in TBS-T (antibodies from Cell Signaling)
blocking solution (cytochemistry)	2 % donkey serum, 0,5 % BSA (w/v) in PBS (SY5Y cells) or 8 % donkey serum in PBS (primary neurons)
coating solution (coverslips)	Poly-D-lysine (P7886, Sigma-Aldrich) and Collagen type I (#354236, BD Laboratories) solubilized in 17 mM acetic acid (ratio 1:1:3)
cryoprotectant (free-floating sections)	100 g glycerol, 100 g ethylenglykol in 200 ml phosphate buffer
detection solution	Peroxide/Luminol Enhancer solution (#34077 or #34095, Thermo Scientific)
DAPI	staining of the nuclei, routinely used in immunocytochemistry experiments (1:5000 in PBS) (#10236276001, Roche)
DNA-loading buffer (10x)	0.25 % bromphenol blue (w/v), 0.25 % xylencyanol (w/v), 30 % glycerol (w/v)
HEPES-buffered sucrose	0.32 M sucrose, 4 mM HEPES pH 7.4
„Hot shot“ base buffer	1.25 M NaOH, 1mM EDTA
„Hot Shot“ neutralization buffer	2M Tris-HCl; pH 5
Laemmli buffer (4x)	12 % SDS (w/v), 30 % glycerol (w/v), 150 mM Tris-HCl (pH 7), 0,05 % Coomassie brilliant blue (w/v)
low TE buffer	10 mM Tris-HCl, 1 mM EDTA; pH 8.0
lysis buffer (bacteria)	200 mM NaOH, 1% SDS
neutralization buffer (Mini Prep)	3.0 M potassium acetate; pH 5.5
0.1 M phosphate buffer (Gomori buffer) pH 7.4	77.4 ml 1M Na ₂ HPO ₄ , 22.6 ml 1M NaH ₂ PO ₄ in 1 l H ₂ O
protein lysis buffer	1 % NP-40, 1 % Triton X-100 (w/v), 50 mM Tris-HCl (pH 7,4),

Material and methods

	300 mM NaCl, 5 mM EDTA; supplemented with protease (#05 892 791 001, Roche) and phosphatase inhibitors (#78440, Thermo Scientific)
PBS	1.5 M NaCl, 80 mM Na ₂ HPO ₄ , 20 mM NaH ₂ PO ₄
4 % PFA	4 % paraformaldehyde (w/v) in PBS
4 % PFA, buffered	4 % PFA, pH 7, purchased from Roth (#P087.5, Roth)
Ponceau S	0.1 % (w/v) Ponceau S in 5 % (v/v) acetic acid
resuspension buffer (Mini Prep)	50 mM Tris-HCl, 10 mM EDTA, 100 µg/ml RNase A; pH 8.0
SDS-PAGE running buffer	196 mM glycine, 0.1% SDS, 50 mM Tris-HCl; pH 8.4
solution A	20 mM Tris-HCl, 2 mM MgCl ₂ , 0.25 mM sucrose, pH 7.5; supplemented with protease and phosphatase inhibitors
SSC (20x)	3M NaCl, 0.3M Na ₃ Citrat; pH 7.0
SSC washing buffer I	2x SSC, 0.1 % SDS
SSC washing buffer II	0.1x SSC, 0.5 % SDS
TAE buffer	40 mM Tris-HCl, 1 mM EDTA, 20 mM glacial acetic acid; pH 8.0
tail buffer	10 mM Tris-HCl, 0.3 M Na-Acetate, 0.1 mM EDTA, 1 % SDS, 0.5 mg/ml proteinase K; pH 7
TBS-T (10x)	1,37 mM NaCl, 27 mM KCl, 0,25 M Tris, 1 % Tween (v/v); pH 7,4
transfer buffer (Tris-glycine)	25 mM Tris-HCl, 192 mM glycine

Buffers and solutions are diluted in bidest water if not otherwise stated.

5.1.4. Bacteria strains and mammalian cells

For amplification of plasmid DNA, *Escherichia (E.) coli* strains XL1blue or DH5α were used. All cloning steps, involving gateway-compatible plasmids were carried out in Stb13 bacterial cells (10268-019, Life Technologies).

Cell culture experiments were carried out in SY5Y cells (CRL-2266, ATCC), stably transfected with the APP695 isoform and either SORLA^{wt} or SORLA^{ΔCD} (kindly provided by Dr. V. Schmidt, Max-Delbrueck-Centrum, Berlin).

5.1.5. Chemicals

Chemicals were purchased from Sigma-Aldrich or Roth if not stated otherwise.

5.2. MOUSE-BASED EXPERIMENTS

All incubation steps were carried out at room temperature (RT) if not stated differently.

Animal experimentation

Mice were kept at standard conditions according to the German animal protection act. All studies involving animals were performed in accordance with institutional guidelines.

Wild-type mice had a mixed genetic background (129SvEmcTer x C57BL/6N and 129SvEmcTer x Balb/c) and were bred in house. *Sor11*-deficient mice (129SvEmcTer x C57BL/6N) were generated by targeted gene disruption as described (Andersen, Reiche et al. 2005).

Alzheimer's disease mouse model 5xFAD was purchased from Jackson Laboratory. Animals express human transgenes APP695 carrying the Swedish, Florida, and London familial Alzheimer's disease (FAD) mutation as well as Presenilin 1 (PSEN1) harbouring two FAD mutations. Expression is regulated by the neural-specific *Thy1* promoter (Oakley, Cole et al. 2006). Although carrying two transgenes, 5xFAD mice breed as single transgenics. Therefore, a test for the abundance of one transgene is sufficient.

A cre transgenic mouse strain was used to delete the loxP-flanked neomycin-conferring resistance cassette ubiquitously (Schwenk, Baron et al. 1995). The generation of transgenic mice is described in the result part of this study. The genotype of each animal was determined after birth.

5.2.1. Brain tissue sections

Brains were fixed by transcardiac perfusion with 4 % PFA, post-fixed at 4°C for 24 h in 4 % PFA, rinsed thoroughly using PBS and stored in 30 % sucrose at 4°C until further processing. Hemibrains were either cut into 40 µm thick free-floating sagittal sections using the sliding microtome SM2000R (Leica Biosystems) (and stored in cryoprotectant), or dehydrated as follows: ethanol (70 %, 90 %, 2 x 96 %, 3 x 100 %), 3 x Roti-Histol, 2 x paraffin (each step 1 hour). Subsequently, dehydrated sections were embedded in paraffin and cut into 5 µm sagittal sections using a Rotary Microtome HM 355S (Thermo Scientific).

Nissl staining

Paraffin sections were deparaffinized in xylene (3 x 5 min) and rehydrated through washing series as follows: Roti-Histol (3 x 2 min), ethanol (3 x 100 %, 80 %, 70 %, 50 %, 30 %, 2 min each) and H₂O (2 min), and subsequently stained with thionine acetate (pH 3.8) for 30 min followed by incubation steps in ethanol (90 % ethanol, 10 s; 100 % ethanol, 1 min). The sections were mounted onto glass slides using Roti-Histokitt II (#T160.2, Roth).

Immunohistochemistry on free-floating sections

Free-floating sections were incubated for 1 h in Triton X-100 (0.5 % in PBS), washed (3 x PBS, 10 min each) and incubated in blocking solution for 1 h. Sections were incubated in primary antibody solution overnight. A washing step (3 x PBS, 10 min each) was carried out before incubating the sections in fluorophore-coupled secondary antibody solution (1:250 in PBS, 2 h). Unbound antibody was removed (3 x PBS, 10 min each) before mounting the sections onto glass slides using fluorescent mounting medium.

5.2.2. Preparation and immunocytochemistry of primary neurons

Primary hippocampal neurons were prepared from newborn mice (day 1 postnatal). Animals were sacrificed by decapitation. Hippocampus was dissected in HBSS (4°C), incubated at 37°C in 1 ml enzyme solution (pre-carbonized for 15 min and preincubated for 1 hour after adding papain at 37°C) for 1 hour with continuous shaking at 900 rpm. Enzymatic reaction was stopped by incubating the tissue for 5 min in 1 ml stop solution. Cells were dissociated in 250 µl dissociation medium, collected by centrifugation for 10 min at 80 x g and resuspended in neuronal medium. Cells were plated (1 hippocampus/6 wells in a 24 well-plate) on coated coverslips and kept at 37°C/5 % CO₂.

After 48 hours, FUDR (8,1 mM 2'-deoxy-5-fluorouridine, 20.4 mM uridine in DMEM) was added (1:25) to prevent growth of non-neuronal cells (glia cells, fibroblasts). 300 µl fresh medium (containing FUDR) was added after 4 days. Experiments were started after five days in culture if not stated differently.

Primary neurons were fixed in 4 % PFA (buffered) for 10 min at RT and stored in PBS at 4°C. Permeabilization (0.15 % Triton X-100 in PBS, 15 min) was followed by a 1 hour incubation in blocking buffer. The cells were stained using various antibodies overnight at 4°C. After an incubation with fluorophore-conjugated antibodies (1:2000, 1 hour) the cells were mounted onto glass slides and analyzed by confocal microscopy.

5.2.3. Isolation of proteins from mouse brains

Purification of membrane proteins

To separate membranous and cytoplasmic proteins, brain tissue was homogenized in Solution A using an T10 basic Ultra Turrax (IKA). After 20 minutes, nuclei and cellular debris was removed by a centrifugation step (1000 x g, 10 min). The membrane fraction in the supernatant was pelleted (100000 x g, 1 hour), resuspended in lysis buffer and stored at -80°C. The supernatant (soluble fraction) was aliquoted and stored at -80 °C. All steps were carried out at 4°C.

Fractionation of nervous tissue

To allow quantitative conclusions about the relative localization of a protein at the synapse, brains of mice were subdissected and desired parts (here: cortex) were homogenized in 10 volumes of HEPES-buffered sucrose in a motor driven glass teflon homogenizer at 900 rpm (10 strokes) (PotterS, Braun Biotech). The homogenate was centrifuged (1000 x g, 10 min) and the supernatant subjected to another round of centrifugation (9200 x g, 15 min) to obtain the crude synaptosomal fraction in the pellet (P2). The supernatant was centrifuged (150000 x g, 1 h) to collect the pelleted light membrane fraction (P3). All steps were carried out at 4°C.

5.3. CELL CULTURE BASED EXPERIMENTS

5.3.1. Cultivation and storage of SH-SY5Y cells

SH-SY5Y cells were grown in the indicated medium at 37°C and 5 % CO₂ atmosphere. When reaching semi-confluency, cells were washed once in PBS and subsequently treated with 0.05 % trypsin/EDTA (#25300, Life Technologies) for 5 min at 37°C. The reaction was stopped by adding double the amount of medium. Cells were separated by pipetting, and split as desired.

For freezing, cells were harvested using 0.05 % trypsin/EDTA, pelleted (500 x g, 3 min), resuspended in SY5Y freezing medium and frozen at -80°C.

Frozen cells were quickly thawed at 37°C, transferred into SY5Y cultivation medium, centrifuged (500 x g, 3 min) and resuspended in SY5Y cultivation medium before plating.

5.3.2. Experimental procedures

siRNA treatment

30 % confluent SH-SY5Y cells, plated one day prior to the experiment, were washed with PBS and treated with siRNA medium supplemented with 1 pM siRNA or scrambled control siRNA. Cells were cultivated at 37°C and 5 % CO₂ atmosphere for 72 hours. After removing the supernatant and a washing step with PBS, fresh SY5Y medium was added and conditioned for 24 hours. Then, medium was collected for analysis. Remaining medium was aliquoted and stored at -80°C. Cells were washed with PBS, harvested with a cell scraper and pelleted (500x g, 3 min) prior to protein isolation.

Immunocytochemistry

SH-SY5Y cells were grown on coated coverslips and fixed using 4 % PFA (buffered) for 10 min. Cells were permeabilized (0.15 % Triton X-100 in PBS), washed in PBS and incubated in blocking solution. After incubation overnight in antibody solution, cells were washed (3 x PBS, 10 min each) and treated with fluorophore-conjugated antibodies (1:2000, 1 hour).

Several washing steps with PBS precluded mounting and analysis by confocal microscopy.

Protein isolation from eukaryotic cells

SH-SY5Y cells were scraped off the petri dish in PBS and centrifuged (500x g, 3 min). The cell pellet was lysed in protein lysis buffer for 40 min at 4°C. Cell debris was removed by centrifugation (16000 x g, 10 min, 4°C). Protein concentration of the supernatant was determined and further processed.

5.4. PROTEINBIOCHEMISTRY

Determination of protein concentration

Determination of protein concentration in soluble and membrane fraction of brain tissue and cellular lysate and supernatant was carried out according to the manufacturer's protocol (#23227, Thermo Scientific).

Dephosphorylation of protein lysates

Prior to protein concentration determination, protein lysates were treated with phosphatase (200 U, 1 hour, 37°C) (10108138001, Roche) to confirm the phosphospecificity of an antibody detecting phosphorylated Thr⁶⁶⁸ in the cytoplasmic tail of APP (#3823, Cell Signaling).

SDS-PAGE (polyacrylamide gel electrophoresis)

4 x Laemmli buffer was added to protein lysates and heated for 5 min (95°C). Lysate was loaded on continuous or gradient Tris-Glycine gels purchased from Invitrogen or Lonza. Proteins were separated according to their molecular weight in SDS-PAGE running buffer at 90V. Subsequently, gels were subjected to western blotting.

Western blotting / Immunoblotting

Western blotting procedure was used for immunodetection of proteins separated by SDS-PAGE. Protein transfer was carried out in transfer buffer at 18V overnight using commercial transfer chambers (Bio-Rad). The efficiency of transfer was verified by a Ponceau S staining. Then the blotting membrane (RPN303E, GE Healthcare) was incubated in blocking solution for 1 hour followed by an overnight incubation in primary antibody solution at 4°C on a rocking platform. Washing in TBS-T was carried out to remove unspecifically bound antibodies. Subsequently, the membrane was incubated with peroxidase-conjugated secondary antibody (1:5000 in TBS-T) for 1 hour. After extensive washing in TBS-T and incubation in detection solution (SuperSignal West Femto/Pico Maximum Sensitivity Kits, Thermo Scientific) immunoreactivity was visualized using the LAS-1000 (Fuji) device.

Biological assays

Human APP processing products (sAPP α , sAPP β , A β ₄₀ and A β ₄₂) were determined in multiplex biological assays (#K15120W, #K151BUE, #K15141, Meso Scale discovery) using the SECTOR Imager 2400 (Meso Scale discovery) as a read-out device. All measurements were carried out as described or according to the manufacturer's protocol.

BACE1 activity in SY5Y cells was assessed using a BACE1 fluorescence resonance energy transfer (FRET) assay kit (P2985, Life Technologies). The theoretical background is explained in the result section. In detail, siRNA treated cells were lysed in assay buffer supplemented with 1 % Triton X-100 (w/v) for 1 hour at 4°C. Cell debris was removed by centrifugation (16000 x g, 10 min, 4°C). Protein concentration was determined and the lysate was subsequently used for assaying BACE1 activity according to the manufacturer's protocol. To determine relative fluorescence units, fluorophores in the sample were excited at 545 nm. Emission was read out at 585 nm using the Synergy HT Multi-Mode Microplate Reader (Bio-Tek).

5.5. MOLECULAR BIOLOGY

5.5.1. Molecular cloning

Enzymatic digest of DNA

Plasmid or genomic DNA was incubated with 0.5 U restriction enzyme/ μg DNA and buffered according to the manufacturer's protocol. All restriction enzymes were obtained from New England Biolabs (NEB).

Amplification of DNA fragments by polymerase chain reaction

For cloning, polymerase chain reaction (PCR) was carried out using Phusion polymerase (F530, Finnzymes). The reaction was set up according to manufacturer's instructions. The following cycling conditions were used:

(1) initial denaturation (3 min, 98°C), (2) denaturation (30 s, 98°C), (3) annealing (30 s, 50 - 70°C), (4) elongation (1 min/kb, 72°C), (5) elongation (7 min, 72°C). Steps (2)-(4) were repeated 30-35 times. Annealing temperature depends on the primer sequence and was calculated using an online tool (<http://www.thermoscientificbio.com/webtools/tmc/>).

Agarose gel electrophoresis of DNA

DNA fragments were separated according to their molecular weight on 0.8 – 1.5 % (w/v) agarose gels in TAE buffer. Ethidium bromide was added to the gel (0.5 $\mu\text{g}/\text{ml}$) to visualize DNA fragments.

Isolation of DNA from agarose gels

PCR products or DNA digests were separated on 0.8 – 1.5 % (w/v) agarose gels containing ethidium bromide. By exposing the agarose gel to UV-light, the DNA was visualized and bands of interest were cut out from the gel. The DNA was extracted using the „High Pure PCR product purification kit“ (#11732668001, Roche) according to manufacturer's instructions.

Determination of DNA concentration

DNA concentration was measured using the NanoDrop ND-1000 spectrophotometer (Thermo Scientific) according to the manufacturer's instructions.

Ligation of DNA fragments

Ligation of PCR products into the pGEM-T Easy Vector (#A1360, Promega) was carried out according to manufacturer's instructions.

For ligation of DNA fragments into other plasmids, insert and plasmid DNA were digested with restriction enzymes and purified using commercially available tools (#28104, Qiagen).

Ligation was carried out as follows:

For a 10 μ l ligation reaction, x ng plasmid DNA was mixed with y ng insert DNA (maximally 300 ng in total).

$$x = \text{number of nucleotides of the plasmid}/1000$$

$$y = 5 * \text{number of nucleotides of the insert}/1000$$

Ligation was carried out according to the manufacturer's protocol (#M0202, NEB) at 16 °C overnight. 2 μ l of the ligation reaction was used to transform electro-competent *E. coli*.

DNA transformation of bacteria

Electro-competent *E. coli* were transformed with purified plasmid DNA or with DNA-ligation reactions. Bacteria were thawed on ice and subsequently electroporated with 10 ng of plasmid DNA or 2 μ l of the ligation reaction at 1.8 kV.

The suspension was transferred into a 2.0 ml tube, mixed with 1 ml of SOC medium and incubated at 37°C for 30 min. Cells were collected (2500 x g; 5 min), resuspended in 100 μ l LB medium and plated on a LB agar plate containing the appropriate selective antibiotic.

Cryopreservation of bacteria

1 ml of an overnight (LB-)culture of *E.coli* was mixed with 1 ml 100 % glycerol and immediately frozen at -80 °C.

Isolation of plasmid DNA from bacteria

5 ml of LB medium was inoculated with a single colony of *E.coli* grown on a LB agar plate containing the appropriate selective antibiotic. The LB culture was grown overnight at 37°C with vigorous shaking. The next day the cells were harvested by centrifugation (14000 x g; 5 min). The pellet was resuspended in resuspension buffer and subsequently lysed by adding an equal volume of lysis buffer. The solution was mixed with an equal volume of neutralization buffer and incubated on ice for 15 min. Cellular debris and genomic DNA were removed by centrifugation of the solution (14000 x g; 20 min; 4°C). Plasmid DNA was collected by adding LiCl (3 M, 0.1 x volume) and 100 % isopropanol (2.5 x volume) to the supernatant, followed by a centrifugation step (14000 x g, 30 min, 4°C). Centrifugation was repeated after washing the pellet in 70 % ethanol. Plasmid DNA in the pellet was resuspended in lowTE and stored at -20°C. For isolation of larger amounts of plasmid DNA, a DNA isolation Kit (#12143, Qiagen) was used according to manufacturer's instructions.

Sequencing of DNA

DNA sequencing was performed using the BigDye Terminator v3.1 Cycle Sequencing Kit (4337455, Life Technologies) according to manufacturer's instructions. Amplification was performed as follows: (1) initial denaturation (96°C, 1 min), (2) denaturation (96°C, 10 sec), (3) annealing (55°C, 5 sec), (4) elongation (60°C, 4 min). Steps (2) to (4) were repeated 30 times. DNA was purified using Sephadex G-50 (# 17004101, GE Healthcare), sequenced with an ABI PRISM 377 DNA Sequencer (Perkin Elmer) and analyzed using Lasergene DNA Star SeqMan software (Version 7.0.0).

5.5.2. DNA isolation and genotyping

Isolation of genomic DNA for southern blot

In order to isolate DNA, embryonic stem cells were grown in gelatine-coated 96-well plates and harvested when reaching confluency. DNA from adult mice was isolated from a tail biopsy.

Genotyping was performed as follows: Embryonic stem cells or a tail biopsy were subjected to an overnight incubation in tail buffer (52°C), followed by mixing the lysate with an equal volume of phenol/chloroform/isoamylalcohol (25:24:1). After a centrifugation step (14000 x g; 5 min) the DNA-containing upper phase was mixed with 100 % ethanol (2.5 volumes). The precipitate was collected by centrifugation (14000 x g, 10 min, 4°C) washed with 70 % ethanol and, after an additional centrifugation step (14000 x g, 10 min, 4°C) carefully redissolved in low TE buffer. Isolated genomic DNA was stored at 4°C.

Isolation of genomic DNA for genotyping by PCR

For PCR genotyping of adult mice, tissue was obtained by subjecting mice to an ear punch biopsy. Tissue was incubated in base buffer (75 µl; 95°C; 30 min). After cooling to RT, neutralization buffer (75 µl) was added. Isolated genomic DNA was stored at 4°C.

Genotyping by PCR

PCR genotyping was carried out using the Taq polymerase and 10 x thermoPol buffer (#M0267, NEB). The following cycling conditions were used: (1) initial denaturation (3 min, 94°C), (2) denaturation (15 sec, 94°C), (3) annealing (15 sec, 54-60°C, depending on the length of the primers used), (4) elongation (1 min, 72°C). Steps (2) to (4) were repeated 39 times.

PCR was used to genotype various transgene insertions (tg) and mutations in the used mouse lines. Below, the name of the transgenes or loci are listed. Additionally, annealing temperature is given (in brackets).

ROSA26 (55°C), *CAG-ROSA26* (53°C), *tgCre* (60°C), *tgPSEN1* (60°C), *Sor11* (57°C)

Corresponding primer sequences and concentrations are listed above.

For transgenes, heterozygous insertion in the genome was confirmed using a primer pair (cre: cre_fw and cre_rev; PSEN1: PSEN1_fw and PSEN1_rev).

Three primers were used to genotype both alleles of the *Rosa26* (*ROSA_rev_tg*, *ROSA/CAG_rev_wt*, *ROSA/CAG_fw*) (*CAG_rev_tg*, *ROSA/CAG_rev_wt*, *ROSA/CAG_fw*) or the *Sor11* (*Sor11_rev*, *Sor11_KO_fw*, *Sor11_wt_fw*) locus, respectively.

Genotyping by southern blot

Restriction enzymes Hind III or Nsi I were used to digest genomic DNA overnight according to the manufacturer's protocol. DNA was loaded on a 1 % agarose gel and subjected to electrophoresis at 80 V for approximately 6 hours in TAE buffer. The gel was incubated in NaOH (0.4 M, 30 min) to denature the double stranded DNA. The transfer of the DNA to a nylon membrane (# RPN303S, GE Healthcare) was performed in 0.4 M NaOH overnight according to the following setup: a stack is build up containing 2 sheets of Whatman paper reaching a reservoir with 0.4 M NaOH, agarose gel, nylon membrane, 2 sheets of Whatman paper and a pack of paper towels. The next day, membrane was heated in a 80°C oven for 10 min and exposed to ultraviolet radiation (0.01 Joule, Crosslinker, Bio-Link) to permanently attach the DNA to the membrane.

A DNA probe (probe HBE was used when analysing a targeting approach of the *Rosa26* locus, probe N was used to screen for a targeting event at the *Sor11* locus) was radioactively labelled using the Prime-It II Random Primer Labelling Kit (#300385, Stratagene) according to manufacturer's instructions and subsequently added to the membrane that was before incubated in rapid-hyb buffer (1 hr, 65°C, (#RPN1635, GE Healthcare)). Hybridization was performed overnight. The next day, the membrane was washed (4 x 5 min SSC washing buffer I, 2 x 5 min SSC washing buffer II, 65°C). To visualize the DNA fragments the membrane was exposed to an imaging plate (Fuji) for 12 hours and analyzed using the FLA 3000-2R radioluminographic scanner (Fuji).

5.6. MICROSCOPY

Confocal microscopy was performed in the MDC imaging core facility headed by Dr. A. Sporbert using a SPE or SP5 Laser Scanning Microscope (Leica). For all scans, a pinhole of one airy unit was chosen.

Stereo microscopy was performed using Leica MZ16F.

Images were processed in Photoshop (Adobe).

5.7. STATISTICAL ANALYSIS

Statistical testing

All quantitative data are shown as the mean +/- standard error of the mean. Statistical significance was determined using Graph Pad Prism 5.0 (Student's *t*-test).

Densitometric scanning of western blots

To quantify the intensity of specific bands in immunoblots, densitometric scanning was performed using the Fiji software (www.fiji.sc) or Aida Image Analysis V3.52, respectively. In detail, upon background subtraction, band intensity was measured and related to the band intensity of a protein loading control on the same blot.

Colocalization analysis

For image analysis, stacks of z-sections (0.17 μm) (1024 x 1024 pixels) were sequentially acquired using a SP5 laser scanning microscope. Images were acquired with a 63x oil objective (NA = 1.4) with a 4x zoom.

Image analysis was carried out using Fiji software. In detail, for each picture an ROI was defined, surrounding the cell of interest. Thresholded Mander's values (tM) and the Pearson's correlation coefficient (r) were measured.

The Pearson's correlation coefficient adopt values from +1 to -1 and represents a measure of the pixel's covariance of two channels in a picture. Whereas +1 indicates a positive relationship between the fluorescent intensities -1 describes a negative relationship.

tM values range from 0 (no colocalization) to 1 (perfect colocalization) and denote the degree of overlap of signals in one channel with those in the other channel.

5.8. GENERATION OF MOUSE MODELS

5.8.1. Cloning of the targeting vector

Targeting of the Sorll locus

The generation of mice expressing a mutated form of SORLA was approached by targeting the endogenous *Sorll* locus in embryonic stem cells. Therefore, I engineered a targeting vector carrying mutations in *Sorll* to replace the wild-type sequence following homologous recombination in embryonic stem cells.

The backbone of the targeting vector pKO Scrambler/Select/DT (Lexicon Genetics) contains an ampicillin resistance cassette and the diphtheria Toxin A (DTA) cDNA under control of the PGK promoter. For a positive selection in embryonic stem cells, the vector comprises a cassette conferring resistance against neomycin and kanamycin. Upon expression of cre, two FRT sites flanking the cassette facilitate an excision. Sequences homologous to the *Sorll* gene locus were amplified from bacterial artificial chromosome DNA by F. Lin and have been placed 5' and 3' to the FRT sites.

Two different targeting vectors were generated targeting either Exon 47 (F²¹⁷⁰SAF²¹⁷⁴ → A²¹⁷⁰AAA²¹⁷⁴) (referred to as FSAF mutation) or exon 47 and exon 48 of *Sorll* (D²¹⁹¹DLGEDDED²¹⁹⁹ → A²¹⁹¹ALGAAAAA²¹⁹⁹) (referred to as acidic mutation). The respective mutations were introduced by site-directed mutagenesis using primers listed above (FSAF_mut or acidic_mut_47 and acidic_mut_48). After verification of the sequence by sequencing, the vector was electroporated into embryonic stem cells.

Targeting of the Rosa26 locus

To study various effects of SORLA mutants in mice, a knock-in strategy was elaborated. For that purpose, human SORLA cDNA variants were flanked with genomic sequences of the *Rosa26* locus to enable homologous recombination.

Two different mutations (FSAF or acidic, for details see above) were inserted into the cytoplasmic tail of SORLA. To that end, site-directed mutagenesis was performed to replace the two different sequences in the cytoplasmic tail of SORLA using primers listed above

(FSAF_mut or acidic_mut fw or acidic_mut rev). The targeting constructs contain a loxP-flanked expression cassette, conferring resistance against the antibiotic neomycin followed by a 5' splice acceptor site, the SORLA cDNA and a tpA transcriptional stop sequence. This unit is flanked by genomic *Rosa26* sequences for homologous recombination at the *Rosa26* locus. To achieve a cDNA expression driven by the endogenous ROSA26 promoter, the pROSA26-DEST vector was chosen (Hohenstein, Slight et al. 2008).

As a second approach, pROSA26-DEST was modified by cloning the cytomegalovirus early enhancer in combination with the chicken beta-actin promoter (CAG) 5' to the splice acceptor site to additionally couple the cDNA expression to the exogenous CAG promoter (provided by P.Mort, University of Edinburgh).

Using the Gateway technology approach (#11791, Life Technologies) human SORLA cDNA variants were inserted into the above named vectors resulting in plasmids that were ready for targeting of embryonic stem cells. Prior to targeting, SORLA cDNA in the vectors was sequenced (primers: SORLA cDNA 1-10).

5.8.2. Embryonic stem cell culture

Cultivation of embryonic stem cells

Embryonic stem cells were grown in petri dishes or plates coated with 0.1 % gelatine (in PBS) and an inactivated feeder layer (neomycin-resistant, non-proliferating mouse fibroblasts, kindly provided by Dr. T. Breiderhoff, Max-Delbrueck-Centrum) unless otherwise stated.

When reaching a certain colony size and confluency, cells were washed once in PBS and subsequently treated with 0.25 % trypsin/EDTA (#25200-056, Life Technologies) for 5 min at 37°C. The reaction was stopped by adding twice the amount of ES cell medium. The cells were separated by pipetting up and down and split as desired.

Electroporation of embryonic stem cells

50 µg vector DNA was electroporated with half of an ICp4-(inner cell mass, passage 4) embryonic stem cell-containing 10 cm petri dish derived from 129S7/SvEvBrd-Hprt mice.

The cells were electroporated with a pulse of 250 V and 5 μ F. After electroporation, the cells were seeded on a 10 cm petri dish.

Isolation of embryonic stem cell clones

Two days after electroporation, targeted embryonic stem cell clones were selected by adding 0.18 mg/ml geneticin (#10131-027, Life Technologies) to the ES cell culture medium. After 6-8 days, individual cell clones were picked, transferred into a 96-well plate and incubated with 0.25 % trypsin/EDTA (30 μ l, 37°C, 3 min). ES cell medium (70 μ l) was added and cells were separated by pipetting. After 2–3 days, cells were split 1:4 onto four 96-well plates: two 96-well plates were coated but do not contain a feeder layer. They were used as a source for the isolation of genomic DNA for southern blot analysis; the other two 96-well plates were frozen. Individual clones were thawed after southern blot analysis and used for injection in blastocysts.

Freezing of embryonic stem cell clones

Embryonic stem cells were washed once in PBS before adding 0.25 % trypsin/EDTA (30 μ l, 7 min, 37°C) to ensure separating into single cells. Reaction was stopped adding ES cell medium (70 μ l). Finally, ES cell freezing medium (100 μ l) was added and cells were slowly frozen at -80 °C.

Injection of embryonic stem cell clones into blastocysts

Targeted embryonic stem cell clones were thawed at 37°C in ES cell medium and transferred into 24-well plates. After 2 days, cells were trypsinized and transferred in 6-well plates. Cells were trypsinized, washed twice with PBS, resuspended in ES cell medium (250 μ l) and, finally, injected into blastocysts from C57BL/6 mice (carried out by Annette and Ernst-Martin Fuechtbauer, Aarhus University, Denmark). The injected blastocysts were transferred into the uterus of a pseudo pregnant foster mother to obtain chimeras. Germ line transmission of the modified gene was confirmed in the offspring of the chimeras by southern blot analysis.

6. ZUSAMMENFASSUNG

„Sortilin-related receptor with low-density lipoprotein receptor class A repeats“ (SORLA) ist ein 250 kDa Typ-I Transmembranprotein, das in Neuronen hauptsächlich im trans-Golgi Netzwerk (TGN) lokalisiert, wo es das „amyloid precursor protein“ (APP) bindet. Diese Interaktion verhindert den Transport von APP in endosomale Kompartimente der Zelle, in denen die Spaltung des Proteins in das Peptid A β , welches das molekulare Merkmal der Alzheimer Krankheit darstellt, stattfindet.

Der zytoplasmatische Bestandteil von SORLA enthält Bindestellen für zytosolische Adapterproteine, die den intrazellulären Aufenthaltsort des SORLA/APP Komplexes in kultivierten Zellen beeinflussen. Allerdings ist die Bedeutung der Adapter für den intrazellulären Transport von SORLA und die Prozessierung von APP *in vivo* nicht bekannt. Ziel meiner Dissertation war es, die Bedeutung zytosolischer Adapter sowohl für den Transport von SORLA als auch für amyloidogene Vorgänge aufzuklären. Dabei habe ich mich auf die Interaktion von SORLA mit zwei Adaptern fokussiert, die im retrograden Proteintransport von Endosomen zurück in das TGN involviert sind.

Dazu habe ich neue, transgene Mausmodelle generiert, die einen mutierten SORLA Rezeptor exprimieren, dem entweder die Bindestelle für den „retromer“ Komplex oder für das „phosphofurin acidic cluster sorting protein“ (PACS) 1 fehlt.

Wie erwartet führen diese Mutationen in primären Neuronen zu einem veränderten Transport von SORLA und APP sowie im Gehirn von Mäusen zu einer erhöhten APP Spaltung. Damit weisen diese Ergebnisse zum ersten Mal auf die Bedeutung von Adapter-vermitteltem retrograden Transport von SORLA für die Prozessierung von APP *in vivo* hin.

Die Bindestelle für PACS1, die in dem von mir generierten Mausmodell mutiert wurde, überlappt mit der Bindestelle für den Adapter AP2. Aus diesem Grund habe ich näher untersucht, welche Funktion speziell PACS1 im Verlauf der Alzheimer Krankheit übernimmt. Der „knockdown“ von PACS1 in Zellen der neuronalen Linie SH-SY5Y führt zu einer verringerten Proteinexpression des Adapters und, wie in dem PACS1-bindedefizienten Mausmodell, zu einem veränderten intrazellulären Transport der SORLA/APP Komplexe sowie zu einer erhöhten Spaltung von APP.

Überraschenderweise bewirkt der „knockdown“ von PACS1 - SORLA-unabhängig - eine Erhöhung der Menge an A β ₄₂. PACS1 ist in den intrazellulären Transport des „cation-independent mannose-6-phosphate receptors“ (CI-MPR) involviert, der für die Reifung der

A β -abbauenden Protease Cathepsin B verantwortlich ist. Eine verringerte Proteinexpression von PACS1 führt darum zu einem fehlerhaften Transport des CI-MPR, was eine geringere Cathepsin B Aktivität und, daraus resultierend, eine Erhöhung der Menge an A β ₄₂ zur Folge hat. Meine Ergebnisse konnten damit sowohl eine SORLA-abhängige als auch eine SORLA-unabhängige Funktion von PACS1 in amyloiden Prozessen aufdecken.

7. SUMMARY

Sortilin-related receptor with low-density lipoprotein receptor class A repeats (SORLA) is a 250 kDa type-I transmembrane protein that mainly resides in the trans-Golgi network (TGN) of neurons where it binds the amyloid precursor protein (APP). Binding to SORLA prevents APP from reaching endosomal compartments where processing into A β peptides, the molecular culprits in Alzheimer's disease (AD), occurs.

The cytoplasmic tail of SORLA harbours binding sites for cytosolic adaptor proteins regulating the intracellular sorting of SORLA/APP complexes in cultured cells. However, the importance of adaptor-mediated routing of SORLA for APP processing *in vivo* remained elusive.

Clarifying the relevance of cytosolic adaptors for sorting of SORLA and for amyloidogenic processes in the brain was the overall goal of my thesis project. More specifically, I focused on the interaction of SORLA with two adaptors that are implicated in the retrograde shuttling of target proteins from endosomes to the TGN.

Towards my aims, I generated novel transgenic mouse models expressing SORLA mutants that lack the binding sites for the retromer complex and the phosphofurin acidic cluster sorting protein (PACS) 1, respectively.

In line with my hypothesis, expression of these receptor variants resulted in an altered trafficking of SORLA and of APP in primary neurons and lead to an increased APP breakdown in the brain of mice. These data, for the first time, ascribed a crucial role for adaptor-mediated retrograde sorting of SORLA in APP processing *in vivo*.

Because the binding motif for PACS1 disrupted in my mouse model overlapped with the binding site for another adaptor AP2, I further substantiate the role for PACS1 as sorting protein for SORLA in Alzheimer's disease-related processes in neurons. To do so, I performed PACS1 knockdown studies in the neuronal cell line SH-SY5Y. In line with findings in mice expressing a SORLA mutant defective in binding PACS1, loss of the adaptor lead to aberrant routing of SORLA/APP complexes and resulted in elevated APP processing rates.

Surprisingly, loss of PACS1 also affected the levels of A β ₄₂ peptides in a manner independent of SORLA activity. I was able to trace the underlying molecular mechanism to the ability of PACS1 to sort the cation-independent mannose-6-phosphate receptor (CI-MPR), a protein implicated in the maturation of cathepsin B, a protease that degrades A β . Consequently, faulty

sorting of CI-MPR in PACS1-depleted cells resulted in impaired cathepsin B activity and in elevated levels of A β ₄₂ peptides. Thus, my cell culture studies also revealed the importance of PACS1 for SORLA-dependent and SORLA-independent mechanisms in amyloidogenic processes.

8. BIBLIOGRAPHY

- Abramov, E., I. Dolev, et al. (2009). "Amyloid-beta as a positive endogenous regulator of release probability at hippocampal synapses." *Nat Neurosci* **12**(12): 1567-1576.
- Allinson, T. M., E. T. Parkin, et al. (2003). "ADAMs family members as amyloid precursor protein alpha-secretases." *J Neurosci Res* **74**(3): 342-352.
- Andersen, O. M., J. Reiche, et al. (2005). "Neuronal sorting protein-related receptor sorLA/LR11 regulates processing of the amyloid precursor protein." *Proc Natl Acad Sci U S A* **102**(38): 13461-13466.
- Andersen, O. M., V. Schmidt, et al. (2006). "Molecular dissection of the interaction between amyloid precursor protein and its neuronal trafficking receptor SorLA/LR11." *Biochemistry* **45**(8): 2618-2628.
- Ando, K., K. I. Iijima, et al. (2001). "Phosphorylation-dependent regulation of the interaction of amyloid precursor protein with Fe65 affects the production of beta-amyloid." *J Biol Chem* **276**(43): 40353-40361.
- Aplin, A. E., G. M. Gibb, et al. (1996). "In vitro phosphorylation of the cytoplasmic domain of the amyloid precursor protein by glycogen synthase kinase-3beta." *J Neurochem* **67**(2): 699-707.
- Arighi, C. N., L. M. Hartnell, et al. (2004). "Role of the mammalian retromer in sorting of the cation-independent mannose 6-phosphate receptor." *J Cell Biol* **165**(1): 123-133.
- Armstrong, R. A. (2011). "The pathogenesis of Alzheimer's disease: a reevaluation of the "amyloid cascade hypothesis"." *Int J Alzheimers Dis* **2011**: 630865.
- Arriagada, P. V., J. H. Growdon, et al. (1992). "Neurofibrillary tangles but not senile plaques parallel duration and severity of Alzheimer's disease." *Neurology* **42**(3 Pt 1): 631-639.
- Back, S., P. Haas, et al. (2007). "beta-amyloid precursor protein can be transported independent of any sorting signal to the axonal and dendritic compartment." *J Neurosci Res* **85**(12): 2580-2590.
- Benjannet, S., A. Elagöz, et al. (2001). "Post-translational processing of beta-secretase (beta-amyloid-converting enzyme) and its ectodomain shedding. The pro- and transmembrane/cytosolic domains affect its cellular activity and amyloid-beta production." *J Biol Chem* **276**(14): 10879-10887.
- Bertram, L., M. B. McQueen, et al. (2007). "Systematic meta-analyses of Alzheimer disease genetic association studies: the AlzGene database." *Nat Genet* **39**(1): 17-23.
- Beyer, K., J. I. Lao, et al. (2001). "Alzheimer's disease and the cystatin C gene polymorphism: an association study." *Neurosci Lett* **315**(1-2): 17-20.
- Bhalla, A., C. P. Vetanovetz, et al. (2012). "The location and trafficking routes of the neuronal retromer and its role in amyloid precursor protein transport." *Neurobiol Dis* **47**(1): 126-134.
- Biernat, J., N. Gustke, et al. (1993). "Phosphorylation of Ser262 strongly reduces binding of tau to microtubules: distinction between PHF-like immunoreactivity and microtubule binding." *Neuron* **11**(1): 153-163.
- Binder, L. I., A. Frankfurter, et al. (1985). "The distribution of tau in the mammalian central nervous system." *J Cell Biol* **101**(4): 1371-1378.
- Blain, J. F., E. Paradis, et al. (2004). "A role for lipoprotein lipase during synaptic remodeling in the adult mouse brain." *Neurobiol Dis* **15**(3): 510-519.
- Bohm, C., N. M. Seibel, et al. (2006). "SorLA signaling by regulated intramembrane proteolysis." *J Biol Chem* **281**(21): 14547-14553.

- Boman, A. L., C. Zhang, et al. (2000). "A family of ADP-ribosylation factor effectors that can alter membrane transport through the trans-Golgi." Mol Biol Cell **11**(4): 1241-1255.
- Bonifacino, J. S. (2004). "The GGA proteins: adaptors on the move." Nat Rev Mol Cell Biol **5**(1): 23-32.
- Bonifacino, J. S. and J. H. Hurley (2008). "Retromer." Curr Opin Cell Biol **20**(4): 427-436.
- Braak, H. and E. Braak (1991). "Neuropathological staging of Alzheimer-related changes." Acta Neuropathol **82**(4): 239-259.
- Burgos, P. V., G. A. Mardones, et al. (2010). "Sorting of the Alzheimer's disease amyloid precursor protein mediated by the AP-4 complex." Dev Cell **18**(3): 425-436.
- Caglayan, S., A. Bauerfeind, et al. (2012). "Identification of Alzheimer disease risk genotype that predicts efficiency of SORL1 expression in the brain." Arch Neurol **69**(3): 373-379.
- Cam, J. A., C. V. Zerbinatti, et al. (2004). "The low density lipoprotein receptor-related protein 1B retains beta-amyloid precursor protein at the cell surface and reduces amyloid-beta peptide production." J Biol Chem **279**(28): 29639-29646.
- Cam, J. A., C. V. Zerbinatti, et al. (2005). "Rapid endocytosis of the low density lipoprotein receptor-related protein modulates cell surface distribution and processing of the beta-amyloid precursor protein." J Biol Chem **280**(15): 15464-15470.
- Cao, X. and T. C. Sudhof (2001). "A transcriptionally [correction of transcriptively] active complex of APP with Fe65 and histone acetyltransferase Tip60." Science **293**(5527): 115-120.
- Carlo, A. S., C. Gustafsen, et al. (2013). The pro-neurotrophin receptor sortilin is a major neuronal apolipoprotein E receptor for catabolism of amyloid-beta peptide in the brain. 33.
- Carlton, J., M. Bujny, et al. (2004). "Sorting nexin-1 mediates tubular endosome-to-TGN transport through coincidence sensing of high- curvature membranes and 3-phosphoinositides." Curr Biol **14**(20): 1791-1800.
- Choy, R. W., Z. Cheng, et al. (2012). "Amyloid precursor protein (APP) traffics from the cell surface via endosomes for amyloid beta (Abeta) production in the trans-Golgi network." Proc Natl Acad Sci U S A **109**(30): E2077-2082.
- Clee, S. M., B. S. Yandell, et al. (2006). "Positional cloning of Sorcs1, a type 2 diabetes quantitative trait locus." Nat Genet **38**(6): 688-693.
- Cozier, G. E., J. Carlton, et al. (2002). "The phox homology (PX) domain-dependent, 3-phosphoinositide-mediated association of sorting nexin-1 with an early sorting endosomal compartment is required for its ability to regulate epidermal growth factor receptor degradation." J Biol Chem **277**(50): 48730-48736.
- Crawford, F. C., M. J. Freeman, et al. (2000). "A polymorphism in the cystatin C gene is a novel risk factor for late-onset Alzheimer's disease." Neurology **55**(6): 763-768.
- Creemers, J. W., D. Ines Dominguez, et al. (2001). "Processing of beta-secretase by furin and other members of the proprotein convertase family." J Biol Chem **276**(6): 4211-4217.
- Crump, C. M., Y. Xiang, et al. (2001). "PACS-1 binding to adaptors is required for acidic cluster motif-mediated protein traffic." EMBO J **20**(9): 2191-2201.
- Daigle, I. and C. Li (1993). "apl-1, a Caenorhabditis elegans gene encoding a protein related to the human beta-amyloid protein precursor." Proc Natl Acad Sci U S A **90**(24): 12045-12049.
- Dawson, G. R., G. R. Seabrook, et al. (1999). "Age-related cognitive deficits, impaired long-term potentiation and reduction in synaptic marker density in mice lacking the beta-amyloid precursor protein." Neuroscience **90**(1): 1-13.
- De Strooper, B. (2003). "Aph-1, Pen-2, and Nicastrin with Presenilin generate an active gamma-Secretase complex." Neuron **38**(1): 9-12.

- De Strooper, B., W. Annaert, et al. (1999). "A presenilin-1-dependent gamma-secretase-like protease mediates release of Notch intracellular domain." *Nature* **398**(6727): 518-522.
- Deinhardt, K., T. Kim, et al. (2011). "Neuronal growth cone retraction relies on proneurotrophin receptor signaling through Rac." *Sci Signal* **4**(202): ra82.
- Dodson, S. E., O. M. Andersen, et al. (2008). "Loss of LR11/SORLA enhances early pathology in a mouse model of amyloidosis: evidence for a proximal role in Alzheimer's disease." *J Neurosci* **28**(48): 12877-12886.
- Eehalt, R., P. Keller, et al. (2003). "Amyloidogenic processing of the Alzheimer beta-amyloid precursor protein depends on lipid rafts." *J Cell Biol* **160**(1): 113-123.
- Farris, W., S. Mansourian, et al. (2003). "Insulin-degrading enzyme regulates the levels of insulin, amyloid beta-protein, and the beta-amyloid precursor protein intracellular domain in vivo." *Proc Natl Acad Sci U S A* **100**(7): 4162-4167.
- Fiete, D., Y. Mi, et al. (2007). "N-linked oligosaccharides on the low density lipoprotein receptor homolog SorLA/LR11 are modified with terminal GalNAc-4-SO₄ in kidney and brain." *J Biol Chem* **282**(3): 1873-1881.
- Fjorback, A. W., M. Seaman, et al. (2012). "Retromer binds the FANSHY sorting motif in SorLA to regulate amyloid precursor protein sorting and processing." *J Neurosci* **32**(4): 1467-1480.
- Friedrich, G. and P. Soriano (1991). "Promoter traps in embryonic stem cells: a genetic screen to identify and mutate developmental genes in mice." *Genes Dev* **5**(9): 1513-1523.
- Fuentealba, R. A., M. I. Barria, et al. (2007). "ApoER2 expression increases Abeta production while decreasing Amyloid Precursor Protein (APP) endocytosis: Possible role in the partitioning of APP into lipid rafts and in the regulation of gamma-secretase activity." *Mol Neurodegener* **2**: 14.
- Fukami, S., K. Watanabe, et al. (2002). "Abeta-degrading endopeptidase, neprilysin, in mouse brain: synaptic and axonal localization inversely correlating with Abeta pathology." *Neurosci Res* **43**(1): 39-56.
- Geng, Z., F. Y. Xu, et al. (2011). "Sorting protein-related receptor SorLA controls regulated secretion of glial cell line-derived neurotrophic factor." *J Biol Chem* **286**(48): 41871-41882.
- Glerup, S., M. Lume, et al. (2013). "SorLA controls neurotrophic activity by sorting of GDNF and its receptors GFRalpha1 and RET." *Cell Rep* **3**(1): 186-199.
- Goedert, M. and M. G. Spillantini (2006). "A century of Alzheimer's disease." *Science* **314**(5800): 777-781.
- Gustafsen, C., S. Glerup, et al. (2013). "Sortilin and SorLA display distinct roles in processing and trafficking of amyloid precursor protein." *J Neurosci* **33**(1): 64-71.
- Haass, C., A. Y. Hung, et al. (1993). "beta-Amyloid peptide and a 3-kDa fragment are derived by distinct cellular mechanisms." *J Biol Chem* **268**(5): 3021-3024.
- Haass, C., E. H. Koo, et al. (1995). "Polarized sorting of beta-amyloid precursor protein and its proteolytic products in MDCK cells is regulated by two independent signals." *J Cell Biol* **128**(4): 537-547.
- Haass, C., E. H. Koo, et al. (1992). "Targeting of cell-surface beta-amyloid precursor protein to lysosomes: alternative processing into amyloid-bearing fragments." *Nature* **357**(6378): 500-503.
- Haass, C., C. A. Lemere, et al. (1995). "The Swedish mutation causes early-onset Alzheimer's disease by beta-secretase cleavage within the secretory pathway." *Nat Med* **1**(12): 1291-1296.
- Haass, C., M. G. Schlossmacher, et al. (1992). "Amyloid beta-peptide is produced by cultured cells during normal metabolism." *Nature* **359**(6393): 322-325.

- Haass, C. and D. J. Selkoe (2007). "Soluble protein oligomers in neurodegeneration: lessons from the Alzheimer's amyloid beta-peptide." *Nat Rev Mol Cell Biol* **8**(2): 101-112.
- Hamazaki, H. (1996). "Cathepsin D is involved in the clearance of Alzheimer's beta-amyloid protein." *FEBS Lett* **396**(2-3): 139-142.
- Harold, D., R. Abraham, et al. (2009). "Genome-wide association study identifies variants at CLU and PICALM associated with Alzheimer's disease." *Nat Genet* **41**(10): 1088-1093.
- He, X., F. Li, et al. (2005). "GGA proteins mediate the recycling pathway of memapsin 2 (BACE)." *J Biol Chem* **280**(12): 11696-11703.
- He, X., G. Zhu, et al. (2003). "Biochemical and structural characterization of the interaction of memapsin 2 (beta-secretase) cytosolic domain with the VHS domain of GGA proteins." *Biochemistry* **42**(42): 12174-12180.
- Heber, S., J. Herms, et al. (2000). "Mice with combined gene knock-outs reveal essential and partially redundant functions of amyloid precursor protein family members." *J Neurosci* **20**(21): 7951-7963.
- Hebert, S. S., L. Serneels, et al. (2006). "Regulated intramembrane proteolysis of amyloid precursor protein and regulation of expression of putative target genes." *EMBO Rep* **7**(7): 739-745.
- Hermans-Borgmeyer, I., W. Hampe, et al. (1998). "Unique expression pattern of a novel mosaic receptor in the developing cerebral cortex." *Mech Dev* **70**(1-2): 65-76.
- Hermey, G., S. S. Sjogaard, et al. (2006). "Tumour necrosis factor alpha-converting enzyme mediates ectodomain shedding of Vps10p-domain receptor family members." *Biochem J* **395**(2): 285-293.
- Herms, J., B. Anliker, et al. (2004). "Cortical dysplasia resembling human type 2 lissencephaly in mice lacking all three APP family members." *EMBO J* **23**(20): 4106-4115.
- Herskowitz, J. H., K. Offe, et al. (2012). "GGA1-mediated endocytic traffic of LR11/SorLA alters APP intracellular distribution and amyloid-beta production." *Mol Biol Cell* **23**(14): 2645-2657.
- Hock, C., A. Maddalena, et al. (2003). "Treatment with the selective muscarinic m1 agonist talsaclidine decreases cerebrospinal fluid levels of A beta 42 in patients with Alzheimer's disease." *Amyloid* **10**(1): 1-6.
- Hoe, H. S., D. Wessner, et al. (2005). "F-spondin interaction with the apolipoprotein E receptor ApoEr2 affects processing of amyloid precursor protein." *Mol Cell Biol* **25**(21): 9259-9268.
- Hohenstein, P., J. Slight, et al. (2008). "High-efficiency Rosa26 knock-in vector construction for Cre-regulated overexpression and RNAi." *Pathogenetics* **1**(1): 3.
- Hong, Z., Y. Yang, et al. (2009). "The retromer component SNX6 interacts with dynactin p150(Glued) and mediates endosome-to-TGN transport." *Cell Res* **19**(12): 1334-1349.
- Hooper, N. M., E. H. Karran, et al. (1997). "Membrane protein secretases." *Biochem J* **321** (Pt 2): 265-279.
- Hopkins, C. R., A. Gibson, et al. (1994). "In migrating fibroblasts, recycling receptors are concentrated in narrow tubules in the pericentriolar area, and then routed to the plasma membrane of the leading lamella." *J Cell Biol* **125**(6): 1265-1274.
- Hu, F., T. Padukkavidana, et al. (2010). "Sortilin-mediated endocytosis determines levels of the frontotemporal dementia protein, progranulin." *Neuron* **68**(4): 654-667.
- Hu, X., W. He, et al. (2008). "Genetic deletion of BACE1 in mice affects remyelination of sciatic nerves." *FASEB J* **22**(8): 2970-2980.

- Huse, J. T., D. S. Pijak, et al. (2000). "Maturation and endosomal targeting of beta-site amyloid precursor protein-cleaving enzyme. The Alzheimer's disease beta-secretase." *J Biol Chem* **275**(43): 33729-33737.
- Iijima, K., K. Ando, et al. (2000). "Neuron-specific phosphorylation of Alzheimer's beta-amyloid precursor protein by cyclin-dependent kinase 5." *J Neurochem* **75**(3): 1085-1091.
- Iwata, N., H. Mizukami, et al. (2004). "Presynaptic localization of neprilysin contributes to efficient clearance of amyloid-beta peptide in mouse brain." *J Neurosci* **24**(4): 991-998.
- Iwata, N., S. Tsubuki, et al. (2001). "Metabolic regulation of brain A β by neprilysin." *Science* **292**(5521): 1550-1552.
- Jacobsen, L., P. Madsen, et al. (2001). "Activation and functional characterization of the mosaic receptor SorLA/LR11." *J Biol Chem* **276**(25): 22788-22796.
- Jacobsen, L., P. Madsen, et al. (1996). "Molecular characterization of a novel human hybrid-type receptor that binds the alpha2-macroglobulin receptor-associated protein." *J Biol Chem* **271**(49): 31379-31383.
- Jacobsen, L., P. Madsen, et al. (2002). "The sorLA cytoplasmic domain interacts with GGA1 and -2 and defines minimum requirements for GGA binding." *FEBS Lett* **511**(1-3): 155-158.
- Jansen, P., K. Giehl, et al. (2007). "Roles for the pro-neurotrophin receptor sortilin in neuronal development, aging and brain injury." *Nat Neurosci* **10**(11): 1449-1457.
- Jellinger, K., H. Braak, et al. (1991). "Alzheimer lesions in the entorhinal region and isocortex in Parkinson's and Alzheimer's diseases." *Ann N Y Acad Sci* **640**: 203-209.
- Jiang, M., H. Bujo, et al. (2008). "Ang II-stimulated migration of vascular smooth muscle cells is dependent on LR11 in mice." *J Clin Invest* **118**(8): 2733-2746.
- Kaether, C., C. Haass, et al. (2006). "Assembly, trafficking and function of gamma-secretase." *Neurodegener Dis* **3**(4-5): 275-283.
- Kamenetz, F., T. Tomita, et al. (2003). "APP processing and synaptic function." *Neuron* **37**(6): 925-937.
- Kanaki, T., H. Bujo, et al. (1998). "Developmental regulation of LR11 expression in murine brain." *DNA Cell Biol* **17**(8): 647-657.
- Kang, J., H. G. Lemaire, et al. (1987). "The precursor of Alzheimer's disease amyloid A4 protein resembles a cell-surface receptor." *Nature* **325**(6106): 733-736.
- Kimberly, W. T., J. B. Zheng, et al. (2005). "Physiological regulation of the beta-amyloid precursor protein signaling domain by c-Jun N-terminal kinase JNK3 during neuronal differentiation." *J Neurosci* **25**(23): 5533-5543.
- Kinoshita, A., H. Fukumoto, et al. (2003). "Demonstration by FRET of BACE interaction with the amyloid precursor protein at the cell surface and in early endosomes." *J Cell Sci* **116**(Pt 16): 3339-3346.
- Kins, S., N. Lauther, et al. (2006). "Subcellular trafficking of the amyloid precursor protein gene family and its pathogenic role in Alzheimer's disease." *Neurodegener Dis* **3**(4-5): 218-226.
- Kjolby, M., O. M. Andersen, et al. (2010). "Sort1, encoded by the cardiovascular risk locus 1p13.3, is a regulator of hepatic lipoprotein export." *Cell Metab* **12**(3): 213-223.
- Klinger, S. C., S. Glerup, et al. (2011). "SorLA regulates the activity of lipoprotein lipase by intracellular trafficking." *J Cell Sci* **124**(Pt 7): 1095-1105.
- Koo, E. H., S. S. Sisodia, et al. (1990). "Precursor of amyloid protein in Alzheimer disease undergoes fast anterograde axonal transport." *Proc Natl Acad Sci U S A* **87**(4): 1561-1565.

- Koo, E. H. and S. L. Squazzo (1994). "Evidence that production and release of amyloid beta-protein involves the endocytic pathway." *J Biol Chem* **269**(26): 17386-17389.
- Kopke, E., Y. C. Tung, et al. (1993). "Microtubule-associated protein tau. Abnormal phosphorylation of a non-paired helical filament pool in Alzheimer disease." *J Biol Chem* **268**(32): 24374-24384.
- Kuhn, P. H., H. Wang, et al. (2010). "ADAM10 is the physiologically relevant, constitutive alpha-secretase of the amyloid precursor protein in primary neurons." *EMBO J* **29**(17): 3020-3032.
- Lai, A., S. S. Sisodia, et al. (1995). "Characterization of sorting signals in the beta-amyloid precursor protein cytoplasmic domain." *J Biol Chem* **270**(8): 3565-3573.
- Lammich, S., E. Kojro, et al. (1999). "Constitutive and regulated alpha-secretase cleavage of Alzheimer's amyloid precursor protein by a disintegrin metalloprotease." *Proc Natl Acad Sci U S A* **96**(7): 3922-3927.
- Lane, R. F., S. M. Raines, et al. (2010). "Diabetes-associated SorCS1 regulates Alzheimer's amyloid-beta metabolism: evidence for involvement of SorL1 and the retromer complex." *J Neurosci* **30**(39): 13110-13115.
- Lee, J. H., K. F. Lau, et al. (2004). "The neuronal adaptor protein X11beta reduces amyloid beta-protein levels and amyloid plaque formation in the brains of transgenic mice." *J Biol Chem* **279**(47): 49099-49104.
- Lee, J. H., K. F. Lau, et al. (2003). "The neuronal adaptor protein X11alpha reduces Abeta levels in the brains of Alzheimer's APP^{swe} Tg2576 transgenic mice." *J Biol Chem* **278**(47): 47025-47029.
- Lee, M. S., S. C. Kao, et al. (2003). "APP processing is regulated by cytoplasmic phosphorylation." *J Cell Biol* **163**(1): 83-95.
- Lesne, S., C. Ali, et al. (2005). "NMDA receptor activation inhibits alpha-secretase and promotes neuronal amyloid-beta production." *J Neurosci* **25**(41): 9367-9377.
- Lewis, J., E. McGowan, et al. (2000). "Neurofibrillary tangles, amyotrophy and progressive motor disturbance in mice expressing mutant (P301L) tau protein." *Nat Genet* **25**(4): 402-405.
- Lombino, F., F. Biundo, et al. (2013). "An Intracellular Threonine of Amyloid-beta Precursor Protein Mediates Synaptic Plasticity Deficits and Memory Loss." *PLoS One* **8**(2): e57120.
- Manders, E. M., F. J. Verbeek, et al. (1993). "Measurement of co-localization of objects in dual-colour confocal images." *Journal of microscopy* **169**(3): 375-382.
- Marcusson, E. G., B. F. Horazdovsky, et al. (1994). "The sorting receptor for yeast vacuolar carboxypeptidase Y is encoded by the VPS10 gene." *Cell* **77**(4): 579-586.
- Matsuda, S., Y. Matsuda, et al. (2003). "Amyloid beta protein precursor (AbetaPP), but not AbetaPP-like protein 2, is bridged to the kinesin light chain by the scaffold protein JNK-interacting protein 1." *J Biol Chem* **278**(40): 38601-38606.
- Meilandt, W. J., M. Cisse, et al. (2009). "Neprilysin overexpression inhibits plaque formation but fails to reduce pathogenic Abeta oligomers and associated cognitive deficits in human amyloid precursor protein transgenic mice." *J Neurosci* **29**(7): 1977-1986.
- Meng, Y., J. H. Lee, et al. (2007). "Association between SORL1 and Alzheimer's disease in a genome-wide study." *Neuroreport* **18**(17): 1761-1764.
- Mort, J. S. and D. J. Buttle (1997). "Cathepsin B." *Int J Biochem Cell Biol* **29**(5): 715-720.
- Morwald, S., H. Yamazaki, et al. (1997). "A novel mosaic protein containing LDL receptor elements is highly conserved in humans and chickens." *Arterioscler Thromb Vasc Biol* **17**(5): 996-1002.
- Motoi, Y., T. Aizawa, et al. (1999). "Neuronal localization of a novel mosaic apolipoprotein E receptor, LR11, in rat and human brain." *Brain Res* **833**(2): 209-215.

- Mueller-Steiner, S., Y. Zhou, et al. (2006). "Antiamyloidogenic and neuroprotective functions of cathepsin B: implications for Alzheimer's disease." Neuron **51**(6): 703-714.
- Muhammad, A., I. Flores, et al. (2008). "Retromer deficiency observed in Alzheimer's disease causes hippocampal dysfunction, neurodegeneration, and Abeta accumulation." Proc Natl Acad Sci U S A **105**(20): 7327-7332.
- Munter, L. M., A. Botev, et al. (2010). "Aberrant amyloid precursor protein (APP) processing in hereditary forms of Alzheimer disease caused by APP familial Alzheimer disease mutations can be rescued by mutations in the APP GxxxG motif." J Biol Chem **285**(28): 21636-21643.
- Munter, L. M., P. Voigt, et al. (2007). "GxxxG motifs within the amyloid precursor protein transmembrane sequence are critical for the etiology of Abeta42." EMBO J **26**(6): 1702-1712.
- Muresan, Z. and V. Muresan (2005). "Coordinated transport of phosphorylated amyloid-beta precursor protein and c-Jun NH2-terminal kinase-interacting protein-1." J Cell Biol **171**(4): 615-625.
- Musa, A., H. Lehrach, et al. (2001). "Distinct expression patterns of two zebrafish homologues of the human APP gene during embryonic development." Dev Genes Evol **211**(11): 563-567.
- Naj, A. C., G. Jun, et al. (2011). "Common variants at MS4A4/MS4A6E, CD2AP, CD33 and EPHA1 are associated with late-onset Alzheimer's disease." Nat Genet **43**(5): 436-441.
- Neve, R. L., E. A. Finch, et al. (1988). "Expression of the Alzheimer amyloid precursor gene transcripts in the human brain." Neuron **1**(8): 669-677.
- Neve, R. L., P. Harris, et al. (1986). "Identification of cDNA clones for the human microtubule-associated protein tau and chromosomal localization of the genes for tau and microtubule-associated protein 2." Brain Res **387**(3): 271-280.
- Nielsen, M. S., C. Gustafsen, et al. (2007). "Sorting by the cytoplasmic domain of the amyloid precursor protein binding receptor SorLA." Mol Cell Biol **27**(19): 6842-6851.
- Nikolaev, A., T. McLaughlin, et al. (2009). "APP binds DR6 to trigger axon pruning and neuron death via distinct caspases." Nature **457**(7232): 981-989.
- Nitsch, R. M., B. E. Slack, et al. (1993). "Receptor-coupled amyloid precursor protein processing." Ann N Y Acad Sci **695**: 122-127.
- Oakley, H., S. L. Cole, et al. (2006). "Intraneuronal beta-amyloid aggregates, neurodegeneration, and neuron loss in transgenic mice with five familial Alzheimer's disease mutations: potential factors in amyloid plaque formation." J Neurosci **26**(40): 10129-10140.
- Offe, K., S. E. Dodson, et al. (2006). "The lipoprotein receptor LR11 regulates amyloid beta production and amyloid precursor protein traffic in endosomal compartments." J Neurosci **26**(5): 1596-1603.
- Park, J. H., D. A. Gimbel, et al. (2006). "Alzheimer precursor protein interaction with the Nogo-66 receptor reduces amyloid-beta plaque deposition." J Neurosci **26**(5): 1386-1395.
- Pasternak, S. H., R. D. Bagshaw, et al. (2003). "Presenilin-1, nicastrin, amyloid precursor protein, and gamma-secretase activity are co-localized in the lysosomal membrane." J Biol Chem **278**(29): 26687-26694.
- Pastorino, L., A. F. Ikin, et al. (2002). "The carboxyl-terminus of BACE contains a sorting signal that regulates BACE trafficking but not the formation of total A(beta)." Mol Cell Neurosci **19**(2): 175-185.
- Patthy, L. (1990). "Homology of a domain of the growth hormone/prolactin receptor family with type III modules of fibronectin." Cell **61**(1): 13-14.

- Perez, R. G., S. Soriano, et al. (1999). "Mutagenesis identifies new signals for beta-amyloid precursor protein endocytosis, turnover, and the generation of secreted fragments, including Abeta42." *J Biol Chem* **274**(27): 18851-18856.
- Perez, R. G., H. Zheng, et al. (1997). "The beta-amyloid precursor protein of Alzheimer's disease enhances neuron viability and modulates neuronal polarity." *J Neurosci* **17**(24): 9407-9414.
- Peter, B. J., H. M. Kent, et al. (2004). "BAR domains as sensors of membrane curvature: the amphiphysin BAR structure." *Science* **303**(5657): 495-499.
- Phinney, A. L., M. E. Calhoun, et al. (1999). "No hippocampal neuron or synaptic bouton loss in learning-impaired aged beta-amyloid precursor protein-null mice." *Neuroscience* **90**(4): 1207-1216.
- Pietrzik, C. U., I. S. Yoon, et al. (2004). "FE65 constitutes the functional link between the low-density lipoprotein receptor-related protein and the amyloid precursor protein." *J Neurosci* **24**(17): 4259-4265.
- Posse De Chaves, E. I., D. E. Vance, et al. (2000). "Uptake of lipoproteins for axonal growth of sympathetic neurons." *J Biol Chem* **275**(26): 19883-19890.
- Postina, R., A. Schroeder, et al. (2004). "A disintegrin-metalloproteinase prevents amyloid plaque formation and hippocampal defects in an Alzheimer disease mouse model." *J Clin Invest* **113**(10): 1456-1464.
- Pottier, C., D. Hannequin, et al. (2012). "High frequency of potentially pathogenic SORL1 mutations in autosomal dominant early-onset Alzheimer disease." *Mol Psychiatry* **17**(9): 875-879.
- Prabhu, Y., P. V. Burgos, et al. (2012). "Adaptor protein 2-mediated endocytosis of the beta-secretase BACE1 is dispensable for amyloid precursor protein processing." *Mol Biol Cell* **23**(12): 2339-2351.
- Puertollano, R., R. C. Aguilar, et al. (2001). "Sorting of mannose 6-phosphate receptors mediated by the GGAs." *Science* **292**(5522): 1712-1716.
- Puertollano, R. and J. S. Bonifacino (2004). "Interactions of GGA3 with the ubiquitin sorting machinery." *Nat Cell Biol* **6**(3): 244-251.
- Puertollano, R., P. A. Randazzo, et al. (2001). "The GGAs promote ARF-dependent recruitment of clathrin to the TGN." *Cell* **105**(1): 93-102.
- Puzzo, D., L. Privitera, et al. (2008). "Picomolar amyloid-beta positively modulates synaptic plasticity and memory in hippocampus." *J Neurosci* **28**(53): 14537-14545.
- Qi-Takahara, Y., M. Morishima-Kawashima, et al. (2005). "Longer forms of amyloid beta protein: implications for the mechanism of intramembrane cleavage by gamma-secretase." *J Neurosci* **25**(2): 436-445.
- Qiu, W. Q., A. Ferreira, et al. (1995). "Cell-surface beta-amyloid precursor protein stimulates neurite outgrowth of hippocampal neurons in an isoform-dependent manner." *J Neurosci* **15**(3 Pt 2): 2157-2167.
- Reitz, C., R. Cheng, et al. (2011). "Meta-analysis of the association between variants in SORL1 and Alzheimer disease." *Arch Neurol* **68**(1): 99-106.
- Richter, L., L. M. Munter, et al. (2010). "Amyloid beta 42 peptide (Abeta42)-lowering compounds directly bind to Abeta and interfere with amyloid precursor protein (APP) transmembrane dimerization." *Proc Natl Acad Sci U S A* **107**(33): 14597-14602.
- Riddell, D. R., G. Christie, et al. (2001). "Compartmentalization of beta-secretase (Asp2) into low-buoyant density, noncaveolar lipid rafts." *Curr Biol* **11**(16): 1288-1293.
- Roberds, S. L., J. Anderson, et al. (2001). "BACE knockout mice are healthy despite lacking the primary beta-secretase activity in brain: implications for Alzheimer's disease therapeutics." *Hum Mol Genet* **10**(12): 1317-1324.

- Rogaeva, E., Y. Meng, et al. (2007). "The neuronal sortilin-related receptor SORL1 is genetically associated with Alzheimer disease." *Nat Genet* **39**(2): 168-177.
- Rohe, M., A. S. Carlo, et al. (2008). "Sortilin-related receptor with A-type repeats (SORLA) affects the amyloid precursor protein-dependent stimulation of ERK signaling and adult neurogenesis." *J Biol Chem* **283**(21): 14826-14834.
- Rohe, M., M. Synowitz, et al. (2009). "Brain-derived neurotrophic factor reduces amyloidogenic processing through control of SORLA gene expression." *J Neurosci* **29**(49): 15472-15478.
- Rojas, R., T. van Vlijmen, et al. (2008). "Regulation of retromer recruitment to endosomes by sequential action of Rab5 and Rab7." *J Cell Biol* **183**(3): 513-526.
- Roques, B. P., F. Noble, et al. (1993). "Neutral endopeptidase 24.11: structure, inhibition, and experimental and clinical pharmacology." *Pharmacol Rev* **45**(1): 87-146.
- Rosen, D. R., L. Martin-Morris, et al. (1989). "A Drosophila gene encoding a protein resembling the human beta-amyloid protein precursor." *Proc Natl Acad Sci U S A* **86**(7): 2478-2482.
- Roshy, S., B. F. Sloane, et al. (2003). "Pericellular cathepsin B and malignant progression." *Cancer Metastasis Rev* **22**(2-3): 271-286.
- Santiard-Baron, D., D. Langui, et al. (2005). "Expression of human FE65 in amyloid precursor protein transgenic mice is associated with a reduction in beta-amyloid load." *J Neurochem* **93**(2): 330-338.
- Scherzer, C. R., K. Offe, et al. (2004). "Loss of apolipoprotein E receptor LR11 in Alzheimer disease." *Arch Neurol* **61**(8): 1200-1205.
- Scheuner, D., C. Eckman, et al. (1996). "Secreted amyloid beta-protein similar to that in the senile plaques of Alzheimer's disease is increased in vivo by the presenilin 1 and 2 and APP mutations linked to familial Alzheimer's disease." *Nat Med* **2**(8): 864-870.
- Schmidt, V., A. Sporbert, et al. (2007). "SorLA/LR11 regulates processing of amyloid precursor protein via interaction with adaptors GGA and PACS-1." *J Biol Chem* **282**(45): 32956-32964.
- Schneider, A., J. Biernat, et al. (1999). "Phosphorylation that detaches tau protein from microtubules (Ser262, Ser214) also protects it against aggregation into Alzheimer paired helical filaments." *Biochemistry* **38**(12): 3549-3558.
- Schweers, O., E. M. Mandelkow, et al. (1995). "Oxidation of cysteine-322 in the repeat domain of microtubule-associated protein tau controls the in vitro assembly of paired helical filaments." *Proc Natl Acad Sci U S A* **92**(18): 8463-8467.
- Schwenk, F., U. Baron, et al. (1995). "A cre-transgenic mouse strain for the ubiquitous deletion of loxP-flanked gene segments including deletion in germ cells." *Nucleic Acids Res* **23**(24): 5080-5081.
- Scott, G. K., H. Fei, et al. (2006). "A PACS-1, GGA3 and CK2 complex regulates CI-MPR trafficking." *EMBO J* **25**(19): 4423-4435.
- Scott, G. K., F. Gu, et al. (2003). "The phosphorylation state of an autoregulatory domain controls PACS-1-directed protein traffic." *EMBO J* **22**(23): 6234-6244.
- Seabrook, G. R., D. W. Smith, et al. (1999). "Mechanisms contributing to the deficits in hippocampal synaptic plasticity in mice lacking amyloid precursor protein." *Neuropharmacology* **38**(3): 349-359.
- Seaman, M. N., E. G. Marcusson, et al. (1997). "Endosome to Golgi retrieval of the vacuolar protein sorting receptor, Vps10p, requires the function of the VPS29, VPS30, and VPS35 gene products." *J Cell Biol* **137**(1): 79-92.
- Seubert, P., C. Vigo-Pelfrey, et al. (1992). "Isolation and quantification of soluble Alzheimer's beta-peptide from biological fluids." *Nature* **359**(6393): 325-327.

- Shankar, G. M., S. Li, et al. (2008). "Amyloid-beta protein dimers isolated directly from Alzheimer's brains impair synaptic plasticity and memory." *Nat Med* **14**(8): 837-842.
- Shoji, M., T. E. Golde, et al. (1992). "Production of the Alzheimer amyloid beta protein by normal proteolytic processing." *Science* **258**(5079): 126-129.
- Sisodia, S. S. (1992). "Beta-amyloid precursor protein cleavage by a membrane-bound protease." *Proc Natl Acad Sci U S A* **89**(13): 6075-6079.
- Sisodia, S. S., E. H. Koo, et al. (1990). "Evidence that beta-amyloid protein in Alzheimer's disease is not derived by normal processing." *Science* **248**(4954): 492-495.
- Slunt, H. H., G. Thinakaran, et al. (1994). "Expression of a ubiquitous, cross-reactive homologue of the mouse beta-amyloid precursor protein (APP)." *J Biol Chem* **269**(4): 2637-2644.
- Soriano, S., A. S. Chyung, et al. (1999). "Expression of beta-amyloid precursor protein-CD3gamma chimeras to demonstrate the selective generation of amyloid beta(1-40) and amyloid beta(1-42) peptides within secretory and endocytic compartments." *J Biol Chem* **274**(45): 32295-32300.
- Spoelgen, R., C. A. von Arnim, et al. (2006). "Interaction of the cytosolic domains of sorLA/LR11 with the amyloid precursor protein (APP) and beta-secretase beta-site APP-cleaving enzyme." *J Neurosci* **26**(2): 418-428.
- Steiner, H. (2008). "The catalytic core of gamma-secretase: presenilin revisited." *Curr Alzheimer Res* **5**(2): 147-157.
- Sun, B., Y. Zhou, et al. (2008). "Cystatin C-cathepsin B axis regulates amyloid beta levels and associated neuronal deficits in an animal model of Alzheimer's disease." *Neuron* **60**(2): 247-257.
- Suzuki, T., M. Oishi, et al. (1994). "Cell cycle-dependent regulation of the phosphorylation and metabolism of the Alzheimer amyloid precursor protein." *EMBO J* **13**(5): 1114-1122.
- Takami, M., Y. Nagashima, et al. (2009). "gamma-Secretase: successive tripeptide and tetrapeptide release from the transmembrane domain of beta-carboxyl terminal fragment." *J Neurosci* **29**(41): 13042-13052.
- Takata, K. and Y. Kitamura (2012). "Molecular approaches to the treatment, prophylaxis, and diagnosis of Alzheimer's disease: tangle formation, amyloid-beta, and microglia in Alzheimer's disease." *J Pharmacol Sci* **118**(3): 331-337.
- Takatsu, H., Y. Katoh, et al. (2001). "Golgi-localizing, gamma-adaptin ear homology domain, ADP-ribosylation factor-binding (GGA) proteins interact with acidic dileucine sequences within the cytoplasmic domains of sorting receptors through their Vps27p/Hrs/STAM (VHS) domains." *J Biol Chem* **276**(30): 28541-28545.
- Takatsu, H., K. Yoshino, et al. (2002). "GGA proteins associate with Golgi membranes through interaction between their GGAH domains and ADP-ribosylation factors." *Biochem J* **365**(Pt 2): 369-378.
- Taru, H., K. Iijima, et al. (2002). "Interaction of Alzheimer's beta -amyloid precursor family proteins with scaffold proteins of the JNK signaling cascade." *J Biol Chem* **277**(22): 20070-20078.
- Taylor, C. J., D. R. Ireland, et al. (2008). "Endogenous secreted amyloid precursor protein-alpha regulates hippocampal NMDA receptor function, long-term potentiation and spatial memory." *Neurobiol Dis* **31**(2): 250-260.
- Tesco, G., Y. H. Koh, et al. (2007). "Depletion of GGA3 stabilizes BACE and enhances beta-secretase activity." *Neuron* **54**(5): 721-737.
- Vardarajan, B. N., S. Y. Bruesegem, et al. (2012). "Identification of Alzheimer disease-associated variants in genes that regulate retromer function." *Neurobiol Aging* **33**(9): 2231 e2215-2231 e2230.

- Vassar, R., B. D. Bennett, et al. (1999). "Beta-secretase cleavage of Alzheimer's amyloid precursor protein by the transmembrane aspartic protease BACE." *Science* **286**(5440): 735-741.
- von Koch, C. S., H. Zheng, et al. (1997). "Generation of APLP2 KO mice and early postnatal lethality in APLP2/APP double KO mice." *Neurobiol Aging* **18**(6): 661-669.
- Wahle, T., D. R. Thal, et al. (2006). "GGA1 is expressed in the human brain and affects the generation of amyloid beta-peptide." *J Neurosci* **26**(49): 12838-12846.
- Waldron, E., S. Isbert, et al. (2008). "Increased AICD generation does not result in increased nuclear translocation or activation of target gene transcription." *Exp Cell Res* **314**(13): 2419-2433.
- Walker, K. R., E. L. Kang, et al. (2012). "Depletion of GGA1 and GGA3 mediates postinjury elevation of BACE1." *J Neurosci* **32**(30): 10423-10437.
- Wan, L., S. S. Molloy, et al. (1998). "PACS-1 defines a novel gene family of cytosolic sorting proteins required for trans-Golgi network localization." *Cell* **94**(2): 205-216.
- Wang, C., B. Sun, et al. (2012). "Cathepsin B degrades amyloid-beta in mice expressing wild-type human amyloid precursor protein." *J Biol Chem* **287**(47): 39834-39841.
- Wang, P., G. Yang, et al. (2005). "Defective neuromuscular synapses in mice lacking amyloid precursor protein (APP) and APP-Like protein 2." *J Neurosci* **25**(5): 1219-1225.
- Wang, Z., B. Wang, et al. (2009). "Presynaptic and postsynaptic interaction of the amyloid precursor protein promotes peripheral and central synaptogenesis." *J Neurosci* **29**(35): 10788-10801.
- Wasco, W., K. Bupp, et al. (1992). "Identification of a mouse brain cDNA that encodes a protein related to the Alzheimer disease-associated amyloid beta protein precursor." *Proc Natl Acad Sci U S A* **89**(22): 10758-10762.
- Wassmer, T., N. Attar, et al. (2009). "The retromer coat complex coordinates endosomal sorting and dynein-mediated transport, with carrier recognition by the trans-Golgi network." *Dev Cell* **17**(1): 110-122.
- Weidemann, A., G. Konig, et al. (1989). "Identification, biogenesis, and localization of precursors of Alzheimer's disease A4 amyloid protein." *Cell* **57**(1): 115-126.
- Weingarten, M. D., A. H. Lockwood, et al. (1975). "A protein factor essential for microtubule assembly." *Proc Natl Acad Sci U S A* **72**(5): 1858-1862.
- Willem, M., A. N. Garratt, et al. (2006). "Control of peripheral nerve myelination by the beta-secretase BACE1." *Science* **314**(5799): 664-666.
- Willnow, T. E., C. M. Petersen, et al. (2008). "VPS10P-domain receptors - regulators of neuronal viability and function." *Nat Rev Neurosci* **9**(12): 899-909.
- Yamazaki, H., H. Bujo, et al. (1996). "Elements of neural adhesion molecules and a yeast vacuolar protein sorting receptor are present in a novel mammalian low density lipoprotein receptor family member." *J Biol Chem* **271**(40): 24761-24768.
- Yamazaki, T., E. H. Koo, et al. (1996). "Trafficking of cell-surface amyloid beta-protein precursor. II. Endocytosis, recycling and lysosomal targeting detected by immunolocalization." *J Cell Sci* **109** (Pt 5): 999-1008.
- Youker, R. T., U. Shinde, et al. (2009). "At the crossroads of homeostasis and disease: roles of the PACS proteins in membrane traffic and apoptosis." *Biochem J* **421**(1): 1-15.
- Zambrowicz, B. P., A. Imamoto, et al. (1997). "Disruption of overlapping transcripts in the ROSA beta geo 26 gene trap strain leads to widespread expression of beta-galactosidase in mouse embryos and hematopoietic cells." *Proc Natl Acad Sci U S A* **94**(8): 3789-3794.
- Zerbinatti, C. V., D. F. Wozniak, et al. (2004). "Increased soluble amyloid-beta peptide and memory deficits in amyloid model mice overexpressing the low-density lipoprotein receptor-related protein." *Proc Natl Acad Sci U S A* **101**(4): 1075-1080.

Bibliography

- Zheng, H., M. Jiang, et al. (1995). "beta-Amyloid precursor protein-deficient mice show reactive gliosis and decreased locomotor activity." *Cell* **81**(4): 525-531.
- Zhu, Y., H. Bujo, et al. (2004). "LR11, an LDL receptor gene family member, is a novel regulator of smooth muscle cell migration." *Circ Res* **94**(6): 752-758.
- Zhu, Y., B. Doray, et al. (2001). "Binding of GGA2 to the lysosomal enzyme sorting motif of the mannose 6-phosphate receptor." *Science* **292**(5522): 1716-1718.

9. PUBLICATIONS

Carlo AS, Gustafsen C, Mastrobuoni G, Nielsen MS, Burgert T, Hartl D, Rohe M, Nykjaer A, Herz J, Heeren J, Kempa S, Petersen CM, Willnow TE.

The pro-neurotrophin receptor sortilin is a major neuronal apolipoprotein E receptor for catabolism of amyloid- β peptide in the brain.

J Neurosci. 2013 Jan 2;33(1):358-70

Safak Caglayan, Shizuka Takagi-Niidome, Anne-Sophie Carlo, Tilman Burgert, Yu Kitago, Ernst-Martin Füchtbauer, Annette Füchtbauer, Junichi Takagi and Thomas E. Willnow

Novel role for SORLA/SORL1 as clearance receptor for amyloid- β peptide is impaired by familial Alzheimer disease mutation

STM paper #3005229 (in revision)

Parts of this work have been reported elsewhere:

Tilman Burgert, Vanessa Schmidt, Safak Caglayan, Fuyu Lin, Annette Füchtbauer, Ernst-Martin Füchtbauer, Anders Nykjaer, Anne-Sophie Carlo, and Thomas E. Willnow

Titel: „SORLA-dependent and –independent functions for PACS1 in control of amyloidogenic processes“

MCB00628-13 (in revision)

Curriculum Vitae

Der Lebenslauf ist in der Online-Version
aus Gründen des Datenschutzes nicht enthalten